Flow Science Incorporated
420 Neff Avenue, Suite 230, Harrisonburg, VA 22801
(540) 442-8433 • FAX (540) 442-8863

Water Purification Demonstration Project: Limnology and Reservoir Detention Study of San Vicente Reservoir - Hydrodynamic Modeling Study

Prepared for

City of San Diego

600 B Street, Suite 600,

San Diego, CA 92101

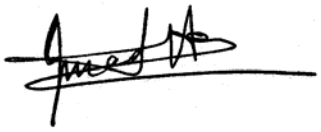

Prepared By
Li Ding, Ph.D., P.E. (VA)
Senior Engineer

Reviewed By
Imad A. Hannoun, Ph.D., P.E. (VA)
President

Reviewed By
E. John List, Ph.D., P.E. (CA)
Principal Consultant

FSI V094005
May 01, 2012

Table of Contents

List of Tables

List of Figures

SUMMARY

BACKGROUND

San Vicente Reservoir (SVR) is located near Lakeside, California, and is used as a source of drinking water supply by the City of San Diego (City), its owner and operator. The reservoir currently has a capacity of about 90,000 acre-feet (see **Figure 1**). It is undergoing an enlargement that will raise the dam 117 feet and increase the reservoir's storage to 247,000 acre-feet at the spillway level (or 242,000 acre-feet at the maximum operation level). The City is considering an option to augment SVR supply by bringing advanced purified recycled water (*i.e.,* purified water) from the advanced water purification facility to SVR. The purified water would be blended with other water in the reservoir. The current project – the Water Purification Demonstration Project (Demonstration Project) – will not actually put any purified water into the reservoir; rather it will study and model the reservoir augmentation process. A component of the Demonstration Project is the Limnology and Reservoir Detention Study of San Vicente Reservoir (Limnology Study).

As part of the Limnology Study, Flow Science Incorporated (FSI) has developed a three-dimensional water quality model that is used to evaluate hydrodynamic and water quality effects of using purified water to augment SVR. After the model was developed, its results were compared to existing field data and documented in the Calibration Technical Memorandum (TM) submitted to the City in 2010 (FSI, 2010). The Calibration TM has been peer-reviewed by the National Water Research Institute Independent Advisory Panel (NWRIIAP) that was assembled for the review of the City's Demonstration Project. After implementing suggestions proposed by the NWRIIAP, the model was deemed by NWRIIAP to be "an effective and robust tool, for 1) simulating thermoclines and hydrodynamics of the San Vicente Reservoir; 2) assessing biological water quality for nutrients; 3) assessing options for the purified water inlet location" (NWRI, 2010).

HYDRODYNAMIC EFFECTS OF RESERVOIR EXPANSION

In order to understand the background conditions where purified water will be stored, the hydrodynamic changes due to the expansion prior to adding purified water were first examined. This was accomplished by running a simulation that uses the same reservoir conditions (climate, inflow and outflow parameters etc.) as the 2006-2007 calibration simulation except for using a higher initial reservoir volume that is close to a full pool. The results from this simulation were compared against those from the original calibration simulation. Based on the comparisons, the following conclusions can be drawn:

- The expanded reservoir is predicted to start stratifying in about March of each year. In the spring and summer, the stratification will intensify. In the fall, the thermocline will start deepening appreciably until the reservoir becomes fully mixed in late fall or early winter. As a result, the reservoir is predicted to be stratified from about March to December, and will be destratified from December to February.

- Reservoir expansion will increase the volume of the hypolimnion but will have a negligible effect on the thermocline depth when the reservoir is stratified. Both surface and bottom reservoir temperatures are expected to remain unchanged due to increased water depth.

RESULTS FOR VARIOUS OPERATING SCENARIOS USING THE DESIGN PURIFIED WATER INLET LOCATION

The main objectives of this study were to use the calibrated and validated SVR computer model to determine the effectiveness of SVR as an environmental buffer and barrier for purified water introduced into SVR, and to evaluate any hydrodynamic changes in SVR induced by the purified water. To achieve these goals, reservoir simulations were conducted to evaluate a number of proposed future reservoir operating scenarios. Firstly, a Base Case simulation was performed to evaluate SVR under expected typical future conditions. This scenario considered a reservoir under median expected storage and normal expected operations. After that, a case was considered whereby no purified water is introduced in the reservoir, enabling a quantification of the effects of purified water addition on the reservoir behavior. Further scenarios were modeled to consider somewhat extreme operations: a scenario with an extended drought and another with emergency drawdown. These scenarios and associated annual flow volumes from various sources are listed in **Table S-1**. The simulations discussed in this section all utilized the Design Purified Water Inlet Location (see **Figure 1** for the location) as the point of release for purified water flow into SVR. Port #2 at the reservoir outlet tower structure was used for all water withdrawals from the reservoir throughout this study.

In these simulations various hypothetical tracers were added to the purified water inflow to illustrate the transport and mixing of the purified water within the reservoir. In particular, decaying tracers (decay rate of 1 log per month, *i.e.*, a reduction in concentration by a factor of 10 per month) were used to study the dilution and inactivation of potential pathogens entering the reservoir and to evaluate the ability of the reservoir to reduce pathogen concentrations before they reach the reservoir outlet. The decaying tracer was continuously released with the purified water inflow at a constant

concentration throughout the entire modeling period. In addition, hypothetical conservative (that is, non-decaying) tracers were added to the purified water inflow in order to simulate the potential effects of elevated concentrations of chemical constituents in the purified water entering SVR after "excursion events" at the water purification facility. These conservative tracers were tracked to determine the dilution and lag time provided by the reservoir (*i.e.*, the time interval between the release of the tracer and peak reservoir outflow concentration). In all simulations, such tracers were added to the reservoir's inflow over a 24-hour period and were thus referred to as 24-hour conservative tracers.

Table S-1. Modeled Operating Scenarios[1,2]

Operating Scenarios	Description	Initial /Final Reservoir Volume (acre-feet)	Annual Purified Water Inflow (acre-feet/year)	Annual Aqueduct inflow (acre-feet/year)	Annual Reservoir Outflow (acre-feet/year)
Base Case	median expected storage and normal expected operations	155,000 /155,000	15,000	3,000	19,000
No Purified Water	no purified water additions and an equal reduction in reservoir outflow	155,000 /155,000	0	3,000	4,000
Extended Drought	a hypothetical two-year drought situation	155,000 /100,000	15,000	3,000	48,000
Emergency Drawdown[3]	a situation where a total of 66,000 acre-feet water is withdrawn from the reservoir in January and February of Year 2 and the reservoir is subsequently refilled by adding 66,000 acre-feet water from the Aqueduct between March and July in Year 2	200,000 /200,000	15,000	69,000	85,000

Note: 1. There are no water transfers from Sutherland Reservoir into SVR.
2. Runoff flow rate is 4,500 acre-feet/year for all scenarios.
3. The table lists the flow volumes for Year 2 for this scenario. Flow volumes for Year 1 are the same as those for the Base Case.

Based on the simulation results, the following conclusions and observations are made for the Base Case:

- The addition of purified water in the expanded reservoir is predicted to slightly deepen the thermocline (*e.g.,* by less than 3 ft in September) and reduce conductivity in the reservoir (compared to the Calibration Run).

- The purified water generally has a lower density (lower conductivity and higher temperature) than the ambient reservoir water. This will cause the purified water to initially spread along the surface of the reservoir near the purified water inlet location. In the stratified reservoir period (typically March to December), the purified water will rapidly mix within the entire epilimnion. As the thermocline gradually deepens, the purified water will gradually approach successively lower ports on the reservoir outlet tower.

- In the unstratified period (December to February), the purified water is predicted to initially flow along the reservoir's surface, but then it will quickly mix over the entire depth, achieving rapid dilution over the entire reservoir volume.

- The proposed withdrawal strategy at SVR will generally utilize deeper ports (Port #2 was considered to be the open port throughout this investigation). Since the purified water will generally flow into the reservoir above the thermocline in the stratified period, it is predicted to typically take several weeks or months for newly released purified water to appear at the reservoir outlet, after undergoing large dilution (*i.e.*, achieving a dilution of at least 2,000). In the reservoir destratified period, the simulations indicate that the purified water can appear at the reservoir outlet within days or weeks after release, but only after undergoing significant dilution (*i.e.*, achieving a dilution of at least 2,000).

- For a decaying tracer released with the purified water (a surrogate for pathogens), the reservoir outflow from the reservoir is predicted to achieve at least a 2-log reduction[1] (100:1 reduction in concentration) in the unstratified period. In the stratified period, the reservoir will provide significantly higher reductions (as high as 9 logs; that is, a 1 trillion reduction).

[1] A log reduction is defined as a 10-fold reduction.

- For a 24-hour conservative tracer that enters the reservoir the simulations indicate that a dilution of at least 2,000 can be obtained in the reservoir outflow.

In the following, conclusions and observations for the Extended Drought and Emergency Drawdown scenarios are listed based on the simulation results. It should be noted that the release dates of the 24-hour conservative tracers for these two scenarios are different from those for the Base Case. The selection of 24-hour conservative tracer release dates for Extended Drought and Emergency Drawdown scenarios was based on identifying critical periods in which the highest reservoir outflow concentrations are most likely to occur (the timings for the 24-hour conservative tracer release for the Base Case were distributed more evenly over the year). From our understanding of the variations in 24-hour conservative tracer release concentrations in the Base Case, the most critical periods are expected to meet the following three conditions: 1) the reservoir is almost or fully mixed vertically; 2) the reservoir water volume is at a minimum; and 3) the occurrence of Santa Ana wind events (events where prevailing winds are expected to rapidly drive purified water introduced at the east side of the reservoir directly toward the reservoir outlet located near the southwest end of the reservoir).

- For a decaying tracer in the purified water inflow under the Extended Drought scenario, the analyses indicate that the reservoir can achieve a 2-log reduction in tracer concentration in the unstratified period and significantly higher values (typically 4-8 log reduction) for the remainder of the year. The minimum predicted dilution and its corresponding lag time for a 24-hour conservative tracer are about 900 and 5 days, respectively, and occurs at the end of Year Two when the reservoir volume is lowest.

- For a decaying tracer in the purified water inflow under the Emergency Drawdown scenario, the results indicate that the reservoir can achieve a 2-log reduction in the unstratified period and significantly higher values (typically 4-10 log reduction) for the remainder of the year. The minimum predicted dilution and its corresponding lag time for a 24-hour conservative tracer are about 1,400 and 8 days, respectively. The minimum predicted dilution here is higher than those obtained from both the Base Case and the Extended Drought scenarios, a result of the larger reservoir volume considered in the Emergency Drawdown Scenario during the winter months.

EFFECT OF PURIFIED WATER INLET LOCATION

Various purified water inlet locations were also evaluated under various operating conditions to examine the effects of varying the purified water inlet location. A total of four different purified water inlet locations were considered under the Base Case operating scenario. These are: the Design Purified Water Inlet Location, Existing Aqueduct Purified Water Inlet Location, New Aqueduct Purified Water Inlet Location, and Barona Arm Purified Water Inlet Location. The Design and New Aqueduct Purified Water Inlet Locations were further evaluated under the Extended Drought operating scenario. All simulations conducted for varying the purified water inlet locations are listed in **Table S-2** and results for the decaying tracer and 24-hour conservative tracers from these simulations are presented in **Table S-3**. Note that the release dates of the 24-hour conservative tracers for these runs are different from those for the runs listed in **Table S-1**.

Based on the simulation results, the conclusions and observations on the effects of varying the purified water inlet location are summarized as follows:

- In the stratified season, utilizing different inlet locations to introduce purified water into SVR is predicted to have little effect on both the decaying and 24-hour conservative tracer concentrations in the reservoir outflow under all scenarios considered (*i.e.*, Base Case and Extend Drought Scenarios).

- For the Design, Existing Aqueduct and Barona Arm Purified Water Inlet Locations, moving the purified water inlet location closer to the reservoir outlet is predicted to generally (but not always) result in slightly higher values in the reservoir outflow concentrations for both the decaying and 24-hour conservative tracers during the unstratified period. However, a minimum 2-log reduction for the decaying tracer and a minimum predicted dilution of 909 for the 24-hour conservative tracer are achieved under all scenarios considered (*i.e.*, Base Case and Extended Drought Scenarios). The lag times for the 24-hour conservative tracer range from 5 to 276 days.

- For the New Aqueduct Purified Water Inlet Location, the modeling shows higher peak concentration values for a 24-hour conservative tracer release in the reservoir outflow in the unstratified period than other purified water inlet locations due to its proximity to the reservoir outlet structure. The minimum achieved dilution is found to be about 385 for the Base Case and 200 for the Extend Drought scenario. The corresponding lag times are typically less than 2 days.

Table S-2. Simulations Conducted for Examining Various Purified Water Inlet Locations

Operating Scenario	Purified Water Inlet Location
Base Case	Design Purified Water Inlet Location
	New Aqueduct Purified Water Inlet Location
	Existing Aqueduct Purified Water Inlet Location
	Barona Arm Purified Water Inlet Location
Extended Drought	Design Purified Water Inlet Location
	New Aqueduct Purified Water Inlet Location

Table S-3. Summary of Simulation Results Using Various Purified Water Inlet Locations

Inlet Location	Operating Scenarios	Minimum Reduction for the Decaying Tracer	Lowest Minimum Dilution for 24-hour Conservative Tracers	Minimum Lag Time[1]
Design Purified Water Inlet Location	Base Case	2-log Reduction	2222	14 days
	Extended Drought	2-log Reduction	909	5 days
Existing Aqueduct Purified Water Inlet Location	Base Case	2-log Reduction	1000	10 days
Barona Arm Purified Water Inlet Location	Base Case	2-log Reduction	1923	39 days
New Aqueduct Purified Water Inlet Location	Base Case	Near 2-log Reduction	385	0.8 days
	Extended Drought	Near 2-log Reduction	196	1.3 days

Note: 1. The minimum lag time does not necessarily correspond to the 24-hour conservative tracer released that results in lowest minimum dilution

1. INTRODUCTION

1.1 BACKGROUND

San Vicente Reservoir (SVR) is located near Lakeside, California, and is used as a drinking water supply by the City of San Diego (City), its owner and operator (**Figure 1**). The reservoir currently has a capacity of about 90,000 acre-feet. It is undergoing an enlargement that will raise the dam by 117 feet and increase the reservoir's storage to 247,000 acre-feet at the spillway level (or 242,000 acre-feet at the maximum operation level).

A water reuse project, entitled Reservoir Augmentation, is being studied by the City. If implemented at full-scale, Reservoir Augmentation would bring advanced purified recycled water (*i.e.,* purified water) from the advanced water purification facility to SVR via a pipeline. The purified water would be blended with other water in the reservoir. The current project – the Water Purification Demonstration Project (Demonstration Project) – will not actually put any purified water into the reservoir; rather it will study and model the Reservoir Augmentation process. A component of the Demonstration Project is the Limnology and Reservoir Detention Study of San Vicente Reservoir (Limnology Study).

As part of the Limnology Study, Flow Science Incorporated (FSI) has developed a three-dimensional water quality model that is used to evaluate hydrodynamic and water quality effects of using purified water to augment SVR. After the model was developed, its results were compared to existing field data and documented in the Calibration Technical Memorandum (TM) submitted to the City in 2010 (FSI, 2010). The Calibration TM has been peer-reviewed by the National Water Research Institute Independent Advisory Panel (NWRIIAP) that was assembled for the review of the City's Demonstration Project. The model was deemed by NWRIIAP, with some fine-tuning, as "an effective and robust tool, for 1) simulating thermoclines and hydrodynamics of the San Vicente Reservoir; 2) assessing biological water quality for nutrients; 3) assessing options for the purified water inlet location" (NWRI, 2010). After the review, all the suggestions by NWRIIAP on fine-tuning the model have been addressed or implemented. Findings and results from the Calibration TM that are relevant to the work presented here are summarized in the next section.

This Technical Memorandum focuses on using the calibrated and validated SVR hydrodynamic model to evaluate the dilution, mixing, and circulation of the purified water in the expanded SVR under various projected reservoir operating scenarios. The detailed results include establishing dilution for purified water in the reservoir; assessing the potential for short-circuiting of purified water between the purified water inlet location and the dam outlet structure; and evaluating various potential purified water

reservoir inlet locations. This work has been performed by Flow Science Incorporated (FSI) of Pasadena, California, under contract to the City of San Diego, California. It is noted that another report that focuses on reservoir water quality (as opposed to hydrodynamics and mixing, which is the focus of this TM) within SVR will be forthcoming.

1.2 DESCRIPTION OF THE SVR MODEL

The three-dimensional SVR model consists of two coupled computer models that simulate both the hydrodynamics and water quality of SVR. These two models are the Estuary Lake and Coastal Ocean DYnamics Model (ELCOM) for hydrodynamic simulation and the Computational Aquatic Ecosystem DYnamics Model (CAEDYM) for water quality simulation. ELCOM requires the user to define boundary conditions, physical inputs, meteorological inputs, and bathymetry in a grid structure. The output from ELCOM consists of predictions for water velocities, temperature, salinity (*i.e.*, conductivity), and concentrations of decaying or conservative tracers in space and time within the body of water. CAEDYM is the water quality module that can be coupled to ELCOM. CAEDYM simulates changes in dissolved oxygen (DO), nutrients, organic matter, pH and chlorophyll *a*. ELCOM can be run independently of CAEDYM, as is the case for the work presented in this report, but CAEDYM requires the use of ELCOM. The coupled models are used to study the spatial and temporal relationships between physical, biological, and chemical variables in SVR. Details on ELCOM and CAEDYM can be found in **Appendix A**.

The modeling domain includes both the existing reservoir as well as the proposed expanded reservoir (**Figure 1**). A grid with a horizontal resolution of 50 × 50 m is used in this investigation – similar to the grid used in the calibration (**Figure 2**). A variable grid size was used in the vertical dimension with a grid size of 1.64 ft (0.5 m) near the surface and expanding in size with depth. This variable size grid enables the highest resolution in regions of steep gradients, while maintaining the execution time of the model within a reasonable span. The calibration was conducted for the two-year period of 2006 and 2007. The input data required by the calibration were either based on the measured data or derived from these data. ELCOM requires limited calibration effort in that the physical aspects of water movements in reservoirs are fairly well understood.

The calibrated model shows good agreement with the measured data for both water temperature and conductivity. The Calibration TM presents various comparisons between model and data. In the following, we discuss the highlights of the Calibration TM. For example, the onset and duration of thermal stratification as well as the deepening rate of the thermocline were predicted accurately by the model (**Figure 3**). In particular both the data and model show that winter water temperatures in the fully mixed reservoir are nearly uniform in the vertical direction at a value near 12 ^{o}C to 13 ^{o}C. By

April, increased solar radiation warms the water surface up to 17 ^{o}C to 18 ^{o}C and thermal stratification starts to develop. This process intensifies and by summer (July through September) the surface temperatures have risen to as high as 28 ^{o}C, while the temperature in the hypolimnion remains nearly unchanged at the winter temperature of 12 ^{o}C to 13 ^{o}C. This large temperature difference indicates that a strong vertical stratification is established in the lake. The thermocline is well defined and located at a depth ranging from 30 to 40 ft as shown in **Figure 3** for both the model and the data. In the fall, surface water temperatures steadily decrease due to reduced solar radiation. This generates convective plumes, which combined with more effective wind mixing, deepens the thermocline to a depth of 60 ft by November. The stratification continues to weaken until the reservoir totally destratifies and becomes fully mixed at the end of the year or beginning of the following year. The variation of conductivity in the reservoir was also well captured by the model (**Figure 4**).

After the model was calibrated, a validation was performed to compare the model against the results of previous tracer field studies. The field studies involved two separate episodes of tracer release in the reservoir (winter 1995 and summer 1995, FSI, 1995). The field studies clearly showed the impacts of stratification (or lack thereof) on the mixing and dispersion of the tracer. The ELCOM model was capable of replicating the main features of the tracer study (**Figures 5** and **6**). In particular, the model was capable of replicating the sinking of the inflow in the winter and its dispersion with time, as well as capturing the magnitude of the dilution (**Figure 5)**. In the summer, the model accurately predicted the insertion of the inflow at the level of the thermocline (**Figure 6)** and the gradual horizontal dispersion and dilution of the inflowing tracer. This validation provides verification and assurance that the model performance is reliable and accurate. Other results of the validation are discussed in the Calibration TM (FSI, 2010).

In conclusion, the SVR model is capable of replicating the stratification, concentration of tracers, as well as water movement in the reservoir. The simulation results are generally in good agreement with the field measurements. Thus the model provides "an effective and robust tool, for simulating thermoclines and hydrodynamics of the San Vicente Reservoir" and for "assessing options for the purified water inlet location" (findings from NWRIIAP, NWRI, 2010). The further ability of the model in "assessing biological water quality for nutrients" will be the subject of a subsequent Technical Memorandum.

1.3 HYDRODYNAMIC EFFECTS OF SVR EXPANSION

The existing SVR has a capacity of 90,000 acre-feet and is currently undergoing an expansion to 247,000 acre-feet that will be completed in 2013. The expanded SVR may then be used to store and dilute purified water from the advanced water purification facility. Thus, it is useful to study hydrodynamic changes due to the expansion prior to

adding purified water and understand the background conditions where purified water will be stored. This was accomplished by running a simulation that uses the same reservoir conditions (climate, inflow and outflow parameters etc.) as the 2006-2007 calibration simulation except for using a higher initial reservoir volume that is close to a full pool. The results from this simulation were compared against those from the original calibration simulation and differences between these two simulations were examined.

Figure 7 shows a comparison of water temperature for the existing reservoir (*i.e.*, the original calibration simulation) and the expanded reservoir (*i.e.*, the calibration simulation with a higher initial reservoir volume). The depth and deepening rate of the thermocline are fairly similar between these two simulations, indicating that the reservoir expansion will cause no major changes in the thickness of the epilimnion and the volume of the epilimnion is somewhat larger, but mostly because of the increase in surface area. However, the thickness and volume of the hypolimnion will be significantly larger for the expanded reservoir. With a larger hypolimnion, the expanded reservoir will destratify a few days later than the existing reservoir in the late fall.

Figure 8 shows a conductivity comparison between the existing and expanded reservoir. Note that conductivity is used to represent salinity in the reservoir throughout this report. As shown, the conductivity decreases in the spring of 2006 for the existing reservoir, a result of the low-conductivity levels from the Aqueduct inflow. For the expanded reservoir, the footprint of the low-conductivity Aqueduct inflow is attenuated in the early spring of 2006 because the Aqueduct inflow mixes with a significantly larger volume of water in the expanded reservoir. This shows that, compared to the existing reservoir, the expanded reservoir will provide a larger buffer that attenuates the effects of fluctuations in the inflow on the water quality in the reservoir. Other than in the spring of 2006, there is little difference in simulated conductivity between the expanded and existing reservoir.

In summary, the reservoir expansion is predicted to cause little change in the temperature, epilimnion depth and water conductivity in the reservoir but it will significantly enlarge the hypolimnion and provide a larger volume of water for dilution.

1.4 TECHNICAL MEMORANDUM ORGANIZATION

This TM provides a detailed description of hydrodynamic effects of discharging purified water into the reservoir, based on the SVR modeling results. **Chapter 2** of the report describes the study objectives and approach. **Chapter 3** presents details of the hydrodynamic simulation results. Conclusions and discussion are provided in **Chapter 4**.

2. STUDY OBJECTIVES AND APPROACH

2.1 STUDY OBJECTIVES

SVR provides a large volume of water for dilution of the repurified water, as well as a storage place where natural assimilation can occur. By holding water for several years on average, the reservoir acts as a settling basin, as well as provides a medium where potential pathogens can decay. In the case of potential spikes in concentration of chemical constituents in the purified water inflow resulting from "excursion events" at the advanced water purification facility, the reservoir also serves as an environmental barrier between the advanced water purification facility upstream and the drinking water treatment facility downstream. The reservoir acts as a barrier in two important ways. First, it offers a large volume of water for dilution and blending of incoming water. Second, the reservoir provides a lag time between the inflows and outflows.

The objectives of this study are to use the calibrated and validated SVR computer model to determine the effectiveness of SVR as an environmental buffer and barrier for purified water and to evaluate hydrodynamic changes in SVR induced by the addition of purified water. Specifically, answers to the following four questions are sought using the SVR model:

- Does purified water cause any hydrodynamic changes in the reservoir?
- Does the reservoir provide a robust year-round pathogen barrier?
- Does the reservoir provide substantial mixing and blending to reduce the effects of potential spikes in concentration of chemical constituents in the purified water inflow resulting from "excursion events" at the advanced water purification facility?
- Does the purified water inlet location within the reservoir affect the above findings?

2.2 APPROACH

To address the aforementioned questions, an analysis approach has been developed in conjunction with the City. It includes using decaying and conservative tracers as surrogates for pathogen and chemical constituents in the purified water to examine the fate and dilution of such constituents that flow into SVR. To achieve that, various tracers were added at specified times to the purified water inflow at a nominal concentration of 100. The movement of purified water in the reservoir is then visually illustrated by

following the contours of the tracer concentration. The dilution achieved by purified water at any location can be obtained by dividing the source tracer concentration (*i.e.*, 100) by the simulated tracer concentration at that location.

It is noted here that the released tracers employed in this study consisted of two types. The first type of tracer was used to simulate viral pathogens that are known to decay with time. As suggested by Welch (2011) and accepted by the NWRIIAP, a first-order exponential decay function with a decay rate of one log per month (half life = 9 days, or decay by a factor of 10 each month) was used to represent a reasonable and conservative method for estimating pathogen decay at SVR. The decaying tracer was continuously released in the purified water inflow at a nominal constant concentration of 100 throughout the whole two-year modeling period. A second type of tracer was used to simulate non-decaying constituents in the purified water that may inadvertently enter the reservoir as a result of a potential excursion event at the advanced water purification facility. In the simulation, such tracers were added to the reservoir's inflow over a 24-hour period and were considered to be conservative (that is, non-decaying). They are thus referred to as 24-hour conservative tracers hereafter.

The specific approaches and methodologies adopted to answer the four questions stated above are the following:

- Comparison of simulated reservoir water temperature and conductivity under various reservoir operation scenarios to examine hydrodynamic changes in the reservoir.

- Comparison of concentrations of the decaying tracer in the reservoir outflow under various reservoir operating scenarios to determine pathogen reduction in the reservoir outflow.

- Selecting critical dates during both the stratified and unstratified periods for the release of the 24-hour conservative tracer (*i.e.*, releasing a conservative tracer for 24 hour period) and then examining the corresponding concentrations and peaking times of these tracers in the reservoir outflow. This allows the calculation of the dilution and lag time provided by the reservoir.

- Comparison of concentrations of decaying and 24-hour conservative tracers in the reservoir outflow originating from different potential purified water inlet locations. This allows the optimal selection of the location where the purified water may be introduced in the reservoir.

3. SCENARIO MODELING RESULTS

In order to help understand the behavior of the reservoir in future conditions if purified water is introduced into SVR, several modeling scenarios were performed. The parameters for these modeling scenarios were determined in collaboration between the City, its consultants, and Flow Science, and based on information provided by the San Diego County Water Authority (SDCWA) about the expected operational schemes for SVR. Firstly, a Base Case simulation was performed to evaluate SVR under expected typical future conditions. This scenario considered a reservoir under median expected storage and normal expected operations. After that, a case was considered whereby no purified water is introduced in the reservoir, enabling a quantification of the effects of purified water addition on the reservoir behavior. Further scenarios were modeled to consider somewhat extreme operations: a scenario with an extended drought and another with emergency drawdown. All preceding operating scenarios utilized the Design Purified Water Inlet Location (see Figure 1 for the location) as the point of release for purified water flow into SVR. Port #2 at the reservoir outlet tower structure was used for all water withdrawals from the reservoir throughout this study. Finally, four alternate inlet locations for the purified water at SVR were evaluated. In the following, we discuss the results of each of these scenarios.

3.1 BASE CASE SCENARIO

The Base Case simulated a two-year period and used the same 2006-2007 meteorological data, Aqueduct inflow water quality data, and other modeling parameters as used in the Calibration, except for the initial reservoir volume, introduction of purified water, and modified inflow and outflow rates as discussed below. The real-world wind data used as inputs for the model included several Santa Ana Wind events that occurred in the winter of each simulated year. The City provided the initial reservoir volume, inflow and outflow rates for the Base Case. The initial reservoir volume for the Base Case is considered to be near the median of the expected future conditions with a volume of 155,000 acre-feet (determined in conjunction with SDCWA). It is considered that the daily flow for all inflows and outflows is constant throughout each month and that there are no water transfers from Sutherland Reservoir into SVR. A new surface inflow, purified water inflow, was added to represent incoming purified water from the advanced water purification facility at an annual rate of 15,000 acre-feet/year. The monthly inflow and outflow volumes for the Base Case are listed in **Table 1**. The purified water inlet for the Base Case is located at the "Design Purified Water Inlet Location" shown in **Figure 1**. As suggested by the City, the multi-year averages of weekly water temperatures at North City Water Reclamation Plant were used to characterize the purified water temperature (**Figure 9**). The salinity of the purified water was considered to be constant at 100 ppm. The available withdrawal elevations on the proposed reservoir outlet are

listed in **Table 2**. In all the simulations presented herein, Port #2 was used for all water withdrawals from the reservoir.

Table 1. Monthly Reservoir Inflow and Outflow Volumes for Base Case Operating Scenario

Month	Aqueduct Inflow (acre-feet)	Runoff Inflow (acre-feet)	Purified Water Inflow (acre-feet)	Withdrawal (acre-feet)
Jan-Year 1	0	0	1440	0
Feb-Year 1	0	1,500	1590	0
Mar-Year 1	0	1,500	1480	0
Apr-Year 1	1,000	1,500	1350	0
May-Year 1	1,000	0	1230	0
Jun-Year 1	1,000	0	1090	0
Jul-Year 1	0	0	900	2200
Aug-Year 1	0	0	1020	4200
Sep-Year 1	0	0	1090	4200
Oct-Year 1	0	0	1120	4200
Nov-Year 1	0	0	1210	4200
Dec-Year 1	0	0	1480	0
Jan-Year 2	0	0	1440	0
Feb-Year 2	0	1,500	1590	0
Mar-Year 2	0	1,500	1480	0
Apr-Year 2	1,000	1,500	1350	0
May-Year 2	1,000	0	1230	0
Jun-Year 2	1,000	0	1090	0
Jul-Year 2	0	0	900	2200
Aug-Year 2	0	0	1020	4200
Sep-Year 2	0	0	1090	4200
Oct-Year 2	0	0	1120	4200
Nov-Year 2	0	0	1210	4200
Dec-Year 2	0	0	1480	0

Table 2. Available Withdrawal Elevations on Proposed Reservoir Outlet Tower

Port	Withdrawal Elevation
6	733 ft
5	708 ft
4	683 ft
3	653 ft
2	623 ft
1	593 ft

Figure 10 shows time-sequenced profiles of simulated temperature and conductivity at Station A (see **Figure 1** for Station A location) for the Base Case. In general, simulated temperatures from the Base Case are similar to those from the Calibration (**Figure 3**) in terms of range of temperature and the development and vertical location of the thermocline. The main difference between the Base Case and the Calibration is the larger hypolimnion in the larger reservoir. The simulated conductivity values for the Base case vary between 740 and 820 µS/cm and are lower than those from the calibration (*i.e.*, 740 – 880 µS/cm). This reduction is mainly due to year-round inflow of purified water with relatively low conductivity.

Figure 11 presents contours of the temperature and decaying tracer along a profile path joining the Design Purified Water Inlet Location to the reservoir outlet near the dam (See **Figure 1** for the path). On the left hand side of **Figure 11** are three snapshots of the temperature contours on 7/1 and 11/30 of Year 1 as well as 1/8 of Year 2. On the right hand side of the figure are decaying tracer concentration contours on the same date. As shown in the top frame, a strong temperature stratification exists on 7/1. At that time, the highest concentrations of the decaying tracer are above the thermocline. This is a result of the fact that the purified water has a lower density than the ambient reservoir water (combination of elevated temperature and lower salinity than the ambient). The purified water initially flows near the surface and then is quickly mixed throughout the epilimnion. While there is some horizontal gradient in tracer concentration, the values above the thermocline are nearly uniform. As the thermocline deepens (11/30 of Year 1), the decaying tracer persists in the entire epilimnion albeit at a lower concentration (due to larger volume in the epilimnion). The concentrations of tracer in the hypolimnion are very low. When the lake completely destratifies (1/8 of Year 2), the decaying tracer concentration is nearly uniform throughout the reservoir. The animations in **Appendix B** show the above phenomena on a daily cycle. Note that the animations are not included in this copy of the report and the reader can contact the City to obtain the animations if needed.

Figure 12 shows the time series of simulated decaying tracer concentrations at all available withdrawal levels (*i.e.*, ports) at the reservoir outlet tower. It should be noted

that water was only withdrawn from Port #2 and the other ports were closed during the simulation. However, it is believed that concentrations sampled at the other ports (aside from Port #2) would approximately represent the reservoir outflow concentrations if that sampled port was open and actually used for withdrawal. Also note that the y-axis in **Figure 12** features a logarithmic scale. This means, for example, with the initial purified water tracer concentration set at 100, a reservoir outflow tracer concentration at 10^{-4} represents a 6-log reduction in concentration (*i.e.*, a million-fold reduction in concentration).

As shown in **Figure 12** and in the animations in **Appendix B**, Port #5, the shallowest port, is generally located inside the epilimnion in which the incoming purified water initially resides. The decaying tracer concentrations at Port #5 remain close to 1 (2-log reduction, this is equivalent to a 100:1 reduction) throughout the simulation period. At Port #1, the deepest port on the reservoir outlet tower, decaying tracer concentrations are generally similar to those at Port #5 during the destratified winter periods, but gradually decrease at the approximate rate of 1-log per month after the onset of stratification (when Port #1 is in the hypolimnion).

As discussed above, the thermocline in the summer months serves as a barrier to inhibit mixing between the epilimnion and hypolimnion. Thus the hypolimnion becomes isolated from the newly added purified water. As a result, hypolimnetic decaying tracer concentrations drop at a rate of 1-log per month throughout the stratified period. When the deepening thermocline reaches the elevation of Port #1 in late fall or early winter, tracer concentrations rise sharply to the level present in the epilimnion. The variation patterns of tracer concentrations at other ports are similar to those at Port #1. The main difference lies in the timing when the tracer concentrations start to rise: a shallower port exhibits an earlier rise in the decaying tracer concentrations in the fall. For reservoir outflow from Port #2, the simulation results show that decaying tracer achieves a 6-log reduction during the summer months and at least a 2-log reduction for the rest of the year.

Figure 13 shows the reservoir outflow concentrations of simulated releases of 24-hour conservative tracers. The tracer releases occurred on 2/1, 4/1, 7/1, 10/1 and 12/30 in the first year of the simulation period and each release lasted for 24 hours. The general trend for all tracers is that concentrations in the reservoir outflow remain very low until the thermocline reaches the level of Port #2. Subsequently, the concentrations rise quickly to a fixed level and stay near that level for the rest of the simulation period (the fixed concentration level can be estimated by considering that the tracer is well mixed in the layer above the port). Details on the maximum tracer concentration as well as the lag time to reach the maximum after release are listed in **Table 3**.

The maximum concentrations for all 24-hour conservative tracers released with purified water remain below 0.05 in the reservoir outflow, indicating a minimum dilution

of 2,000 prior to withdrawal at Port #2 (minimum dilution is computed as the initial concentration, 100 in this case, divided by the maximum observed concentration). The shortest lag time between the release of the 24-hour conservative tracer and peak reservoir outflow concentration (*i.e.*, lag time) is about 31 days and occurs for the tracer released on 12/30, Year 1, a period of reservoir destratification. The longest lag time is about 276 days and corresponds to the tracer released in early spring when the thermocline begins to form. This implies that the time it takes for purified water tracer to reach the reservoir outflow is more controlled by vertical mixing than by horizontal advection and dispersion.

Table 3. Summary of 24-hour Conservative Tracer Simulation Results for the Base Case

Date of Release	Reservoir Outflow Peak Tracer Concentration (%) / Minimum Dilution	Lag Time* (days)
2/1, Year 1	0.037 / 2703	49
4/1, Year 1	0.045 / 2222	276
7/1, Year 1	0.031 / 3226	185
10/1, Year 1	0.037 / 2703	93
12/30, Year 1	0.030 / 3333	31

Note: * Lag Time – time interval between the start of tracer release and occurrence of a concentration peak in the reservoir outflow at Port #2.

3.2 NO PURIFIED WATER SCENARIO

A scenario with no purified water addition was investigated. The inputs for this scenario are similar to those for the Base Case scenario, except for no purified water additions and an equal reduction in reservoir outflow volume. **Table 4** presents the monthly water volumes of inflows and outflow for the No Purified Water scenario. The purpose of conducting this simulation was, by comparing results with the Base Case, to evaluate the hydrodynamic effects of purified water addition on the expanded SVR.

Figures 14 and **15** show comparisons between the Base Case and No Purified Water scenarios for temperature and conductivity, respectively. Note that we use elevation as y-axis in all the figures hereafter to allow labeling the port elevations. The temperature patterns are fairly similar between these two scenarios with similar thermocline development patterns. However, note that the thermocline is slightly deeper for the Base Case (*e.g.*, less than 3 ft in September), a result of adding water in the epilimnion. Without addition of low-conductivity purified water, conductivity is higher for the No Purified Water scenario, especially in the epilimnion (**Figure 15**).

Table 4. Monthly Reservoir Inflow and Outflow Volumes for No Purified Water Scenario

Month	Aqueduct Inflow (acre-feet)	Runoff Inflow (acre-feet)	Purified Water Inflow (acre-feet)	Withdrawal (acre-feet)
Jan-Year 1	0	0	0	0
Feb-Year 1	0	1500	0	0
Mar-Year 1	0	1500	0	0
Apr-Year 1	1000	1500	0	0
May-Year 1	1000	0	0	0
Jun-Year 1	1000	0	0	0
Jul-Year 1	0	0	0	800
Aug-Year 1	0	0	0	800
Sep-Year 1	0	0	0	800
Oct-Year 1	0	0	0	800
Nov-Year 1	0	0	0	800
Dec-Year 1	0	0	0	0
Jan-Year 2	0	0	0	0
Feb-Year 2	0	1500	0	0
Mar-Year 2	0	1500	0	0
Apr-Year 2	1000	1500	0	0
May-Year 2	1000	0	0	0
Jun-Year 2	1000	0	0	0
Jul-Year 2	0	0	0	800
Aug-Year 2	0	0	0	800
Sep-Year 2	0	0	0	800
Oct-Year 2	0	0	0	800
Nov-Year 2	0	0	0	800
Dec-Year 2	0	0	0	0

3.3 EXTENDED DROUGHT AND EMERGENCY DRAWDOWN SCENARIOS

The Extended Drought scenario represents a hypothetical multi-year drought situation where a large and constant volume of water is withdrawn monthly from the reservoir without importing additional water (as compared to the Base Case) to refill the reservoir. **Table 5** lists the monthly inflow and outflow water volumes for this scenario while **Figure 16** shows an inflow and outflow rate comparison between this scenario and the

Base Case. Under the Extended Drought scenario, the volume of water stored in SVR decreases steadily throughout the modeling period from an initial 155,000 acre-feet to slightly below 100,000 acre-feet at the end of the simulation (**Figure 17**). This corresponds to a WSEL (water surface elevation) reduction from 710 ft to about 660 ft. In comparison, the volume of water stored in SVR for the Base Case remains above the initial volume of 155,000 acre-feet and reaches as high as about 170,000 acre-feet (WSEL of about 720 ft) in the middle of the simulation year (**Figure 17**).

Table 5. Monthly Reservoir Inflow and Outflow Volumes for the Extended Drought Scenario

Month	Aqueduct Inflow (acre-feet)	Runoff Inflow (acre-feet)	Purified Water Inflow (acre-feet)	Withdrawal (acre-feet)
Jan-Year 1	0	0	1440	4000
Feb-Year 1	0	1500	1590	4000
Mar-Year 1	0	1500	1480	4000
Apr-Year 1	1000	1500	1350	4000
May-Year 1	1000	0	1230	4000
Jun-Year 1	1000	0	1090	4000
Jul-Year 1	0	0	900	4000
Aug-Year 1	0	0	1020	4000
Sep-Year 1	0	0	1090	4000
Oct-Year 1	0	0	1120	4000
Nov-Year 1	0	0	1210	4000
Dec-Year 1	0	0	1480	4000
Jan-Year 2	0	0	1440	4000
Feb-Year 2	0	1500	1590	4000
Mar-Year 2	0	1500	1480	4000
Apr-Year 2	1000	1500	1350	4000
May-Year 2	1000	0	1230	4000
Jun-Year 2	1000	0	1090	4000
Jul-Year 2	0	0	900	4000
Aug-Year 2	0	0	1020	4000
Sep-Year 2	0	0	1090	4000
Oct-Year 2	0	0	1120	4000
Nov-Year 2	0	0	1210	4000
Dec-Year 2	0	0	1480	4000

The Emergency Drawdown scenario simulates a situation where a large volume of water is withdrawn from the reservoir in January and February of Year 2 and the reservoir is subsequently refilled by adding water from the Aqueduct between March and July in Year 2. The monthly inflow and outflow rates for this scenario are listed in **Table 6** and are plotted against flow rates from the Base Case and Extended Drought scenario in **Figure 16**. The volume of water stored in SVR over the two-year simulation period under this scenario (as well as the Base Case and Extended Drought) is plotted in **Figure 17**. Note that the initial volume of the Emergency Drawdown scenario is set at 200,000 acre-feet (WSEL of about 738 ft) compared to an initial volume for the Base Case and Extended Drought scenarios of 155,000 acre-feet (WSEL of about 710 ft). During the emergency drawdown period, the reservoir water volume is reduced to about 140,000 acre-feet (WSEL of 690 ft). It then climbs rapidly to above 200,000 acre-feet during the refill period.

The purified water inlet location used for both the Extended Drought and Emergency Drawdown scenarios is the "Design Purified Water Inlet Location" (see **Figure 1**), the same as that for the Base Case.

A comparison of simulated water temperature between the Base Case, Extended Drought, and Emergency Drawdown scenarios is shown in **Figure 18**. All three scenarios have a generally similar epilimnion thickness and thermocline deepening rate. A notable exception is the emergence of a thick epilimnion for the Emergency Drawdown scenario in the spring of the second year, a result of the influx of a large amount of inflow into the epilimnion in a short period of time. Since the epilimnion thickness is generally unchanged amongst these three scenarios, the *elevation* of the thermocline is mostly determined by the WSEL. For example, as a result of the steady decrease in WSEL for the Extended Drought scenario, the thermocline reaches the elevation of Port #2 in early September in Year 2 compared to mid-October for the Base Case. For the Emergency Drawdown scenario, the thermocline reaches the elevation of Port #2 in mid-December, a result of the higher WSEL.

A comparison of simulated conductivity between the Base Case, Extended Drought, and Emergency Drawdown scenarios is shown in **Figure 19**. Note that the values of conductivity in the purified water are lower than those in the Aqueduct water. Thus, the levels of conductivity in the reservoir are elevated in Year 2 of the Emergency Drawdown scenario compared to the other two scenarios, a result of using a large volume of Aqueduct water to refill the reservoir after the emergency drawdown. During the rest of simulation period, the conductivity is fairly similar among these three scenarios.

Table 6. Monthly Reservoir Inflow and Outflow Volumes for the Emergency Drawdown Scenario

Month	Aqueduct Inflow (acre-feet)	Runoff Inflow (acre-feet)	Purified Water Inflow (acre-feet)	Withdrawal (acre-feet)
Jan-Year 1	0	0	1440	0
Feb-Year 1	0	1500	1590	0
Mar-Year 1	0	1500	1480	0
Apr-Year 1	1000	1500	1350	0
May-Year 1	1000	0	1230	0
Jun-Year 1	1000	0	1090	0
Jul-Year 1	0	0	900	2200
Aug-Year 1	0	0	1020	4200
Sep-Year 1	0	0	1090	4200
Oct-Year 1	0	0	1120	4200
Nov-Year 1	0	0	1210	4200
Dec-Year 1	0	0	1480	0
Jan-Year 2	0	0	1440	33000
Feb-Year 2	0	1500	1590	33000
Mar-Year 2	19000	1500	1480	0
Apr-Year 2	15000	1500	1350	0
May-Year 2	12000	0	1230	0
Jun-Year 2	12000	0	1090	0
Jul-Year 2	11000	0	900	2200
Aug-Year 2	0	0	1020	4200
Sep-Year 2	0	0	1090	4200
Oct-Year 2	0	0	1120	4200
Nov-Year 2	0	0	1210	4200
Dec-Year 2	0	0	1480	0

Figure 20 shows a comparison of decaying tracer concentrations in the reservoir outflow at Port #2 between the Base Case, Extended Drought and Emergency Drawdown scenarios. In general, all three scenarios show many similarities: tracer concentrations are highest during the destratified winter period with at least a 2-log reduction, steadily decreasing in the summer due to decay, and rise sharply once the thermocline reaches the elevation of the reservoir outlet port. The main difference between these scenarios is the timing of the rise in reservoir outflow tracer concentration. As discussed previously, the

timing of the thermocline reaching the open reservoir outlet mainly depends on the WSEL: the higher the WSEL, the later is the rise. As such, the Extended Drought scenario has the earliest rise, followed by the Base Case then the Emergency drawdown scenario.

Simulated 24-hour conservative tracer concentrations in the reservoir outflow are shown in **Figures 21** and **22** for the Extended Drought and Emergency Drawdown scenarios respectively. It should be noted that the release dates of the 24-hour conservative tracers for these two scenarios are different from those for the Base Case. The selection of 24-hour conservative tracer release dates for these scenarios was based on identifying critical periods in which the highest reservoir outflow concentrations are most likely to occur (the timings for the 24-hour conservative tracer release for the Base Case were distributed more evenly over the year). From our understanding of the variations in 24-hour conservative tracer release concentrations in the Base Case, the critical periods are most likely to occur when the reservoir is near to, or fully, mixed and the water volume in the reservoir is at the lowest. In addition, Santa Ana winds, a wind event where strong and extremely dry east and northeast winds prevail in Southern California, are expected to rapidly drive purified water introduced at the east side of the reservoir directly toward the reservoir outlet located near the west end of the reservoir. Such an event could minimize dilution and lag time between the time when the water enters the reservoir and the time it reaches the reservoir outlet. Thus, the most critical periods are expected to meet the following three conditions: 1) the reservoir is almost or fully mixed vertically; 2) the reservoir water volume is at a minimum; and 3) the occurrence of Santa Ana wind events.

FSI conducted an analysis of meteorological data at SVR to identify Santa Ana wind events. Based on the analysis and the discussion above, the six 24-hour conservative tracer release dates were considered to be: 12/2 of Year 1, 1/6, 1/14, 1/21, 11/29 and 12/2 of Year 2 for the Extended Drought scenario (note that two release dates at the end of Year 2 were chosen for this scenario due to the lower WSEL at the end of Year 2). For the Emergency Drawdown scenario the dates were 12/2 of Year 1, 1/6, 1/14, 1/21, 2/20 and 2/25 of Year 2.

Figures 21 and **22** present simulated reservoir outflow concentrations for all 24-hour conservative tracer releases. The results are also summarized in **Tables 7** and **8**. For the Extended Drought scenario, the maximum observed concentrations at the outflow range from about 0.03 to 0.11, reflecting a minimum dilution range between 900 and 2,700. The smallest dilution occurs for the 24-hour conservative tracer released on 12/2 of Year 2 when the reservoir volume is near the low end of the range. The lag time ranges from 5 to 25 days. For the Emergency Drawdown scenario, the maximum observed concentrations at the outflow range from about 0.03 to 0.07, reflecting a minimum dilution of about 1,400 to 3,000. The lag time ranges from 8 to 120 days.

Table 7. Summary of 24-hour Conservative Tracer Simulation Results for the Extended Drought Scenario

Date of Release	Reservoir Outflow Peak Tracer Concentration (%) / Minimum Dilution	Lag Time* (days)
12/2, Year 1	0.077 / 1299	11
1/6, Year 2	0.034 / 2941	25
1/14, Year 2	0.037 / 2703	37
1/21, Year 2	0.058 / 1724	8
11/29, Year 2	0.11 / 909	5
12/2, Year 2	0.11 / 909	9

Note: * Lag Time – time interval between the start of tracer release and occurrence of tracer concentration peak in the reservoir outflow at Port #2.

Table 8. Summary of 24-hour Conservative Tracer Simulation Results for the Emergency Drawdown Scenario

Date of Release	Reservoir Outflow Peak Tracer Concentration (%) / Minimum Dilution	Lag Time* (days)
12/2, Year 1	0.043 / 2326	31
1/6, Year 2	0.023 / 4348	33
1/14, Year 2	0.025 / 4000	32
1/21, Year 2	0.042 / 2381	8
2/20, Year 2	0.072 / 1388	8
2/25, Year 2	0.031 / 3226	120

Note: * Lag Time – time interval between the start of tracer release and occurrence of tracer concentration peak in the reservoir outflow at Port #2.

3.4 COMPARISON OF VARIOUS PURIFIED WATER INLET LOCATIONS

All simulations discussed prior to this section utilized the "Design Purified Water Inlet Location" as the point of release for purified water flow into SVR. This section focuses on evaluating other potential purified water inlet locations and investigating the location impact on dilution and mixing under different reservoir operating scenarios. A total of four purified water inlet locations were considered under the Base Case operating scenario. Two of these four locations were further evaluated under the Extended Drought operating scenario.

3.4.1 Evaluation Under Base Case Operating Conditions

Four purified water inlet locations were considered under the Base Case operating scenario. These are: Design Purified Water Inlet Location, Existing Aqueduct Purified Water Inlet Location, New Aqueduct Purified Water Inlet Location, and Barona Arm Purified Water Inlet Location. These four locations are illustrated in **Figure 23**. As shown, the Barona Arm Purified Water Inlet Location is the furthest from the reservoir outlet and the New Aqueduct Purified Water Inlet Location is the nearest to the reservoir outlet.

A comparison of decaying tracer reservoir outflow concentrations for tracers released into these four purified water inlet locations is shown in **Figure 24**. The decaying tracer concentrations in the reservoir outflow are fairly similar for all purified water inlet locations. The Barona Arm Purified Water Inlet Location, the furthest from the reservoir outlet, produces slightly lower reservoir outflow tracer concentrations than the other three purified water inlet locations. On the other hand, the New Aqueduct Purified Water Inlet Location, the release point nearest to the reservoir outlet, produces slightly higher reservoir outflow concentrations than the other three. Overall, the differences in reservoir outflow concentrations between different purified water inlet locations are relatively small. All purified water inlet locations can achieve a 6-log reduction in concentration in the summer months and near a 2-log reduction in the destratified period.

Comparison of the 24-hour conservative tracer concentrations in the reservoir outflow for releases at various purified water inlet locations are presented in **Figures 25 – 30** and results are summarized in **Table 9**. **Figure 25** shows that, for a 24-hour conservative tracer released during the destratified period, the New Aqueduct Purified Water Inlet Location features the shortest lag time for the tracer to reach the reservoir outlet. Furthermore, the New Aqueduct Purified Water Inlet location has the highest concentration and lowest minimum dilution at the reservoir outlet. It is noted, however, that the minimum dilution for the New Aqueduct Purified Water Inlet location is over 1,200 (maximum concentration of 0.08).

For releases between April and October, the purified water inlet location has very little effect on the 24-hour conservative tracer concentration at the reservoir outlet, as shown in **Figures 26 – 28**. This finding is a result of the thermocline isolating the reservoir outflow from the purified water during the stratified season regardless of the purified water inlet location. The 24-hour conservative tracers released during the summer do not reach the reservoir outflow until the following late fall when the reservoir is nearly well mixed.

For the 1/5 and 1/15 of Year 2 tracer releases, the results shown in **Figures 29** and **30** indicate that the New Aqueduct Purified Water Inlet Location features the highest

concentrations and lowest minimum dilutions, followed by the Existing Aqueduct Purified Water Inlet Location, Design Purified Water Inlet Location, and Barona Arm Purified Water Inlet Location. Note that the main differences between the various scenarios during these unstratified periods occur in the first few days after tracer release.

As indicated in **Table 9**, minimum dilutions achieved in the reservoir outflow for these releases range from 385 to 3,448 and the lag times vary from 0.8 to 276 days. The purified water inlet location nearest to the reservoir outlet, the New Aqueduct Purified Water Inlet Location, produces the highest peak concentration (*i.e.*, 0.26, corresponding to a dilution of 385) in the reservoir outflow and the peak reaches the reservoir outflow within two days.

Table 9. Summary of 24-hour Conservative Tracer Simulation Results for Various Purified Water Inlet Locations Under Base Case Conditions

Date of Release	Design Purified Water Inlet Location		Existing Aqueduct Purified Water Inlet Location		New Aqueduct Purified Water Inlet Location		Barona Arm Purified Water Inlet Location	
	C/D*	LT**	C/D	LT	C/D	LT	C/D	LT
1/30 Year 1	0.030 / 3333	51	0.038/ 2632	27	0.081/ 1235	0.8	0.033/ 3030	39
4/1 Year 1	0.045 / 2222	276	0.038/ 2632	275	0.042/ 2381	271	0.052/ 1923	271
7/1 Year 1	0.036 / 2778	178	0.034/ 2941	180	0.032/ 3125	182	0.037/ 2703	180
10/1 Year 1	0.037/ 2703	93	0.041/ 2439	88	0.038/ 2632	87	0.045/ 2222	88
1/5 Year 2	0.033/ 3030	17	0.10/ 1000	10	0.26/ 385	1.5	0.030/ 3333	87
1/15 Year 2	0.031/ 3226	14	0.079/ 1266	10	0.13/ 769	0.8	0.029/ 3448	188

Note: * C/D – Reservoir outflow peak tracer concentration (%) / Minimum Dilution
** LT –lag time in days between the start of tracer release and occurrence of tracer concentration peak in the reservoir outflow Port #2.

3.4.2 Evaluation Under the Extended Drought Operating Conditions

The Design Purified Water Inlet Location and the New Aqueduct Purified Water Inlet Locations were further evaluated under the Extended Drought Operating Scenario. **Figure 31** shows a comparison of reservoir outflow decaying tracer concentrations for

tracer releases at these two purified water inlet locations. In general, the concentrations are fairly similar, but as expected the New Aqueduct Purified Water Inlet Location (location nearest to the reservoir outlet) produces slightly higher concentrations overall.

Figures 32-37 show comparisons of the 24-hour conservative tracer in the reservoir outflow for these two locations. The results are also summarized in **Table 10**. As shown in **Table 10,** the maximum concentrations are higher (and minimum dilutions therefore lower) for the New Aqueduct Purified Water Inlet Location. The maximum concentration and minimum dilution at the reservoir outlet are about 0.51 and 196, respectively, and occur for the 24-hour tracer release on 12/2, Year 2. It is noted that several days after release, any effect of the purified water inlet location has become negligible. Also note that in this analysis, all the purified water 24-hour conservative tracers were released in the destratified period. It is expected that little differences in dilutions between purified water inlet locations would be observed for 24-hour conservative tracers released in the stratified period.

Table 10. Summary of 24-hour Conservative Tracer Simulation Results for Various Purified Water Inlet Locations under the Extended Drought Conditions

Date of Release	Design Purified Water Inlet Location		New Aqueduct Purified Water Inlet Location	
	C/D*	LT**	C/D	LT
12/2, Year 1	0.077 /1299	11	0.15 /667	6
1/6, Year 2	0.034 /2941	25	0.19 /526	1.5
1/14, Year 2	0.037 /2703	37	0.25 /400	1.8
1/21, Year 2	0.058 /1724	8	0.24 /417	1.8
11/25, Year 2	0.11 /909	5	0.47 /213	2.5
12/2, Year 2	0.11 /909	9	0.51 /196	1.3

Note: * C/D – Reservoir outflow peak tracer concentration (%) / Minimum Dilution
** T – time lag in days between the start of tracer release and occurrence of tracer concentration peak in the reservoir outflow at Port #2.

4. CONCLUSIONS

The objectives of this study were to use the calibrated and validated SVR computer model to determine the effectiveness of SVR as an environmental buffer and barrier for purified water introduced into SVR, and to evaluate any hydrodynamic changes in SVR induced by the purified water. To achieve these goals, reservoir simulations were conducted to evaluate a number of proposed future reservoir operating scenarios.

First, the model was used to determine the impacts of reservoir expansion on mixing and dilution in the reservoir, without the introduction of any purified water. The model was then used to investigate the effects of the purified water addition on the general hydrodynamics of the reservoir for several different operational scenarios:

- Base Case ---- This scenario considered a reservoir under median expected storage and normal expected operations. The initial reservoir volume for the Base Case is set at 155,000 acre-feet. The annual flow rates for Aqueduct inflow, Runoff, purified water inflow and dam withdrawal are 3,000, 4,500, 15,000 and 19,000 acre-feet/year respectively. There are no water transfers from Sutherland Reservoir into SVR.

- No Purified Water ---- The inputs for this scenario are similar to those for the Base Case scenario, except for no purified water additions and an equal reduction in reservoir outflow. The initial reservoir volume for this scenario is set at 155,000 acre-feet. The annual flow rates for Aqueduct inflow, Runoff, purified water inflow and dam withdrawal are 3,000, 4,500, 0 and 4,000 acre-feet/year respectively. There are no water transfers from Sutherland Reservoir into SVR.

- Extended Drought ---- This scenario represents a hypothetical two-year drought situation where a large and constant volume of water is withdrawn monthly from the reservoir without importing additional water (as compared to the Base Case) to refill the reservoir. The initial reservoir volume for this scenario is set at 155,000 acre-feet. The annual flow rates for Aqueduct inflow, Runoff, purified water inflow and dam withdrawal are 3,000, 4,500, 15,000 and 48,000 acre-feet/year respectively. There are no water transfers from Sutherland Reservoir into SVR. The volume of water stored in SVR at the end of the two-year simulation period is about 100,000 acre-feet.

- Emergency Drawdown ---- The Emergency Drawdown scenario simulates a situation where a total of 66,000 acre-feet water is withdrawn from the reservoir in January and February of Year 2 and the reservoir is subsequently refilled by adding 66,000 acre-feet water from the Aqueduct between March

and July in Year 2. The rest of flow rates for all inflows and outflows are the same as the Base Case. The initial reservoir volume for this scenario is set at 200,000 acre-feet.

Note that all preceding simulations utilized the Design Purified Water Inlet Location as the point of release of purified water flow into SVR. Port #2 was used for all water withdrawals from the reservoir throughout this investigation.

In these simulations various hypothetical tracers were added to the purified water inflow to illustrate the transport and mixing of the purified water within the reservoir. In particular, decaying tracers (decay rate of 1 log per month, *i.e.*, a reduction in concentration by a factor of 10 per month) were used to study the dilution and inactivation of potential pathogens entering the reservoir and to evaluate the ability of the reservoir to reduce pathogen concentrations before they reach the reservoir outlet. The decaying tracer was continuously released with the purified water inflow at a constant concentration throughout the entire modeling period. In addition, hypothetical conservative (that is, non-decaying) tracers were added to the purified water inflow in order to simulate the potential effects of elevated concentrations of chemical constituents in the purified water entering SVR after "excursion events" at the water purification facility. These conservative tracers were tracked to determine the dilution and lag time provided by the reservoir (*i.e.*, the time interval between the release of the tracer and peak reservoir outflow concentration). In all simulations, such tracers were added to the reservoir's inflow over a 24-hour period and were thus referred to as 24-hour conservative tracers.

Finally, various purified water inlet locations were also evaluated under various operating conditions to examine the effects of varying the purified water inlet location. A total of four different purified water inlet locations were considered under the Base Case operating scenario. These are: the Design Purified Water Inlet Location, Existing Aqueduct Purified Water Inlet Location, New Aqueduct Purified Water Inlet Location, and Barona Arm Purified Water Inlet Location. The Design and New Aqueduct Purified Water Inlet Locations were further evaluated under the Extended Drought operating scenario.

Based on the simulation results, the following conclusions and observations are made:

GENERAL CONCLUSIONS ON RESERVOIR EXPANSION

- The expanded reservoir is predicted to start stratifying in about March of each year. In the spring and summer, the stratification will intensify. In the fall, the thermocline will start deepening appreciably until the reservoir becomes fully mixed in late fall or early winter. As a result, the reservoir is predicted

to be stratified from about March to December, and will be destratified from December to February.

- Reservoir expansion will increase the volume of the hypolimnion but will have a negligible effect on the thermocline depth when the reservoir is stratified. Both surface and bottom reservoir temperatures are expected to remain unchanged due to increased water depth.

CONCLUSIONS FOR BASE CASE (DESIGN PURIFIED WATER INLET LOCATION)

- Under the Base Case scenario, the addition of purified water in the expanded reservoir is predicted to slightly deepen the thermocline (*e.g.,* by less than 3 ft in September) and reduce conductivity in the reservoir (compared to the Calibration Run).

- The purified water generally has a lower density (lower conductivity and higher temperature) than the ambient reservoir water. This will cause the purified water to initially spread along the surface of the reservoir near the purified water inlet location. In the stratified reservoir period (typically March to December), the purified water will rapidly mix within the entire epilimnion. As the thermocline gradually deepens, the purified water will gradually approach successively lower ports on the reservoir outlet tower.

- In the unstratified period (December to February), the purified water is predicted to initially flow along the reservoir's surface, but then it will quickly mix over the entire depth, achieving rapid dilution over the entire reservoir volume.

- The proposed withdrawal strategy at SVR will generally utilize deeper ports (Port #2 was considered to be the open port throughout this investigation). Since the purified water will generally flow into the reservoir above the thermocline in the stratified period, it is predicted to typically take several weeks or months for newly released purified water to appear at the reservoir outlet, after undergoing large dilution (*i.e.*, achieving a dilution of at least 2,000). In the reservoir destratified period, the simulations indicate that the purified water can appear at the reservoir outlet within days or weeks after release, but only after undergoing significant dilution (*i.e.*, achieving a dilution of at least 2,000).

- For a decaying tracer released with the purified water (a surrogate for pathogens), the reservoir outflow from the reservoir is predicted to achieve at least a 2-log reduction[2] (100:1 reduction in concentration) in the unstratified period. In the stratified period, the reservoir will provide significantly higher reductions (as high as 9 logs; that is, a 1 trillion reduction).

- For a 24-hour conservative tracer that enters the reservoir the simulations indicate that a dilution of at least 2,000 can be obtained in the reservoir outflow.

CONCLUSIONS FOR EXTENDED DROUGHT & EMERGENCY DRAWDOWN SCENARIOS (DESIGN PURIFIED WATER INLET LOCATION)

- For a decaying tracer in the purified water inflow under the Extended Drought scenario, the analyses indicate that the reservoir can achieve a 2-log reduction in tracer concentration in the unstratified period and significantly higher values (typically 4-8 log reduction) for the remainder of the year. The minimum predicted dilution and its corresponding lag time for a 24-hour conservative tracer are about 900 and 5 days, respectively, and occurs at the end of Year Two when the reservoir volume is lowest.

- For a decaying tracer in the purified water inflow under the Emergency Drawdown scenario, the results indicate that the reservoir can achieve a 2-log reduction in the unstratified period and significantly higher values (typically 4-10 log reduction) for the remainder of the year. The minimum predicted dilution and its corresponding lag time for a 24-hour conservative tracer are about 1,400 and 8 days, respectively. The minimum predicted dilution here is higher than those obtained from both the Base Case and the Extended Drought scenarios, a result of the larger reservoir volume considered in the Emergency Drawdown Scenario during the winter months.

[2] A log reduction is defined as a 10-fold reduction.

EFFECT OF THE PURIFIED WATER INLET LOCATION

- In the stratified season, utilizing different inlet locations to introduce purified water into SVR is predicted to have little effect on both the decaying and 24-hour conservative tracer concentrations in the reservoir outflow under all scenarios considered (*i.e.*, Base Case and Extend Drought Scenarios).

- For the Design, Existing Aqueduct and Barona Arm Purified Water Inlet Locations, moving the purified water inlet location closer to the reservoir outlet is predicted to generally (but not always) result in slightly higher values in the reservoir outflow concentrations for both the decaying and 24-hour conservative tracers during the unstratified period. However, a minimum 2-log reduction for the decaying tracer and a minimum predicted dilution of 909 for the 24-hour conservative tracer are achieved under all scenarios considered (*i.e.*, Base Case and Extended Drought Scenarios). The lag times for the 24-hour conservative tracer range from 5 to 276 days.

- For the New Aqueduct Purified Water Inlet Location, the modeling shows higher peak concentration values for a 24-hour conservative tracer release in the reservoir outflow in the unstratified period than other purified water inlet locations due to its proximity to the reservoir outlet structure. The minimum achieved dilution is found to be about 385 for the Base Case and 200 for the Extend Drought scenario. The corresponding lag times are typically less than 2 days.

5. REFERENCES

City of San Diego (2008). "IPR Description for BOR Grant 122208 MS," obtained from Jeffery Pasek of the City of San Diego through e-mail on December 23, 2008.

Flow Science Incorporated (1995). "San Vicente Water Reclamation Project: Results of Tracer Studies, prepared for Montgomery Watson", FSI Project No. P941003, Pasadena, CA.

Flow Science Incorporated (2010). "Reservoir Augmentation Demonstration Project: Limnology and Reservoir Detention Study of San Vicente Reservoir – Calibration of the Water Quality Model", FSI Project No. V094005, Pasadena, CA.

National Water Research Institute (2010). "Findings and Recommendations of the Limnology and Reservoir Subcommittee Meeting for the Reservoir Augmentation Demonstration Project's 'Limnology and Reservoir Detention Study of the San Vicente Reservoir' " Memorandum from NWRI Independent Advisory Panel for the City of San Diego's Indirect Potable Reuse/Reservoir Augmentation Demonstration Project, June 7, 2010.

Welch, M.R. (2011). "Potential Pathogen Inactivation at San Vicente Reservoir", dated May, 2011 and submitted to the City of San Diego.

6. GLOSSARY

Advanced Water Purification Facility: The demonstration facility located at the North City Water Reclamation Plant. The facility is considered "advanced" because of the high level of treatment utilizing reverse osmosis and advanced oxidation.

Blending: Mixing or combining one water source with another such as purified water with raw water sources.

Conductivity: see "Salinity".

Constituent: In water, a constituent is a dissolved chemical element or compound or a suspended material that is carried in the water.

Drought: A defined period of time when rainfall and runoff in a geographic area are much less than average.

Epilimnion: Natural thermal stratification exists for much of the year in almost all temperate lakes and reservoirs and creates three vertical zones. The upper, warmer water is called the epilimnion, the deeper, colder water is called the hypolimnion, whereas the middle portion separating these two layers, where the rate of vertical temperature change is greatest, is called the metalimnion, or thermocline.

Excursion events at the advanced purification facility: Events in which the water quality of the recycled water into the advanced purification facility deviates from the normal or expected conditions. They result in that the final outflow from the advanced purification facility may contain chemical constituents at higher level than normal concentrations when no such events occur.

Hypolimnion: see "epilimnion".

Pathogens: Disease-causing organisms. The general groupings of pathogens are viruses, bacteria, protozoa, and fungi.

Periods of mixing: Periods when water temperatures become vertically uniform in the water body and they generally occur in the winter.

Purified water: Recycled water that has been treated to an advanced level beyond tertiary treatment, so that it can be added to water supplies ultimately used for drinking water. The treatment includes membrane filtration with microfiltration or ultrafiltration, reverse osmosis (RO), and advanced oxidation that consists of disinfection with

ultraviolet light (UV) and hydrogen peroxide (H_2O_2). Purified water may be released into a groundwater basin or surface water reservoir that supplies water to a drinking water treatment facility.

Purified water inflow: Purified water that is transported from the advanced purified water treatment facility to the SVR.

Purified water inlet: Point of release in the SVR for purified water inflow. Note that the purified water is assumed to be released at the surface of the SVR.

Recycled water: Water that originated from homes, businesses and drains as municipal wastewater and has undergone a high level of treatment at a reclamation facility so that it can be beneficially reused for a variety of purposes. This is the water that comes into the AWP Facility.

Reservoir: A manmade lake or tank used to collect and store water.

Reservoir augmentation: The process of adding purified water to a surface water reservoir. The purified water undergoes advanced treatment (membrane filtration, reverse osmosis and UV disinfection/advanced oxidation). The purified water is then blended with untreated water in a reservoir. The blended water is then treated and disinfected at a conventional drinking water treatment plant and is distributed into the drinking water delivery system. Also known as "surface water augmentation."

Reservoir outflow: The flow withdrawal through the opening port located at the outlet structure near the dam.

Reservoir outlet: The opening port at the outlet structure near the dam. In this study, the opening port is assumed to be Port #2.

Salinity: The concentration of mineral salts dissolved in water. Salinity may be measured by weight (total dissolved solids or TDS) or by electrical conductivity. Salinity and TDS are both measures of the amount of salt dissolved in water, and the terms are often used interchangeably. Generally, salinity is used when referring to water with a lot of salt (*e.g.*, seawater), whereas TDS is used to refer to water with little salt (*e.g.*, freshwater).

Storage: Water held in a reservoir for later use.

Surface water: Water located on the Earth's surface, in a river, stream, lake, pond or surface water reservoir.

Thermocline: see "epilimnion".

Water Purification Demonstration Project (Demonstration Project): The second phase of the City of San Diego's Water Reuse Program. During this test phase the Advanced Water Purification Facility will operate for approximately one year and will produce 1 million gallons of purified water per day. A study of the San Vicente Reservoir is being conducted to test the key functions of reservoir augmentation and to determine the viability of a full-scale project. No purified water will be sent to the reservoir during the demonstration phase.

Water Measurement Terms

Milligrams per liter (mg/L) ***also known as parts per million (ppm):*** A measurement describing the amount of a substance (such as a mineral, chemical or contaminant) in a liter of water; a unit used to measure concentration of water constituents (parts of something per million parts of water). One part per million is equal to one milligram per liter. (This term is becoming obsolete as instruments measure smaller concentrations.) This is equivalent to one drop of water diluted into 50 liters (roughly the fuel tank capacity of a compact car) or about thirty seconds out of a year.

Acre-foot (AF): A unit of water commonly used in the water industry to measure large volumes of water. It equals the volume of water required to cover one acre to a depth of one foot. An acre-foot is 325,851 gallons (43,560 cubic feet) and is considered enough water to meet the needs of two families of four with a house and yard for one year.

µS/cm: A basic unit of water conductivity. It stands for microSiemens per meter. Distilled water has a conductivity in the range of 0.5 to 3 µS/cm. The conductivity of rivers in the United States generally ranges from 50 to 1500 µS/cm.

FIGURES

Map of San Vicente Reservoir

Plan View of Existing and Expanded Reservoir and Inflow/Outflow Locations

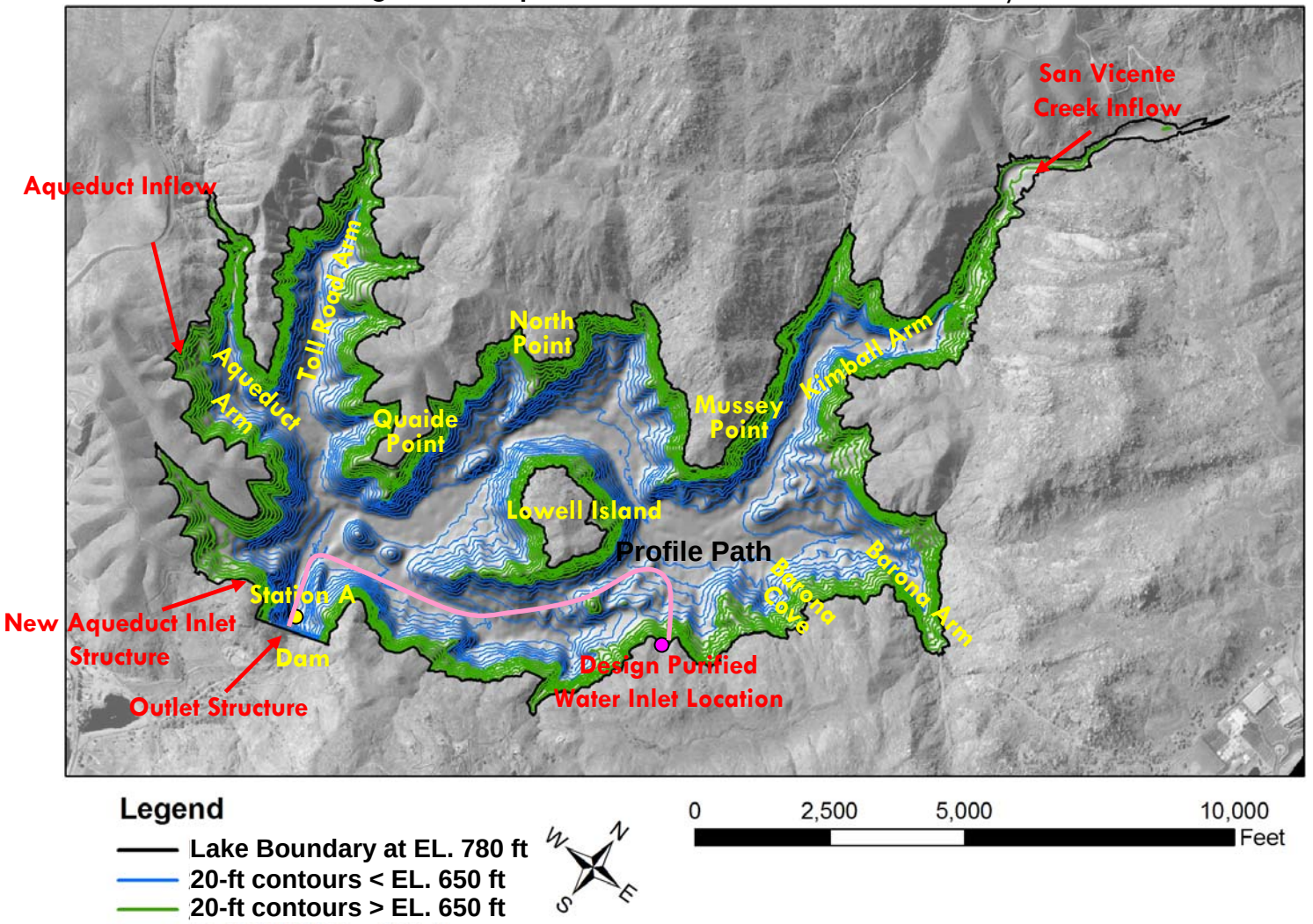

FSI V094005
May 01, 2012

Figure 1

FLOW SCIENCE®

SVR Hydrodynamic Model Grid

(Grid Size = 50 m)

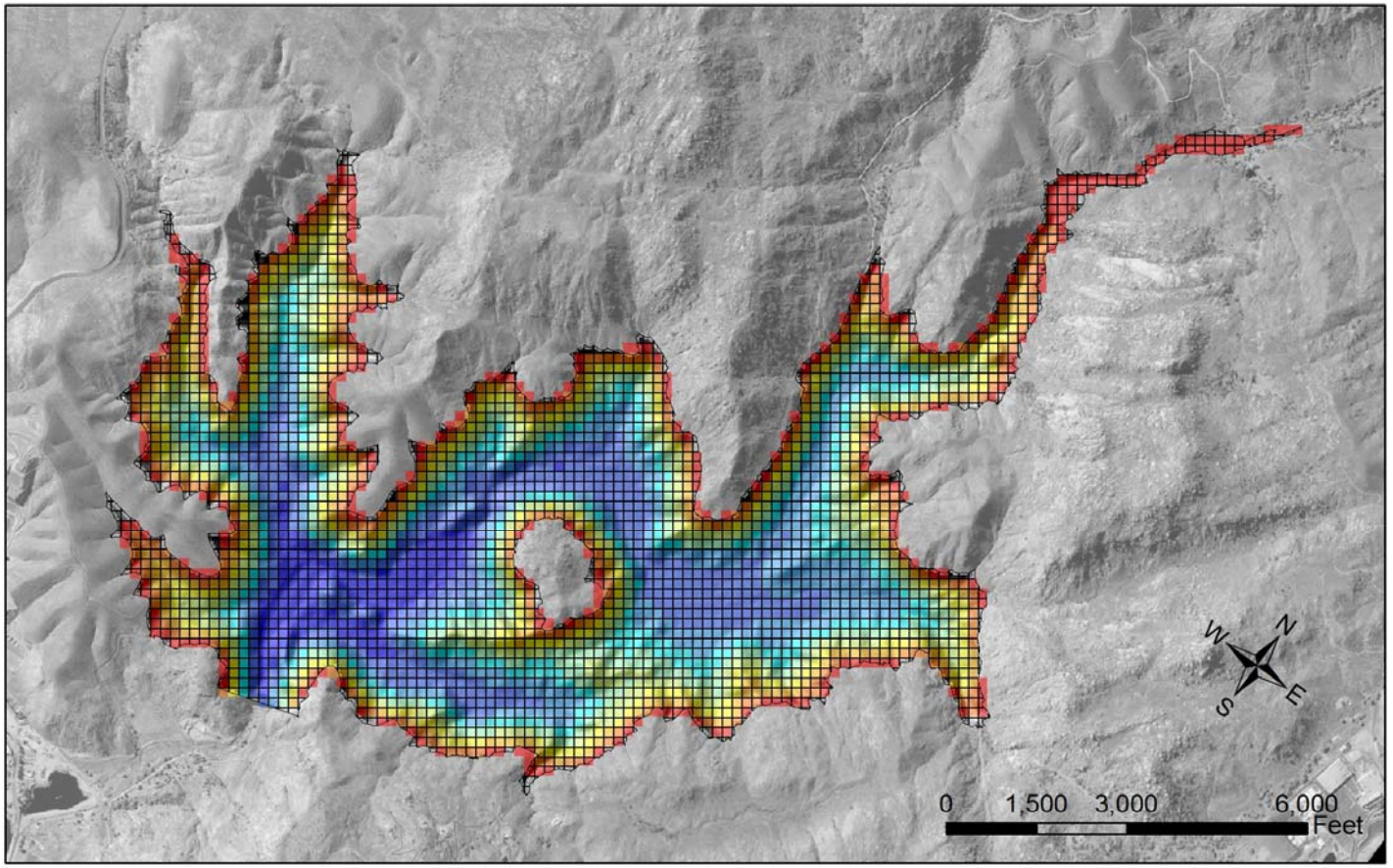

Legend

Lake Boundary at 780 ft

Elevation (ft)

480 - 510
511 - 540
541 - 569
570 - 599
600 - 629
630 - 659
660 - 689
690 - 718
719 - 748
749 - 778

Figure 2

FSI V094005
May 01, 2012

FLOW SCIENCE®

SVR Hydrodynamic Model Calibration Results

Station A – Water Temperature Comparison

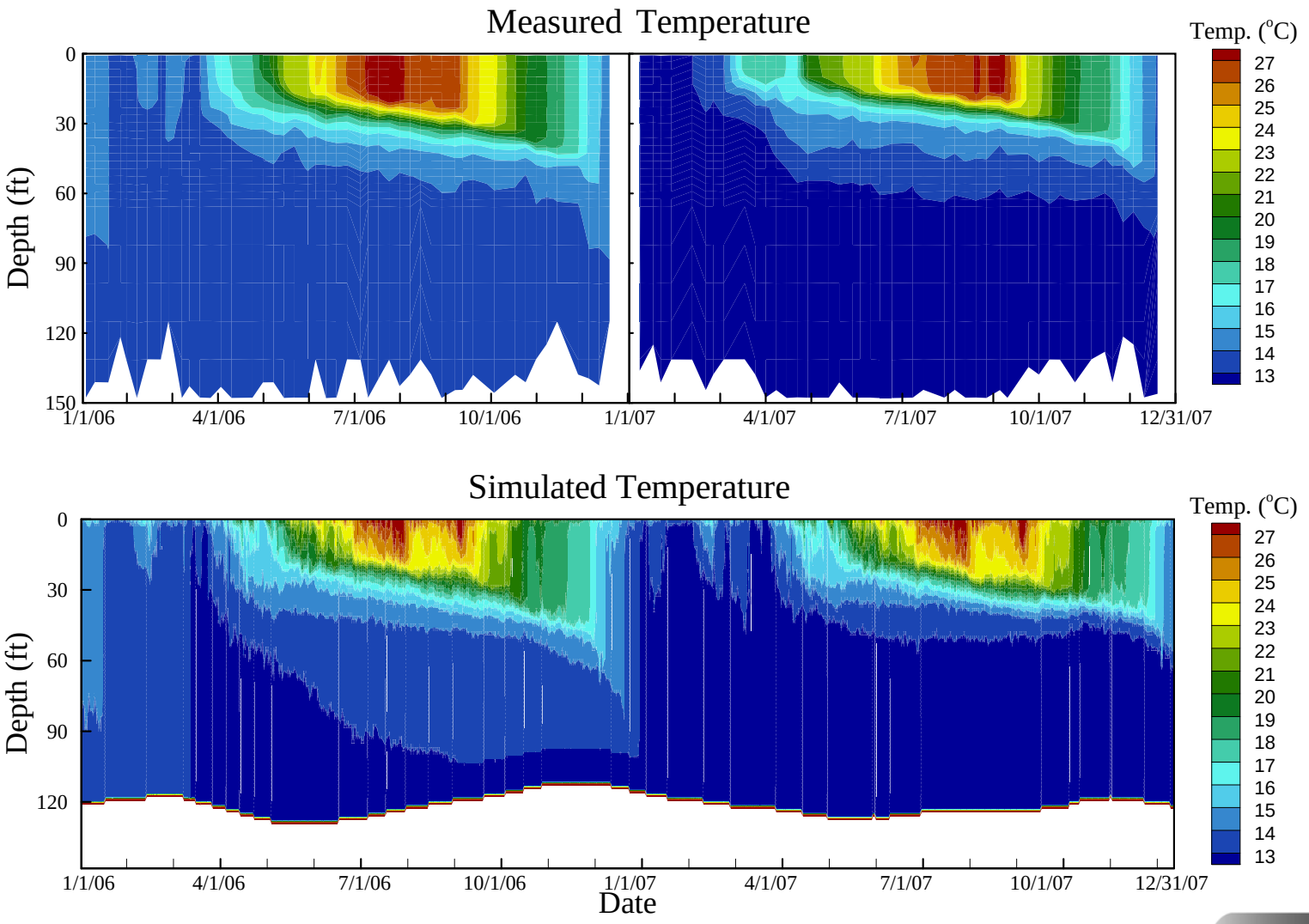

Figure 3

FSI V094005
May 01, 2012

FLOW SCIENCE®

SVR Hydrodynamic Model Calibration Results

Station A – Conductivity Comparison

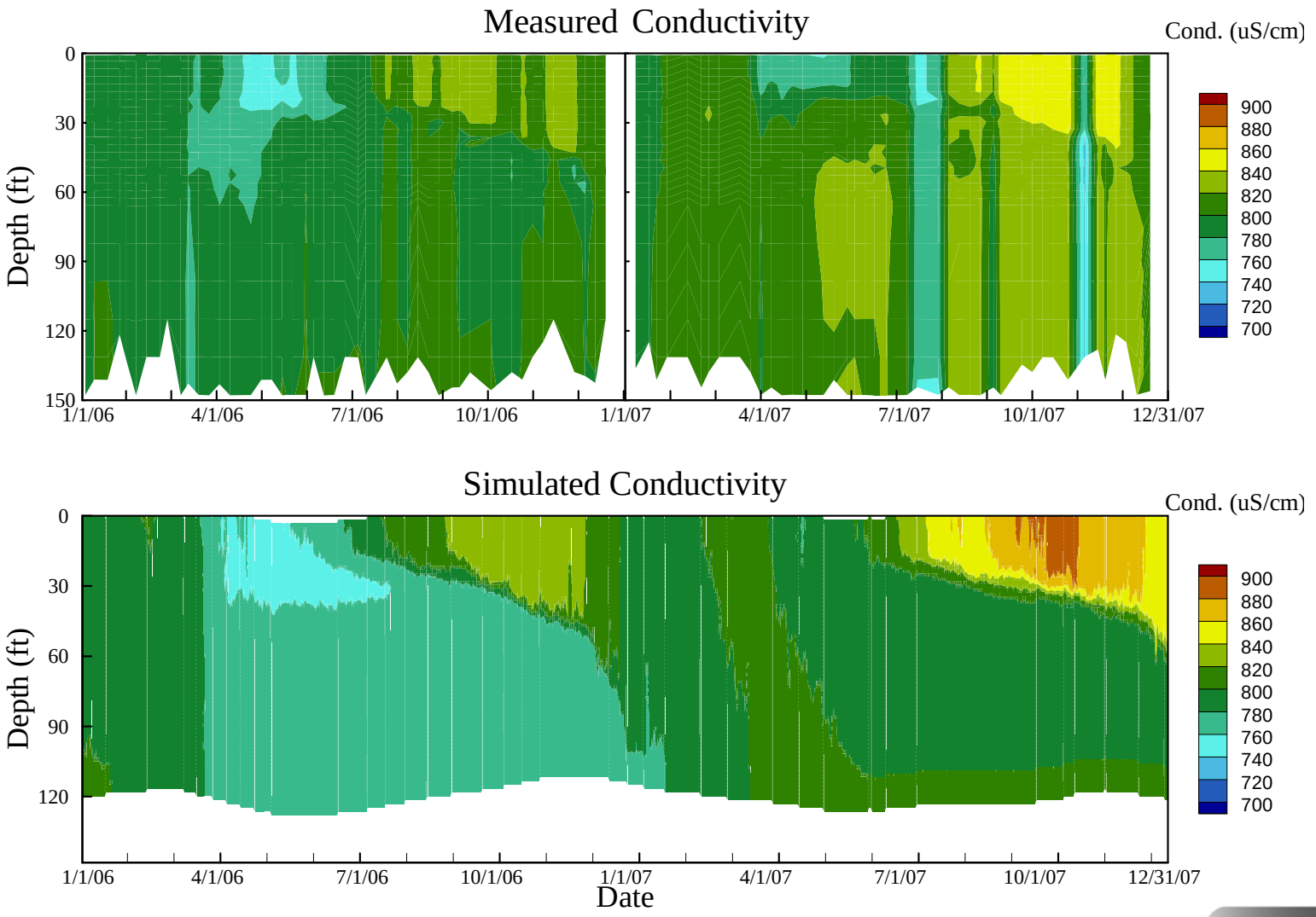

Figure 4

FSI V094005
May 01, 2012

FLOW SCIENCE®

SVR Hydrodynamic Model Calibration Results

1995 Winter Tracer Study – Measured versus Simulated Lanthanum Concentrations

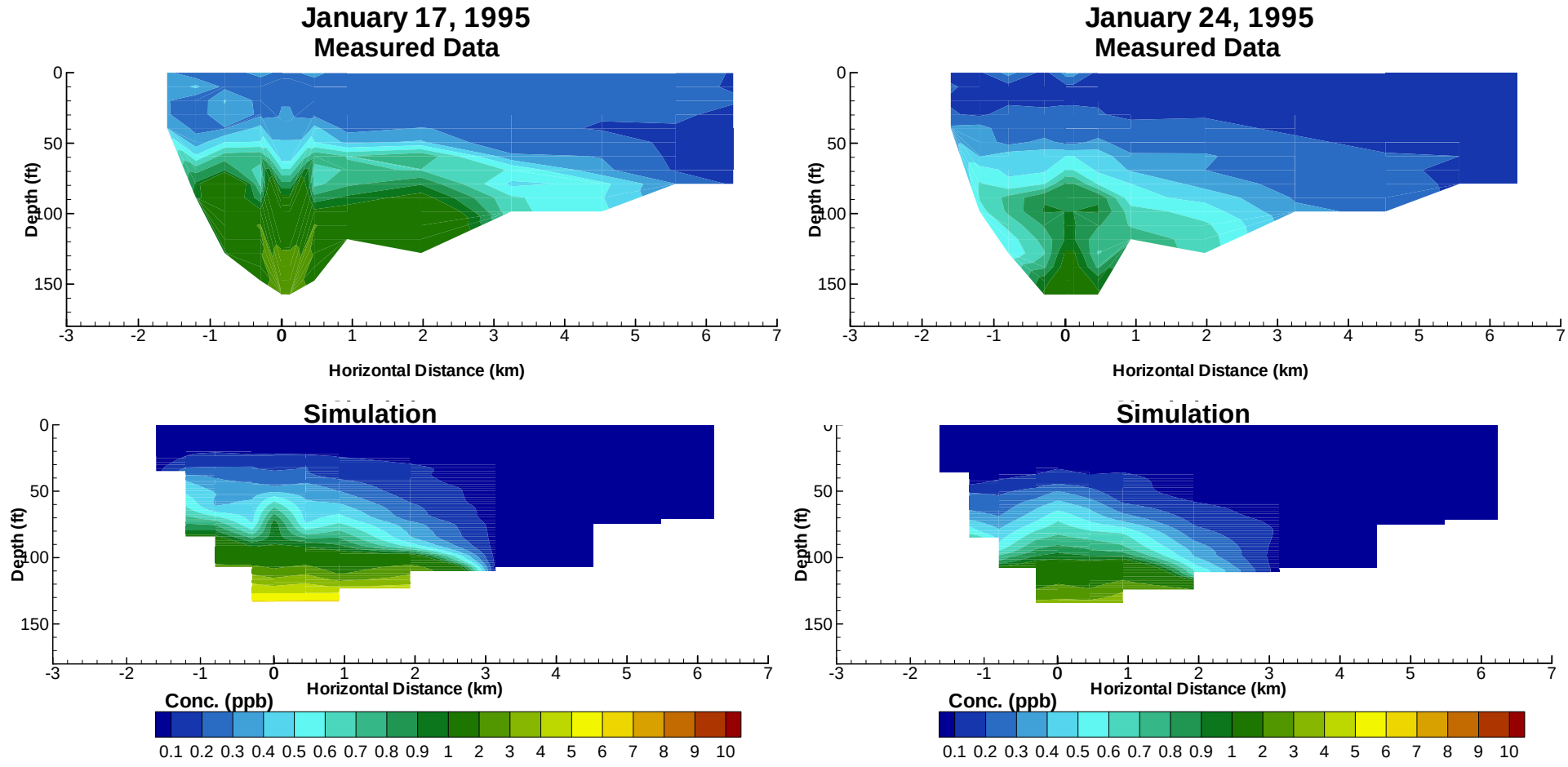

FSI V094005
May 01, 2012

Figure 5

FLOW SCIENCE®

SVR Hydrodynamic Model Calibration Results

1995 Summer Tracer Study – Measured versus Simulated Lanthanum Concentrations

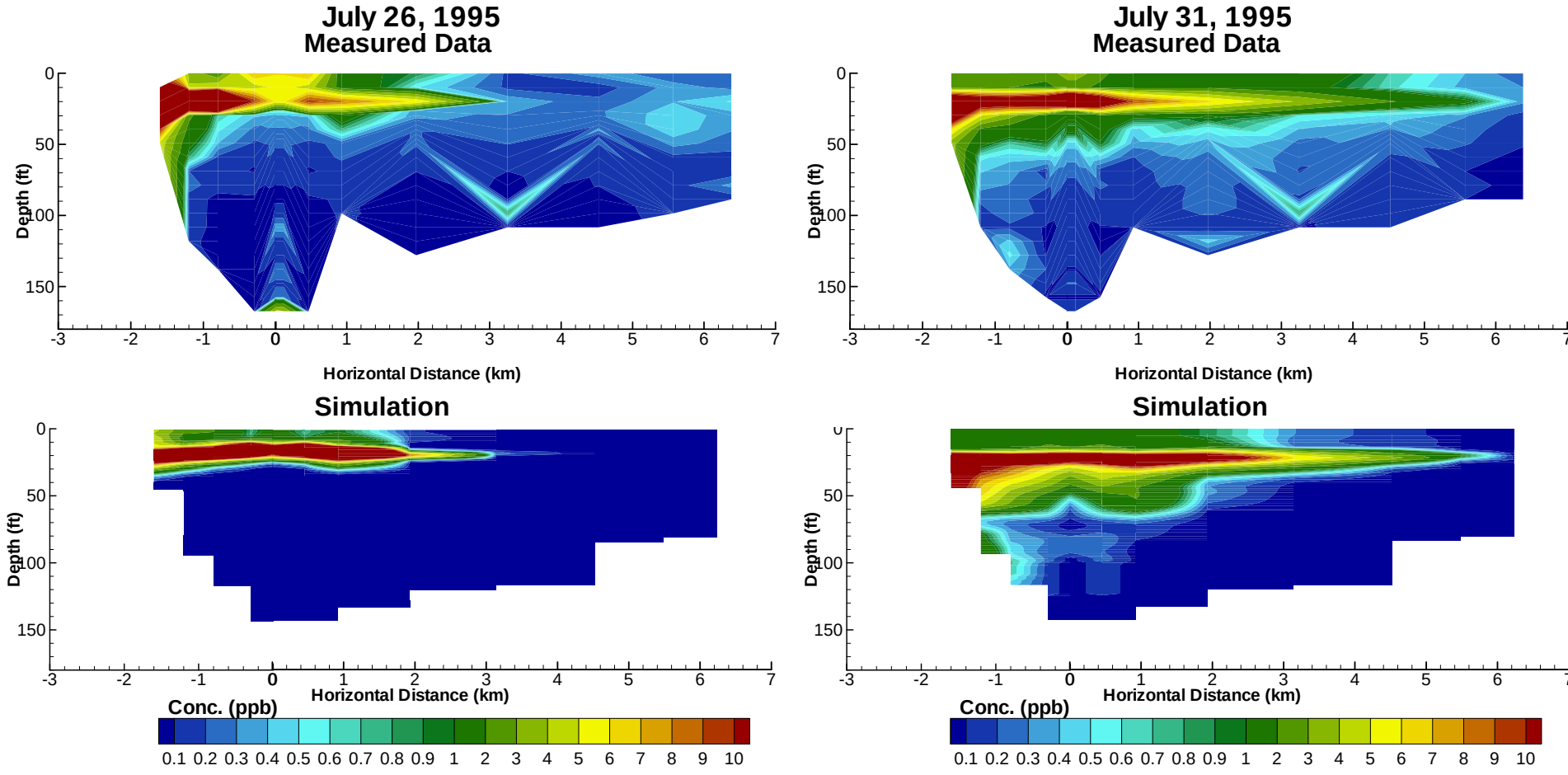

FSI V094005
May 01, 2012

Figure 6

FLOW SCIENCE®

Comparison of Existing and Expanded Reservoir

Simulated Water Temperature at Station A

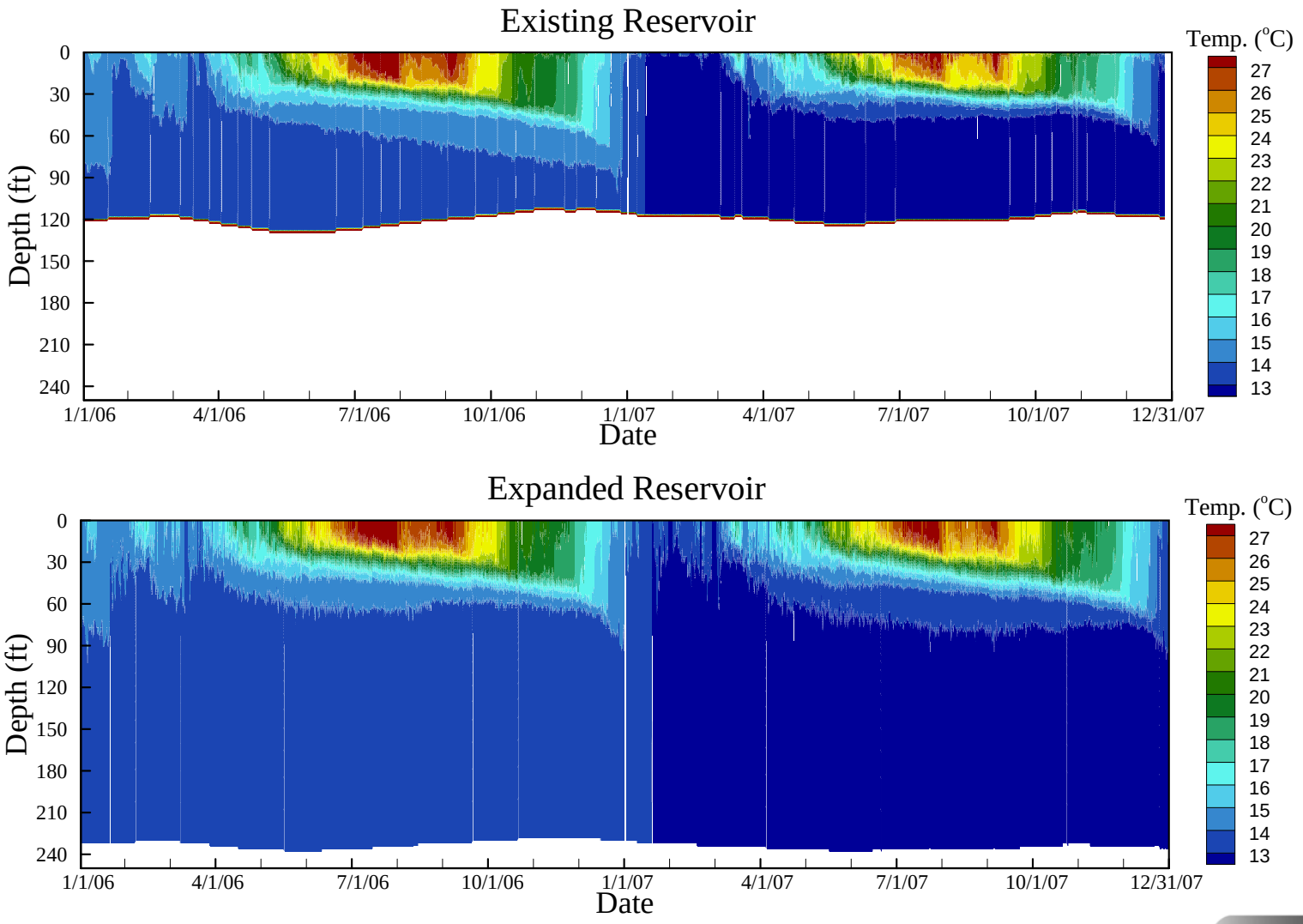

Figure 7

FSI V094005
May 01, 2012

FLOW SCIENCE®

Comparison of Existing and Expanded Reservoir

Simulated Conductivity at Station A

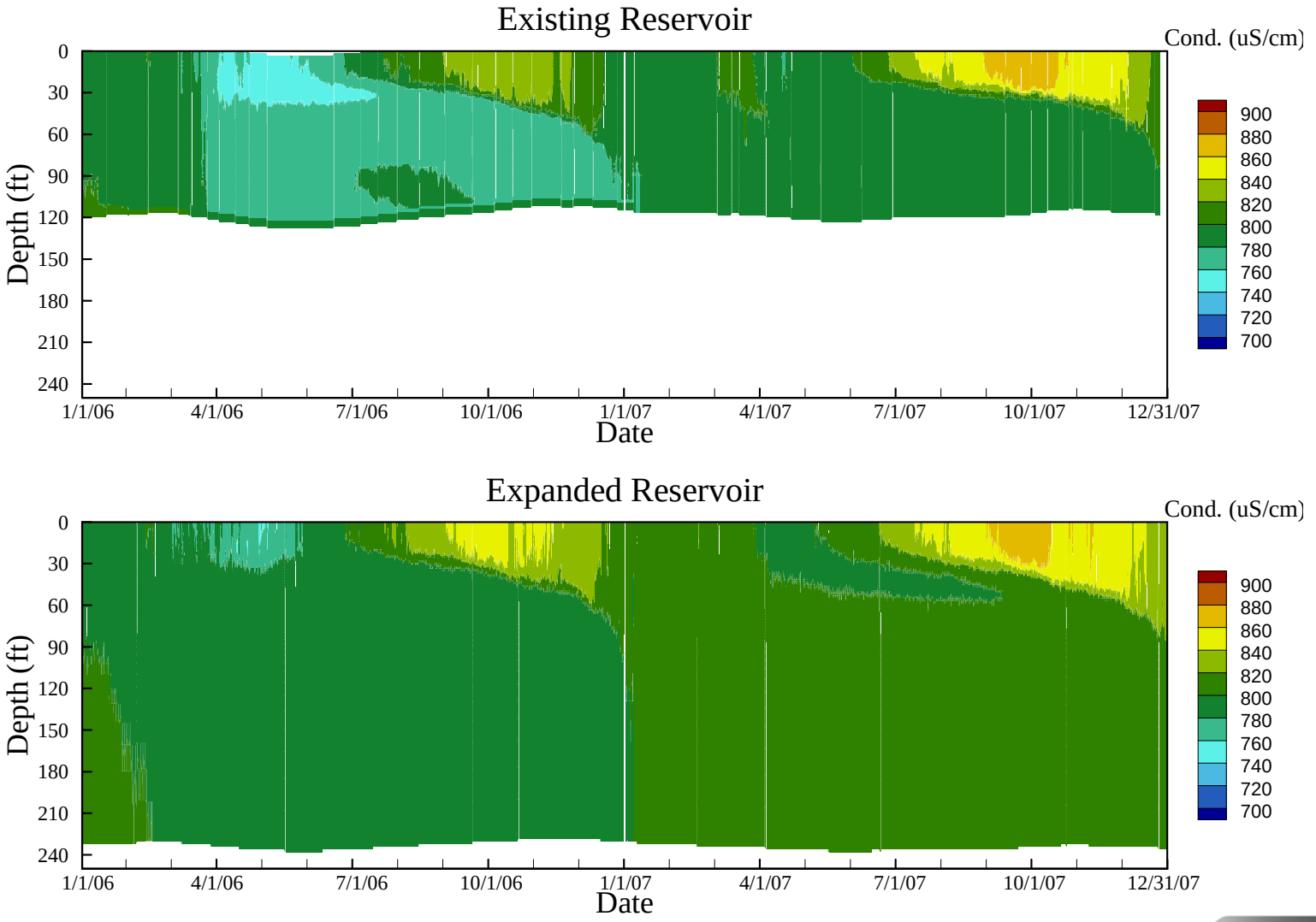

Figure 8

FSI V094005
May 01, 2012

FLOW SCIENCE®

Base Case: Purified Water Inflow Temperature

(Using multi-year averages of weekly water temperatures at North City Water Reclamation Plant; Provided by the City)

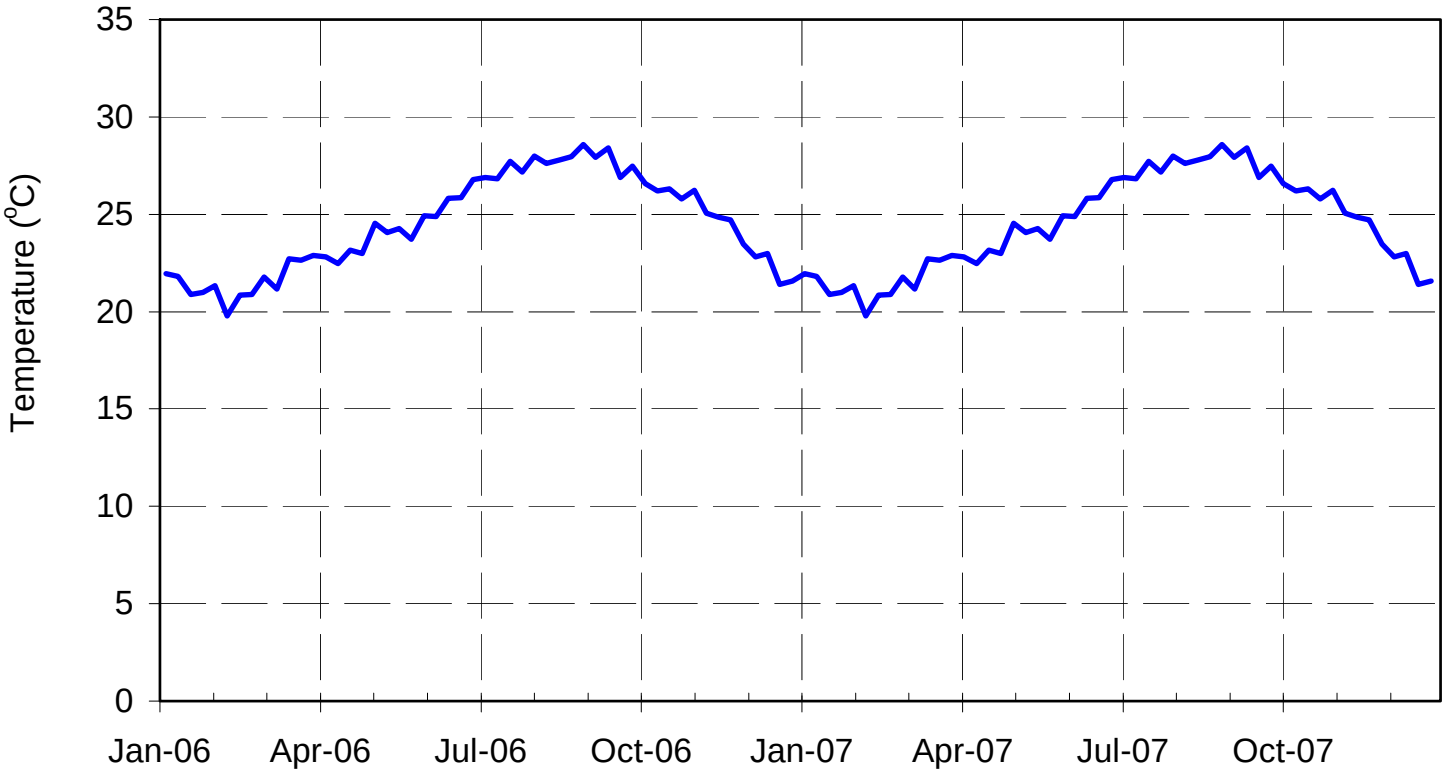

FSI V094005
May 01, 2012

Figure 9

FLOW SCIENCE®

Base Case: Simulated Water Temperature and Conductivity at Station A

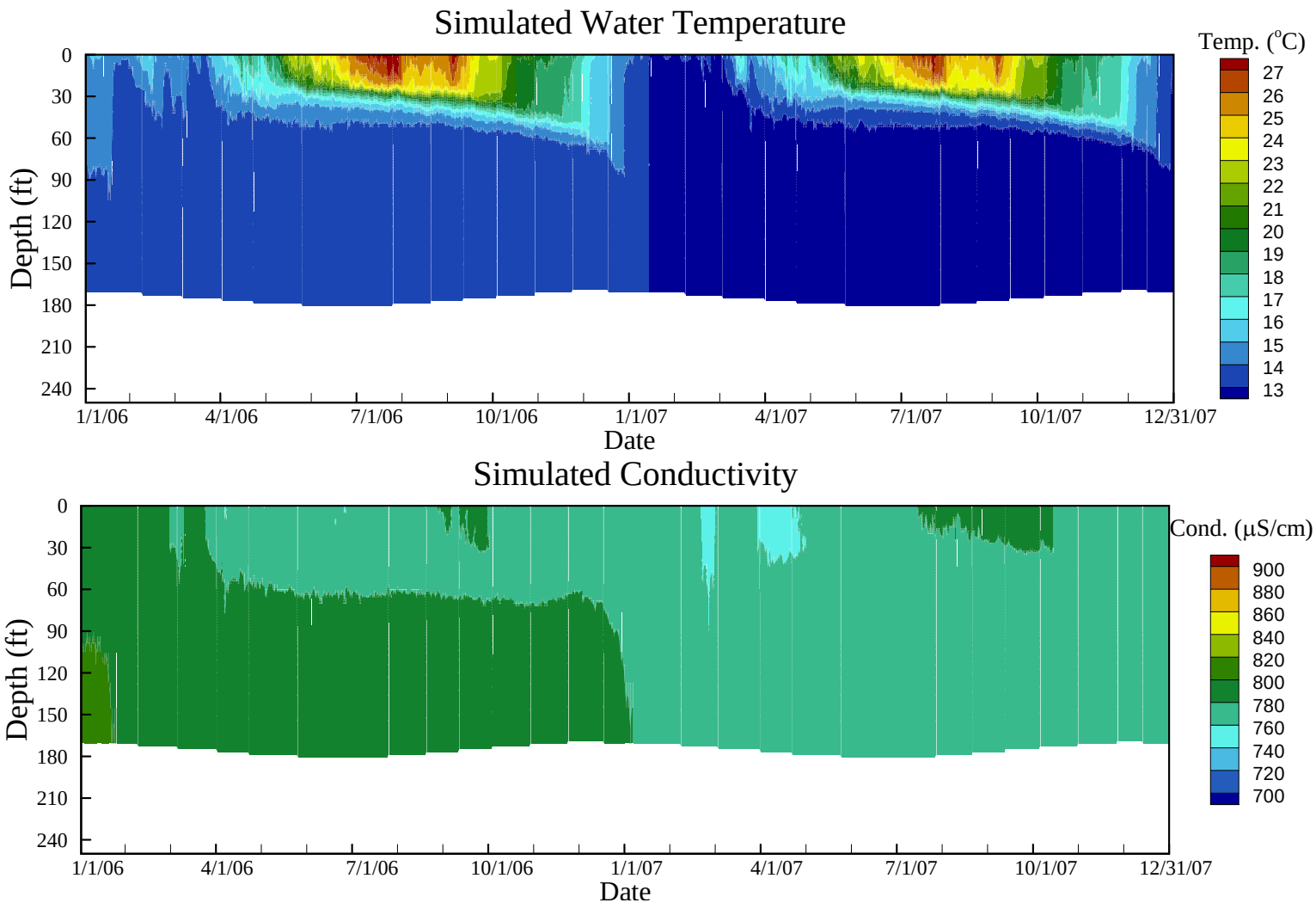

FSI V094005
May 01, 2012

Figure 10

FLOW SCIENCE®

Base Case: Contours of Simulated Temperature and Decaying Tracer

(Initial Inflow Concentration = 100%; Decay Rate = One Log Reduction Per Month)

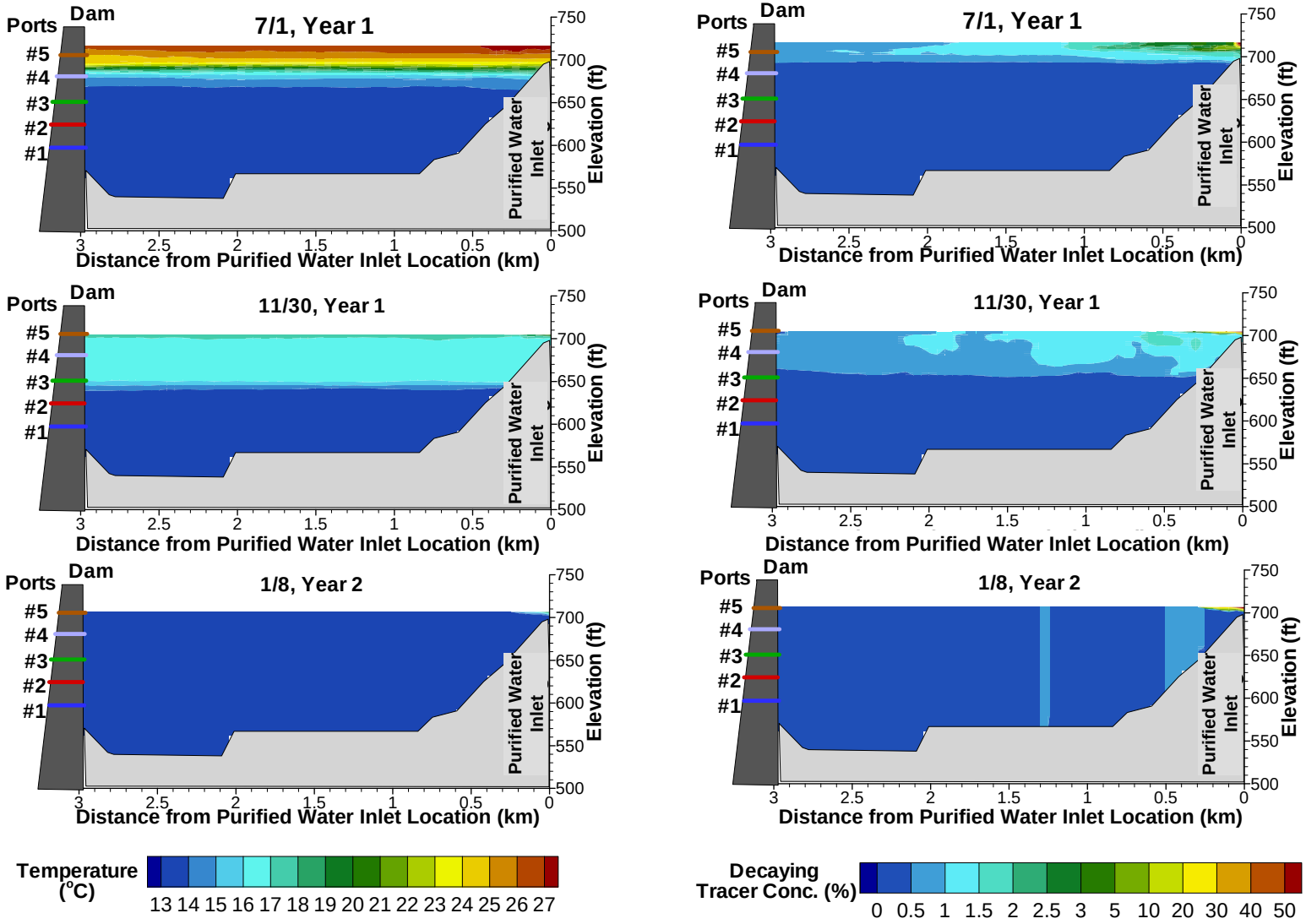

FSI V094005
May 01, 2012

Figure 11

FLOW SCIENCE®

Base Case: Simulated Decaying Tracer at the Reservoir Outlet Tower

(Initial Inflow Concentration = 100%; Decay Rate = One Log Reduction Per Month)

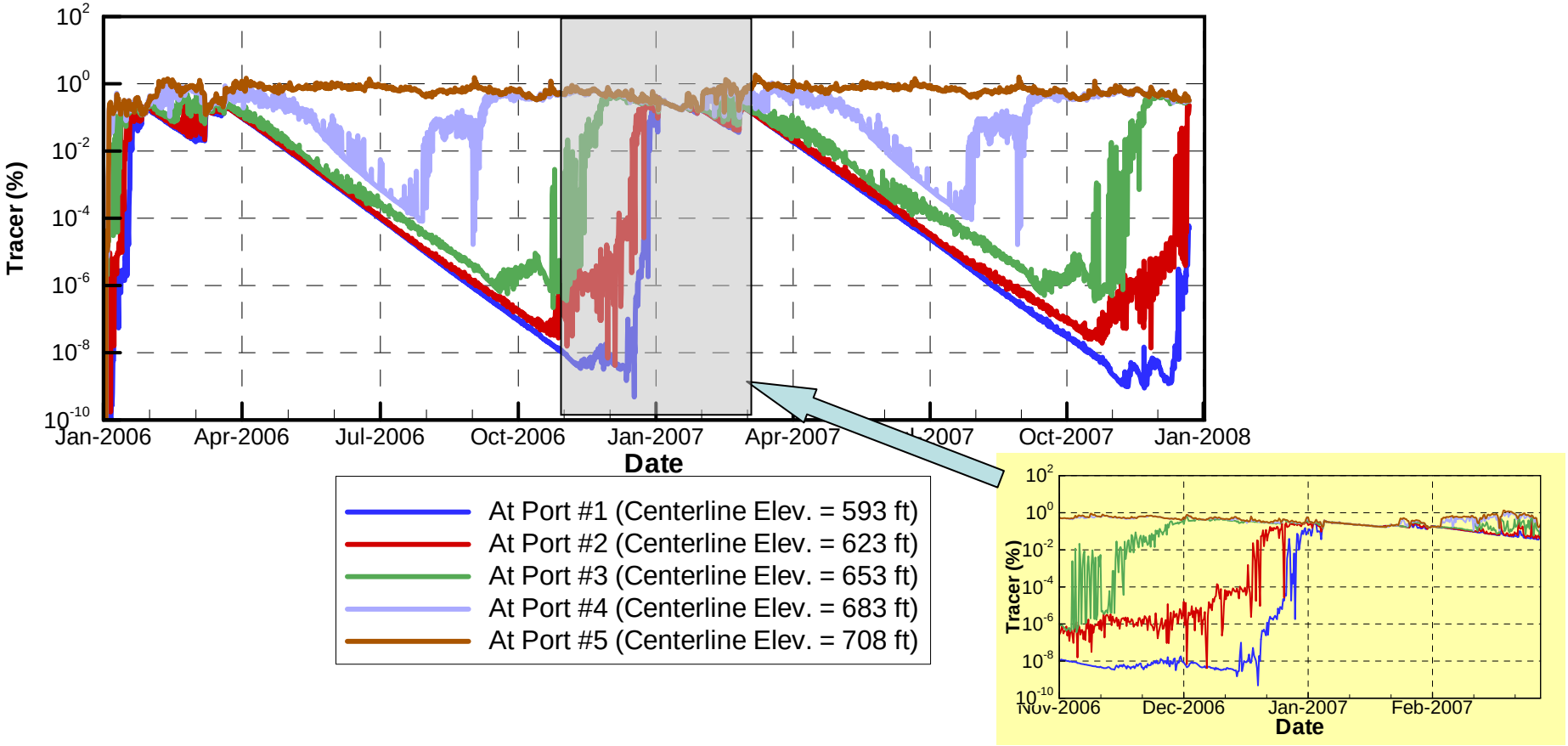

FSI V094005
May 01, 2012

Figure 12

FLOW SCIENCE®

Base Case: Simulated 24-hour Conservative Tracer Concentrations in Reservoir Outflow*

(Initial Inflow Concentration = 100%; Open Port #2)

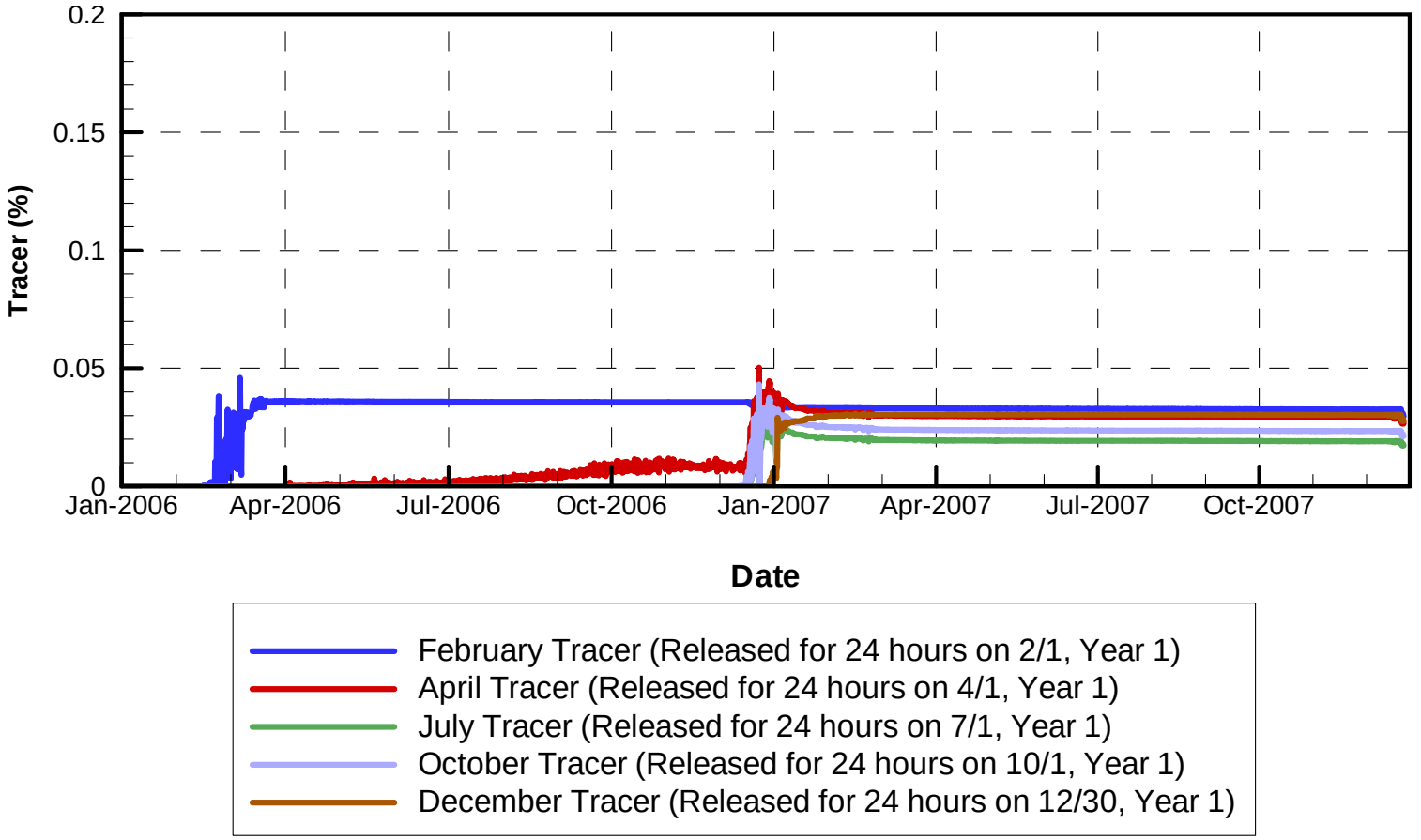

* Concentrations of trace within the reservoir at the outlet tower at the depth of the outlet port

Comparison of Base Case and No Purified Water Scenario

Simulated Water Temperature at Station A

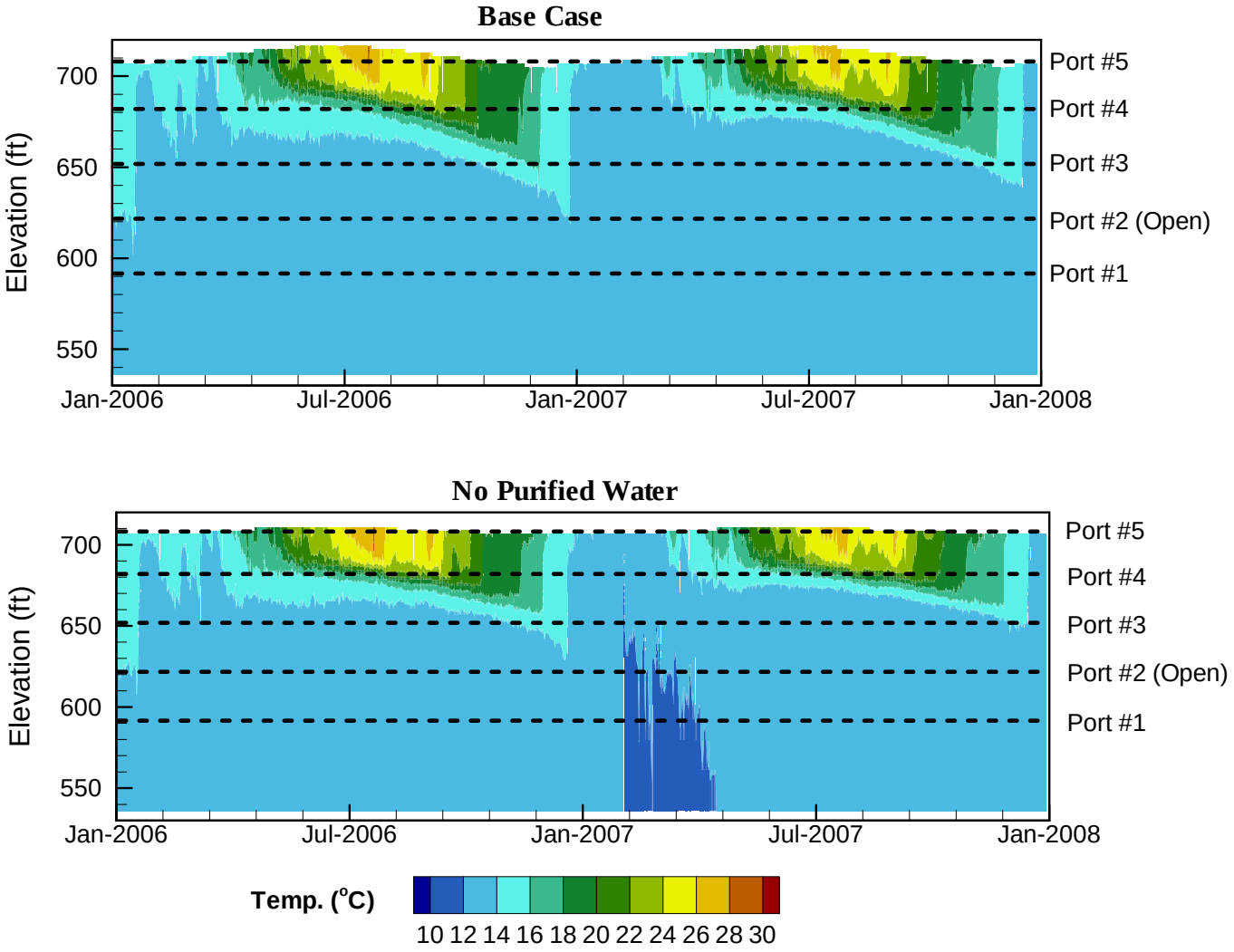

* Note that y-axis in this figure is elevation in ft for allowing labels of the port elevations in the figure

FSI V094005
May 01, 2012

Figure 14

FLOW SCIENCE®

Comparison of Base Case and No Purified Water Scenario

Simulated Conductivity at Station A

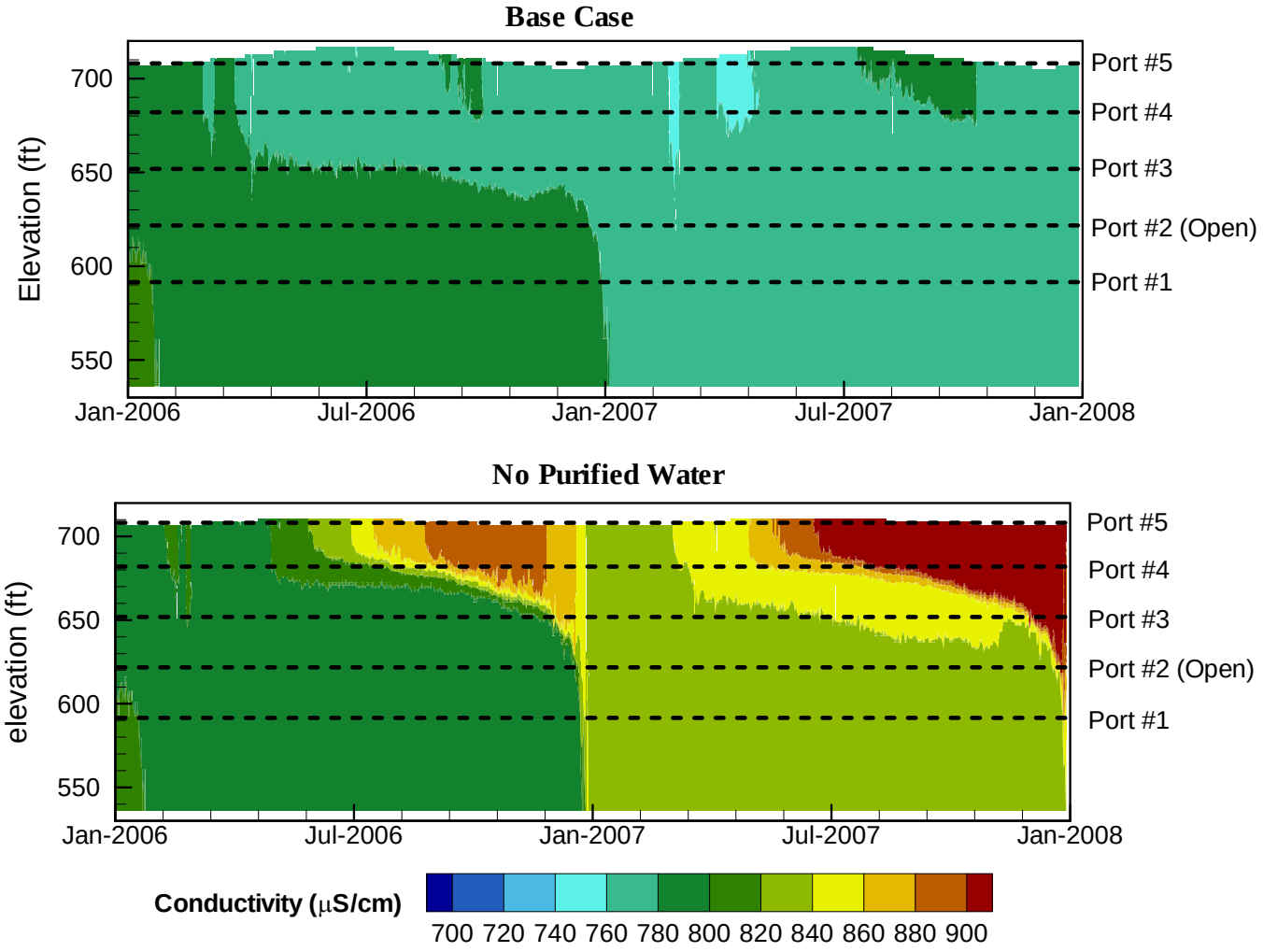

* Note that y-axis in this figure is elevation in ft for allowing labels of the port elevations in the figure

Figure 15

FLOW SCIENCE®

Inflow and Outflow Rates of Base Case, Extended Drought and Emergency Drawdown Scenarios

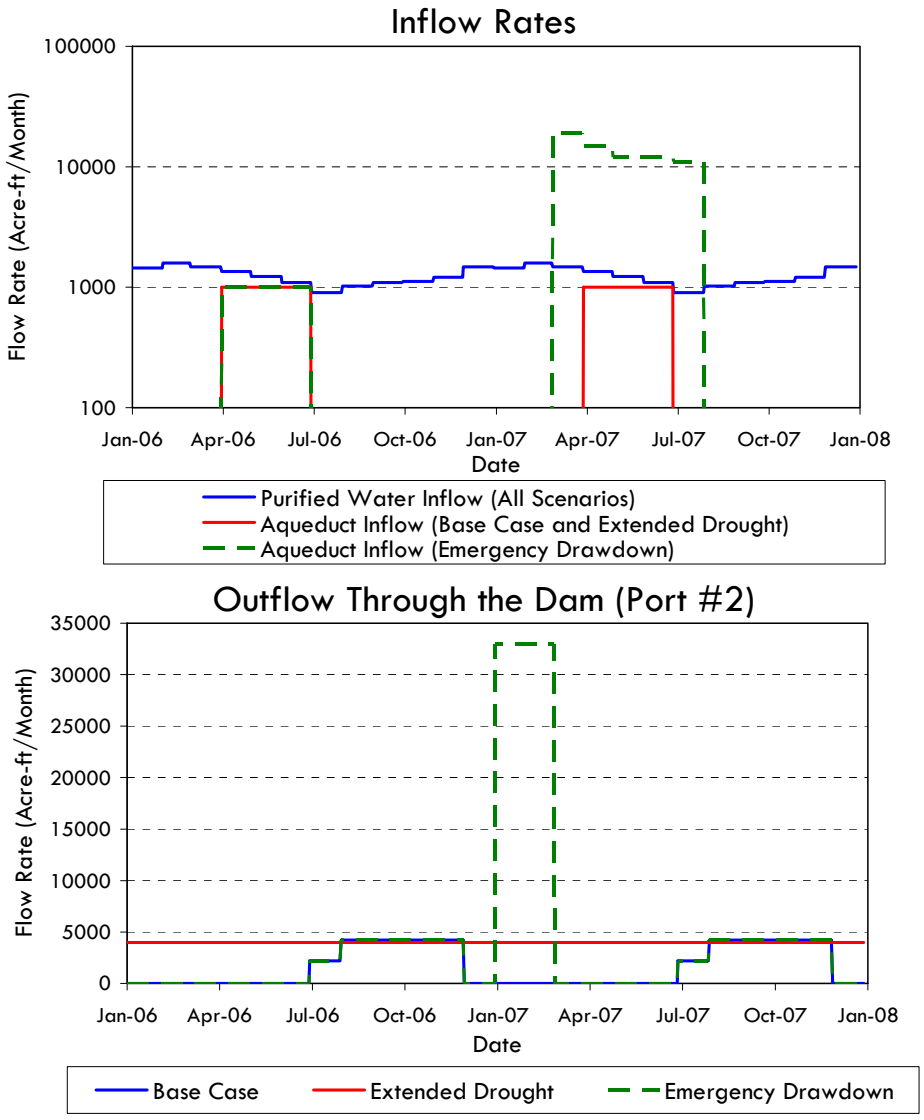

Figure 16

FSI V094005
May 01, 2012

FLOW SCIENCE®

Water Volumes of Base Case, Extended Drought and Emergency Drawdown Scenarios

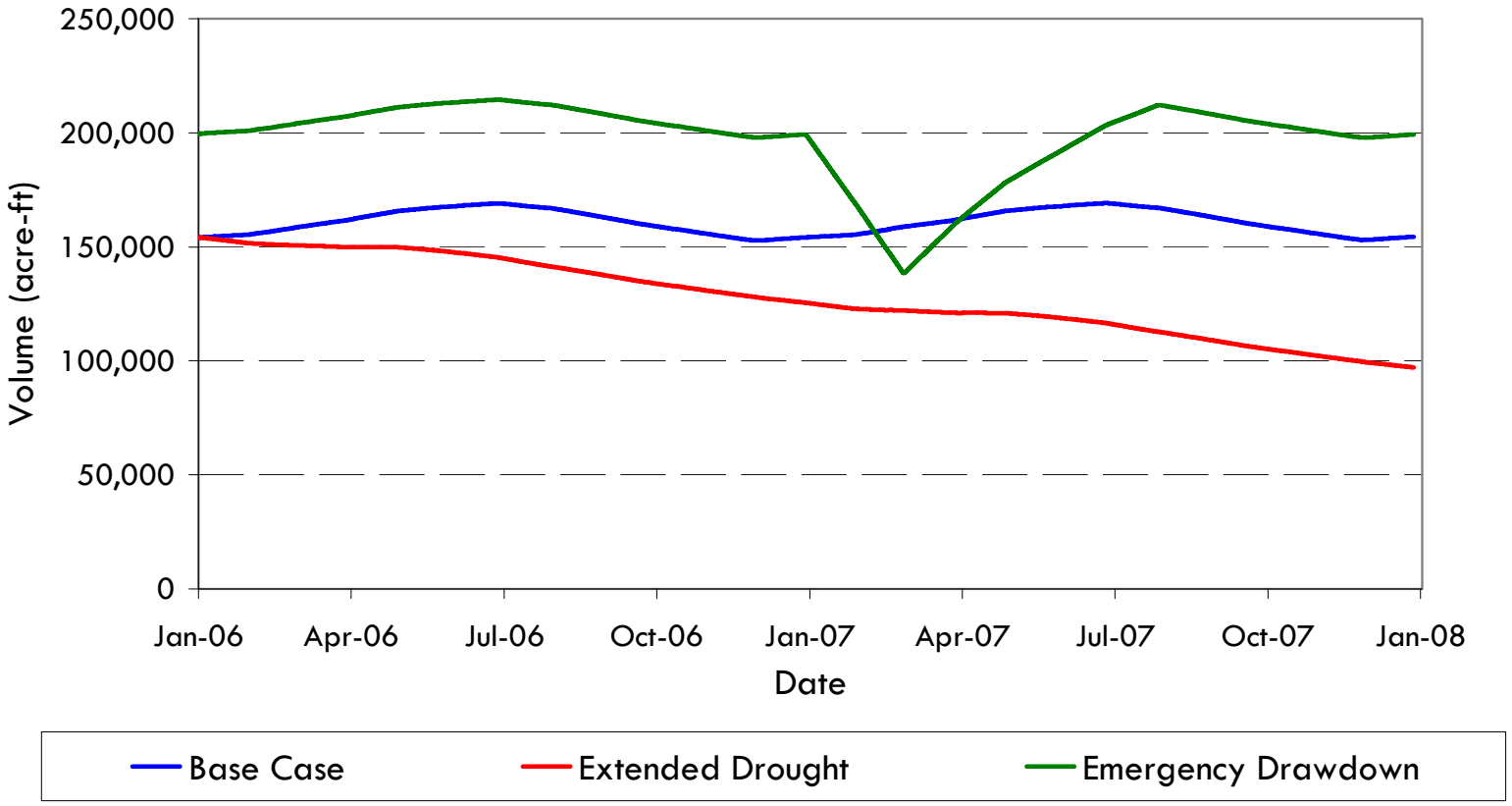

FSI V094005
May 01, 2012

Figure 17

FLOW SCIENCE®

Comparison of Base Case, Extended Drought and Emergency Drawdown Scenarios

Simulated Water Temperature at Station A

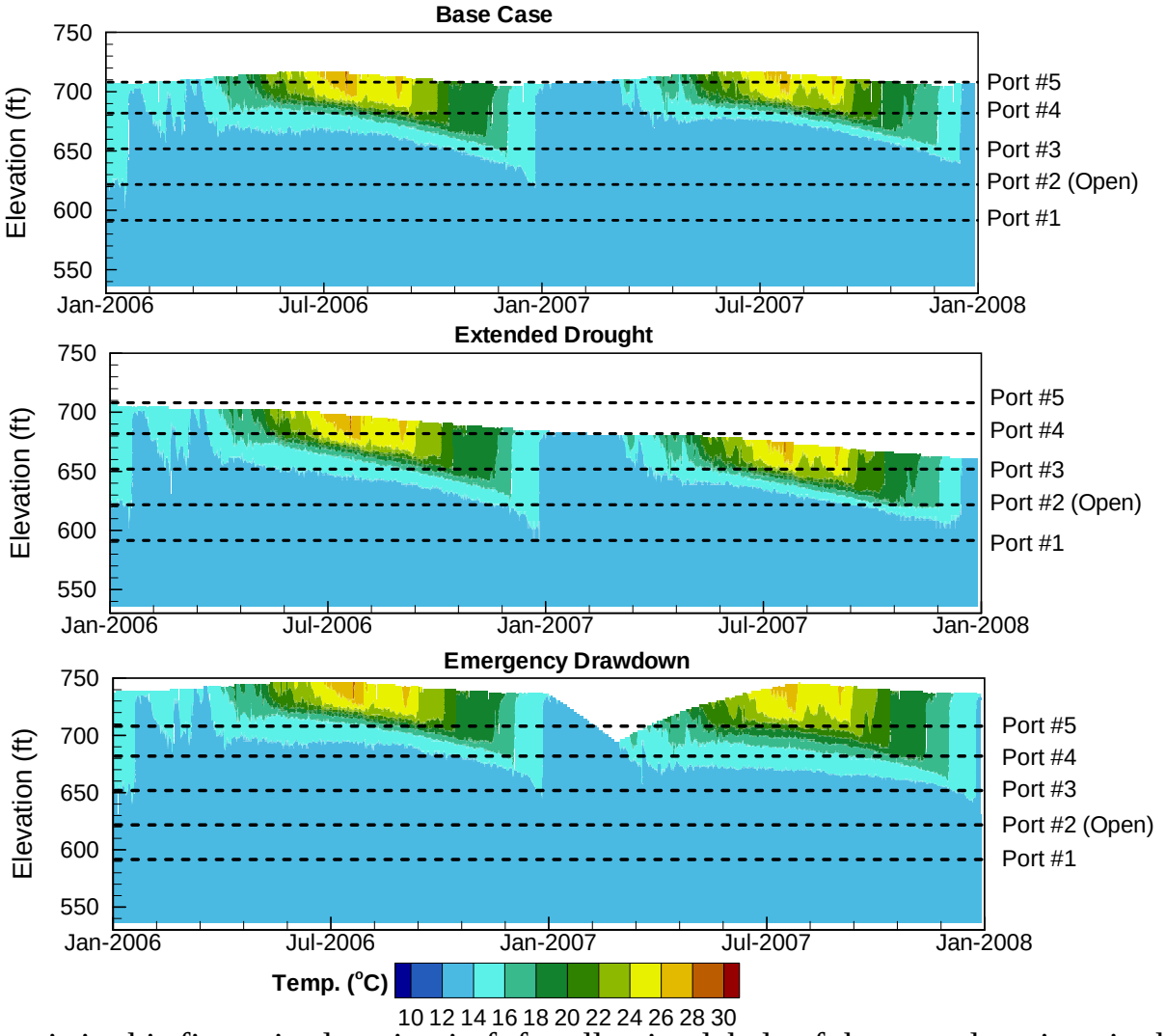

* Note that y-axis in this figure is elevation in ft for allowing labels of the port elevations in the figure

Figure 18

FLOW SCIENCE®

Comparison of Base Case, Extended Drought and Emergency Drawdown Scenarios

Simulated Conductivity at Station A

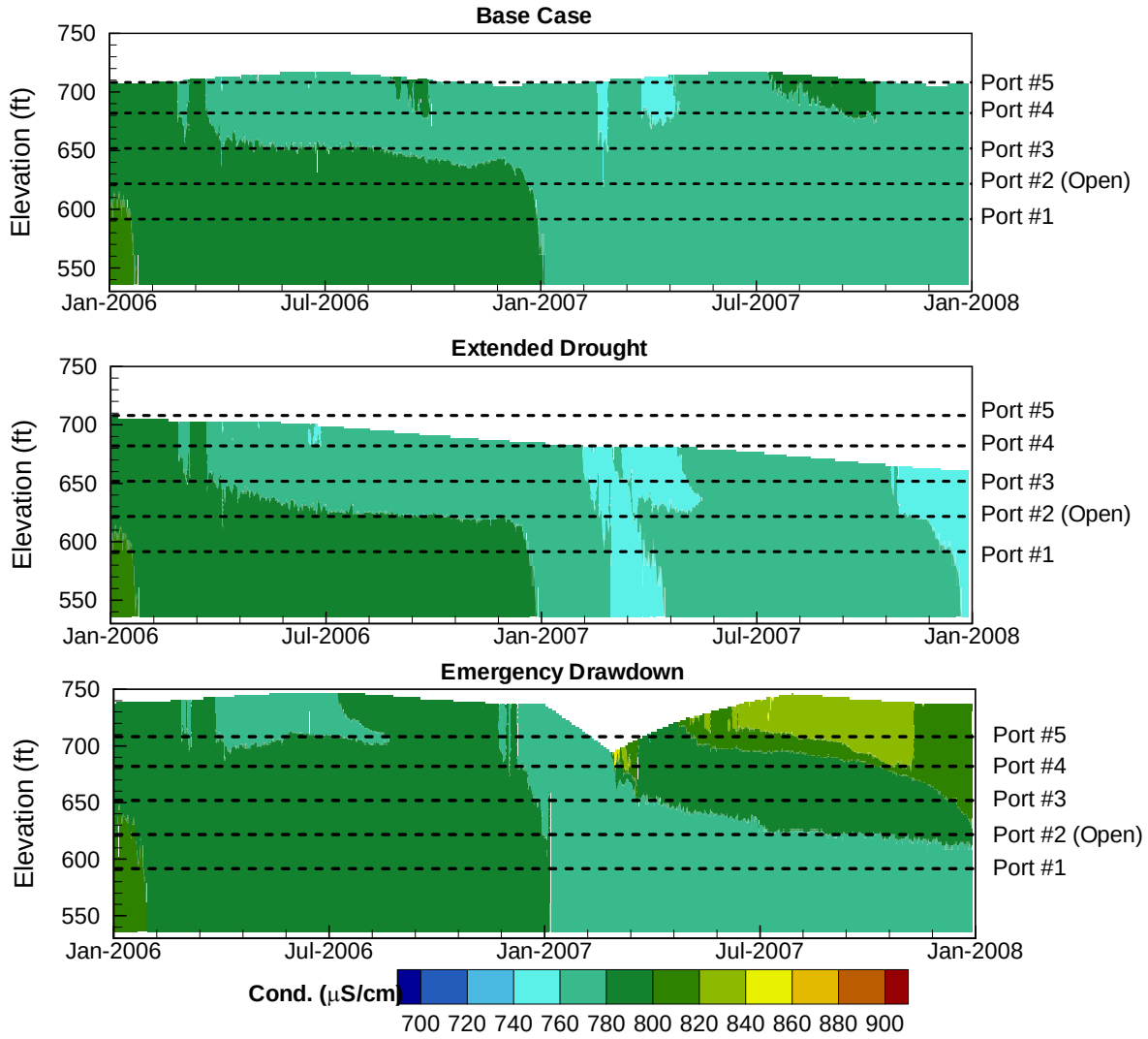

* Note that y-axis in this figure is elevation in ft for allowing labels of the port elevations in the figure

Figure 19

FLOW SCIENCE®

Comparison of Base Case, Extended Drought and Emergency Drawdown Scenarios

Simulated Decaying Tracer Concentrations in the Reservoir Outflow*

(Open Port #2; Initial Inflow Concentration = 100%; Decay Rate = One Log Reduction Per Month)

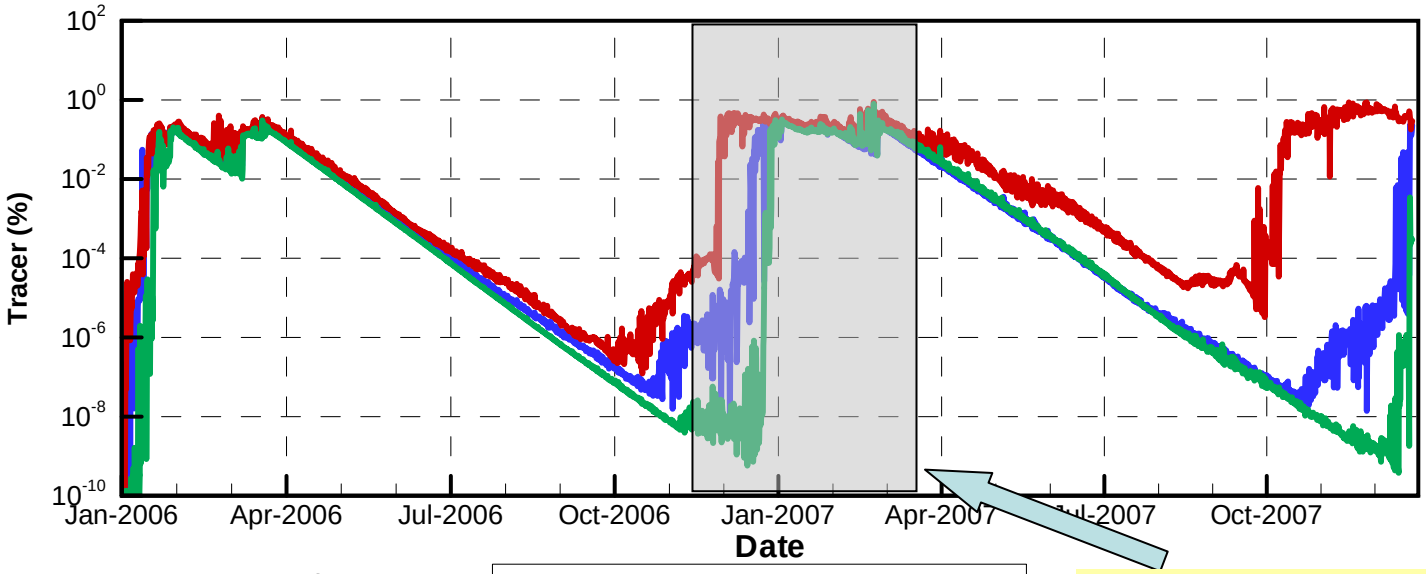

* Concentrations of tracer within the reservoir at the outlet tower at the depth of the open outlet port

Base Case
Extended Drought
Emergency Drawdown

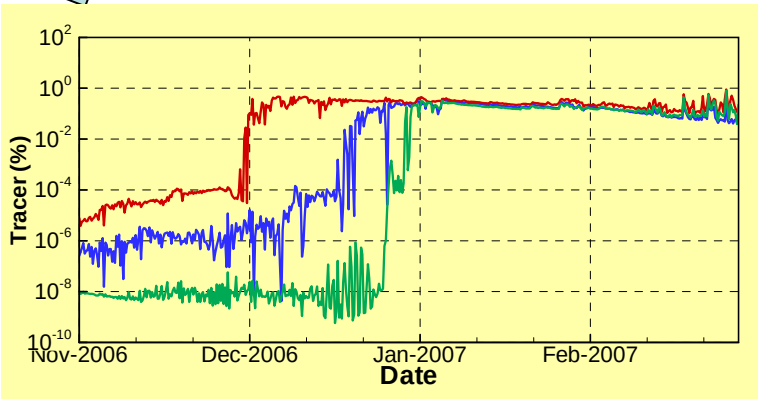

FSI V094005
May 01, 2012

Figure 20

FLOW SCIENCE®

Extended Drought Scenario Simulated 24-hour Conservative Tracer Concentrations in the Reservoir Outflow*

(Open Port #2; Initial Inflow Concentration = 100%)

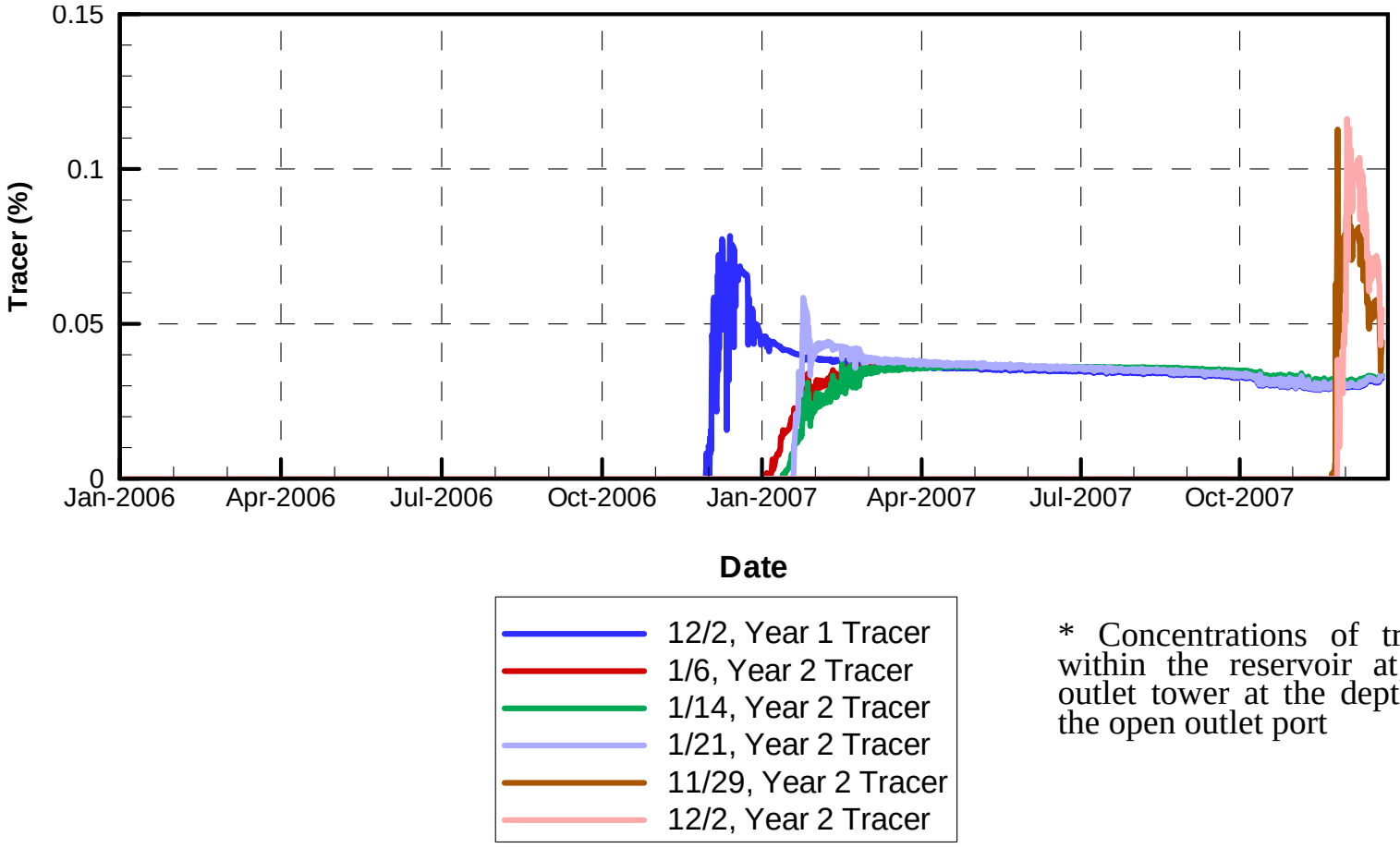

* Concentrations of tracer within the reservoir at the outlet tower at the depth of the open outlet port

FSI V094005
May 01, 2012

Figure 21

FLOW SCIENCE®

Emergency Drawdown Scenario Simulated 24-hour Conservative Tracer Concentrations in the Reservoir Outflow*

(Open Port #2; Initial Inflow Concentration = 100%)

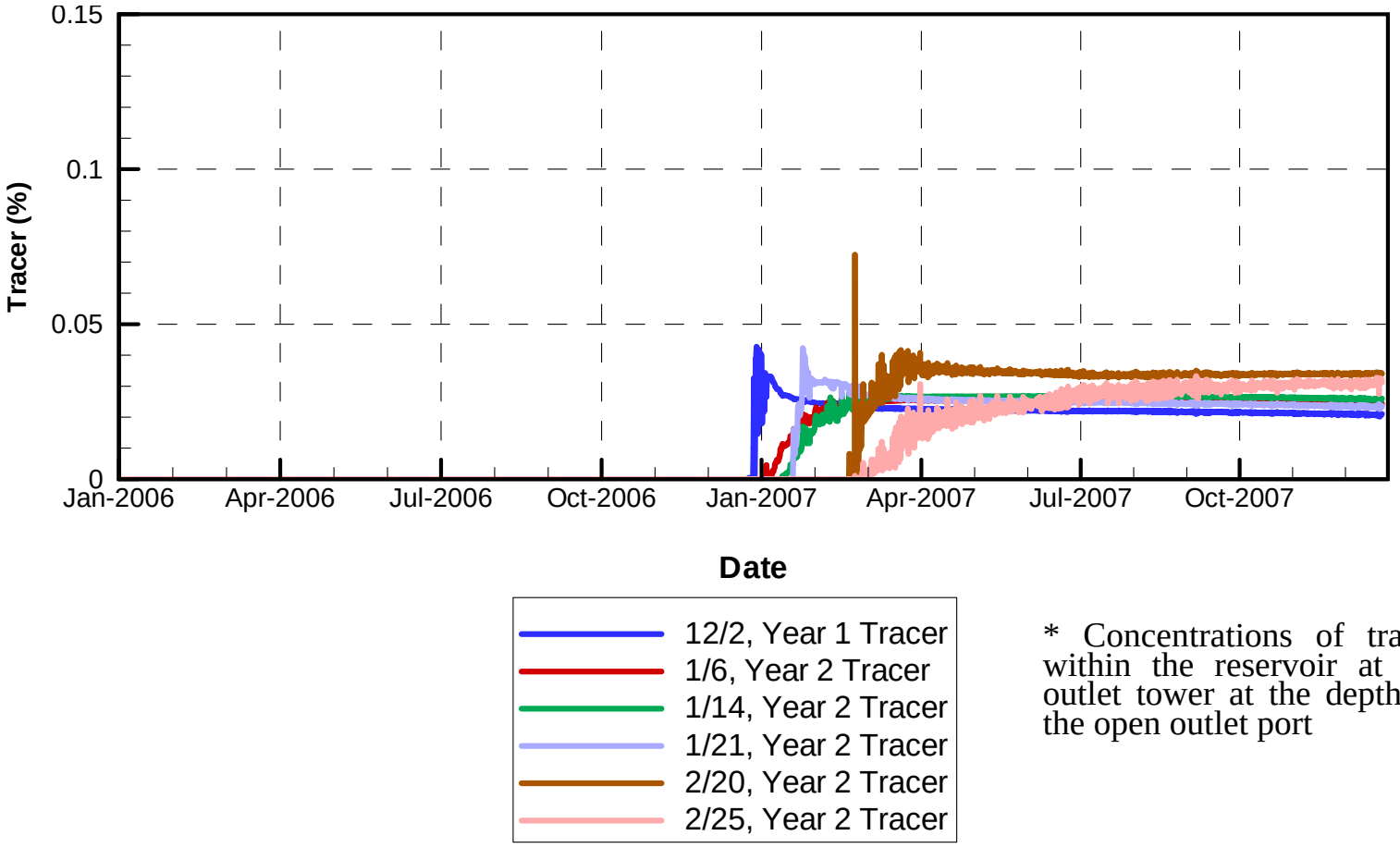

* Concentrations of tracer within the reservoir at the outlet tower at the depth of the open outlet port

FSI V094005
May 01, 2012

Figure 22

FLOW SCIENCE®

Map of Modeled Purified Water Inlet Locations

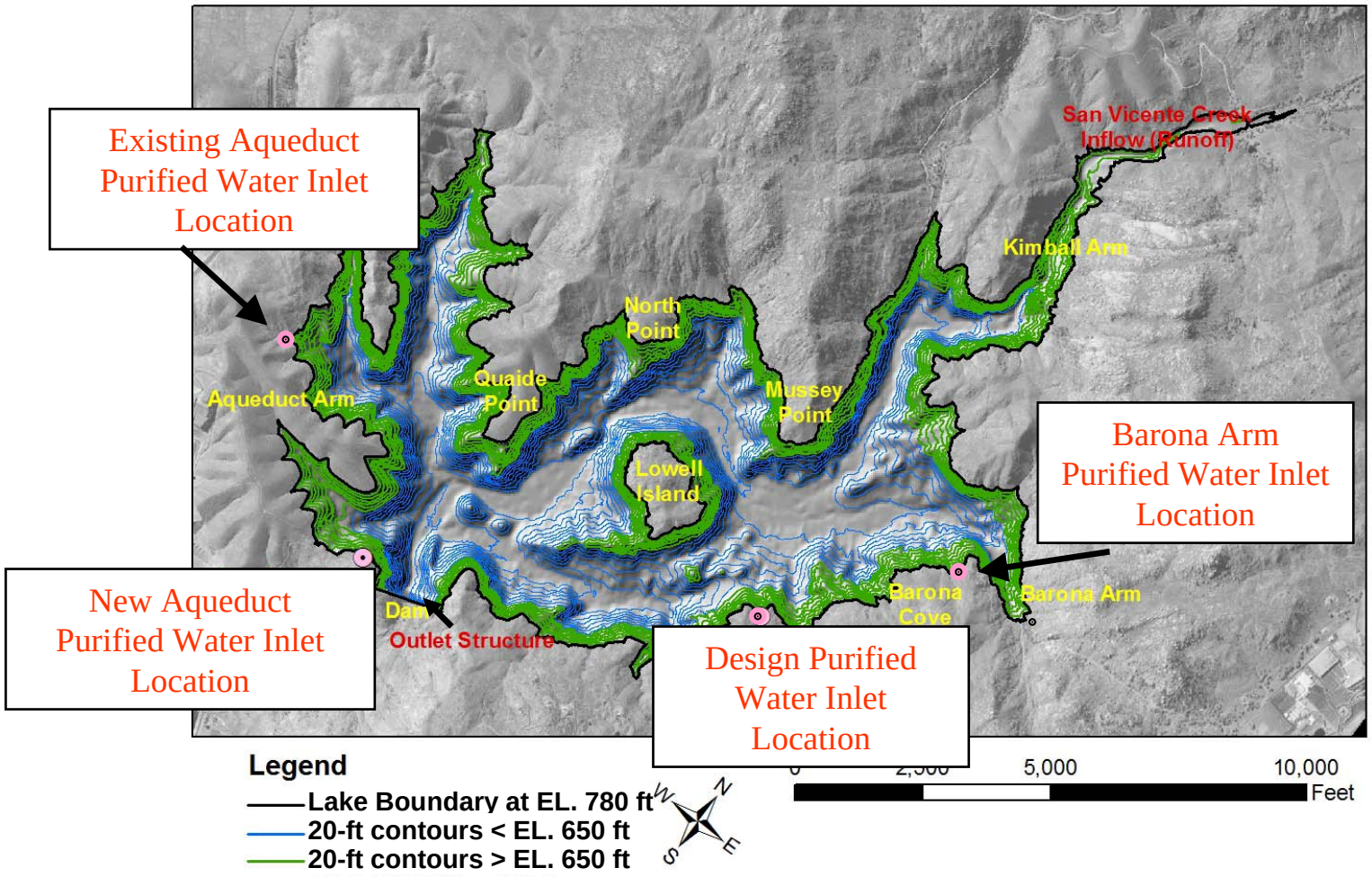

FSI V094005
May 01, 2012

Figure 23

FLOW SCIENCE®

Comparison of Reservoir Outflow Decaying Tracer Concentrations* from Different Purified Water Inlet Locations Under Base Case Operating Scenario

(Open Port #2; Initial Inflow Concentration = 100%;
Decay Rate = One Log Reduction Per Month)

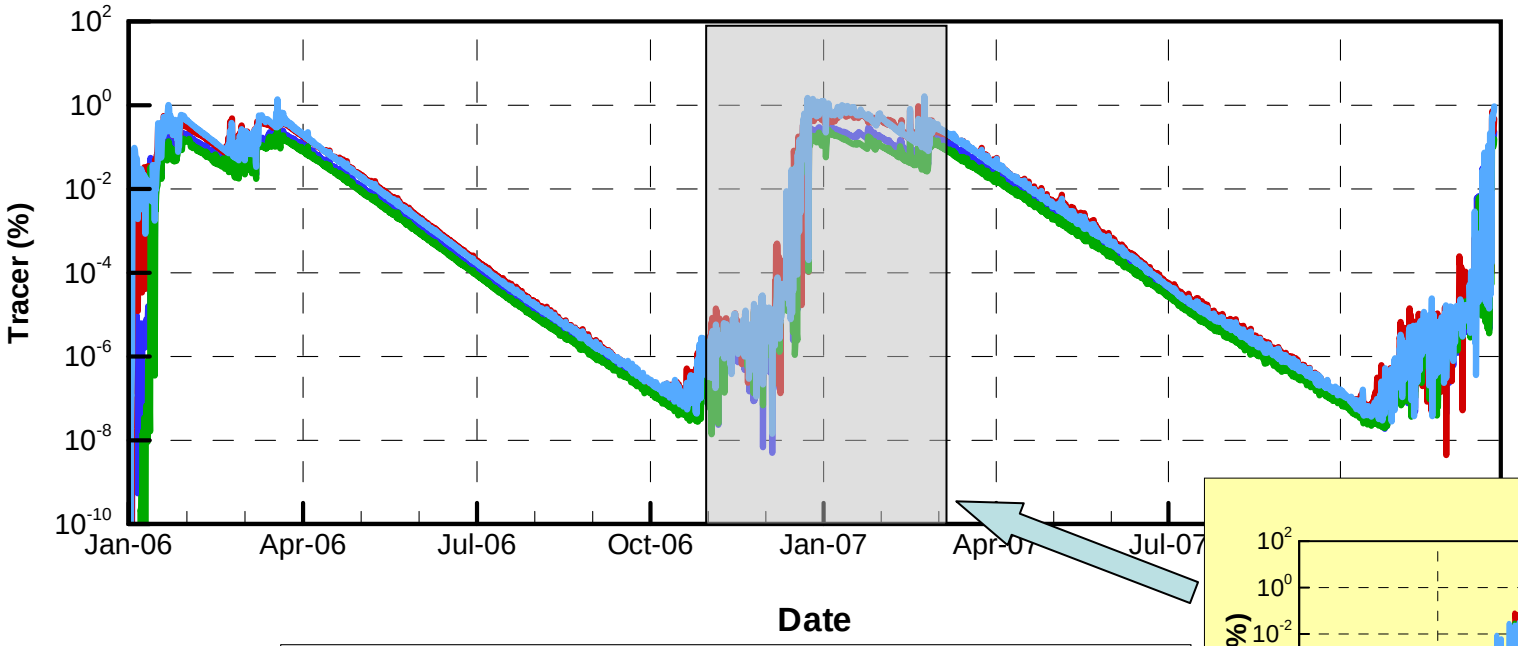

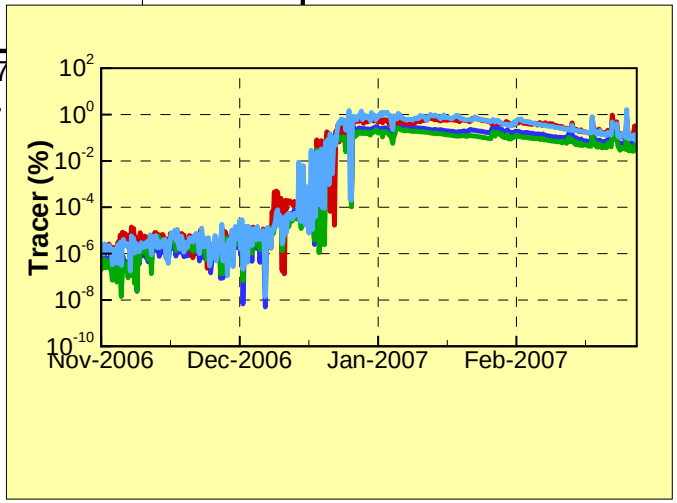

* Concentrations of tracer within the reservoir at the outlet tower at the depth of the open outlet port.

Figure 24

FSI V094005
May 01, 2012

Comparison of Reservoir Outflow 24-hour Conservative Tracer Concentrations* from Different Purified Water Inlet Locations Under Base Case Operating Scenario

Tracer Released on 1/30, Year 1 for 24 hours

(Open Port #2; Initial Inflow Concentration = 100%)

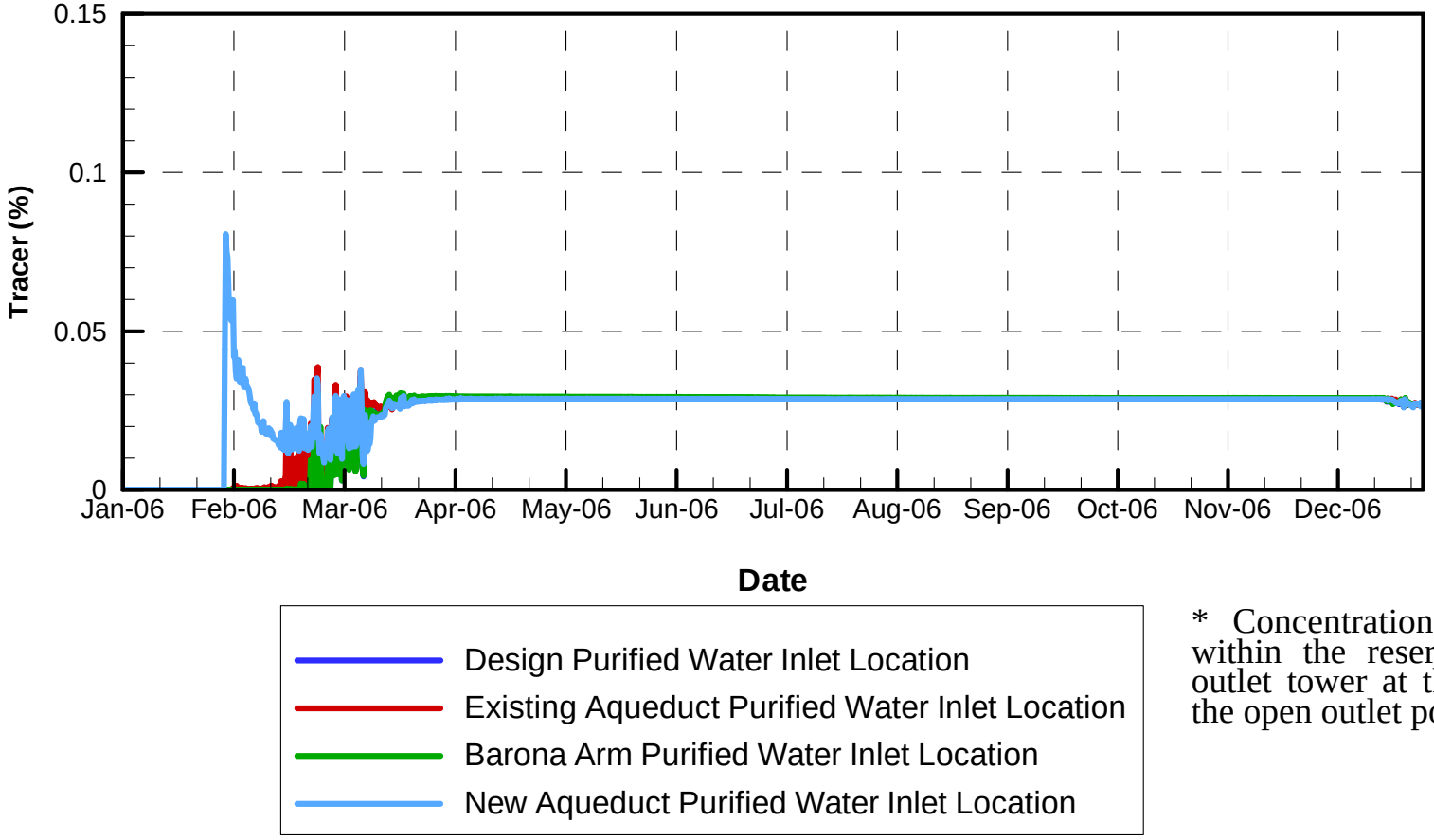

* Concentrations of tracer within the reservoir at the outlet tower at the depth of the open outlet port

Figure 25

FSI V094005
May 01, 2012

FLOW SCIENCE®

Comparison of Reservoir Outflow 24-hour Conservative Tracer Concentrations* from Different Purified Water Inlet Locations Under Base Case Operating Scenario

Tracer released on 4/1, Year 1 for 24 hours

(Open Port #2; Initial Inflow Concentration = 100%)

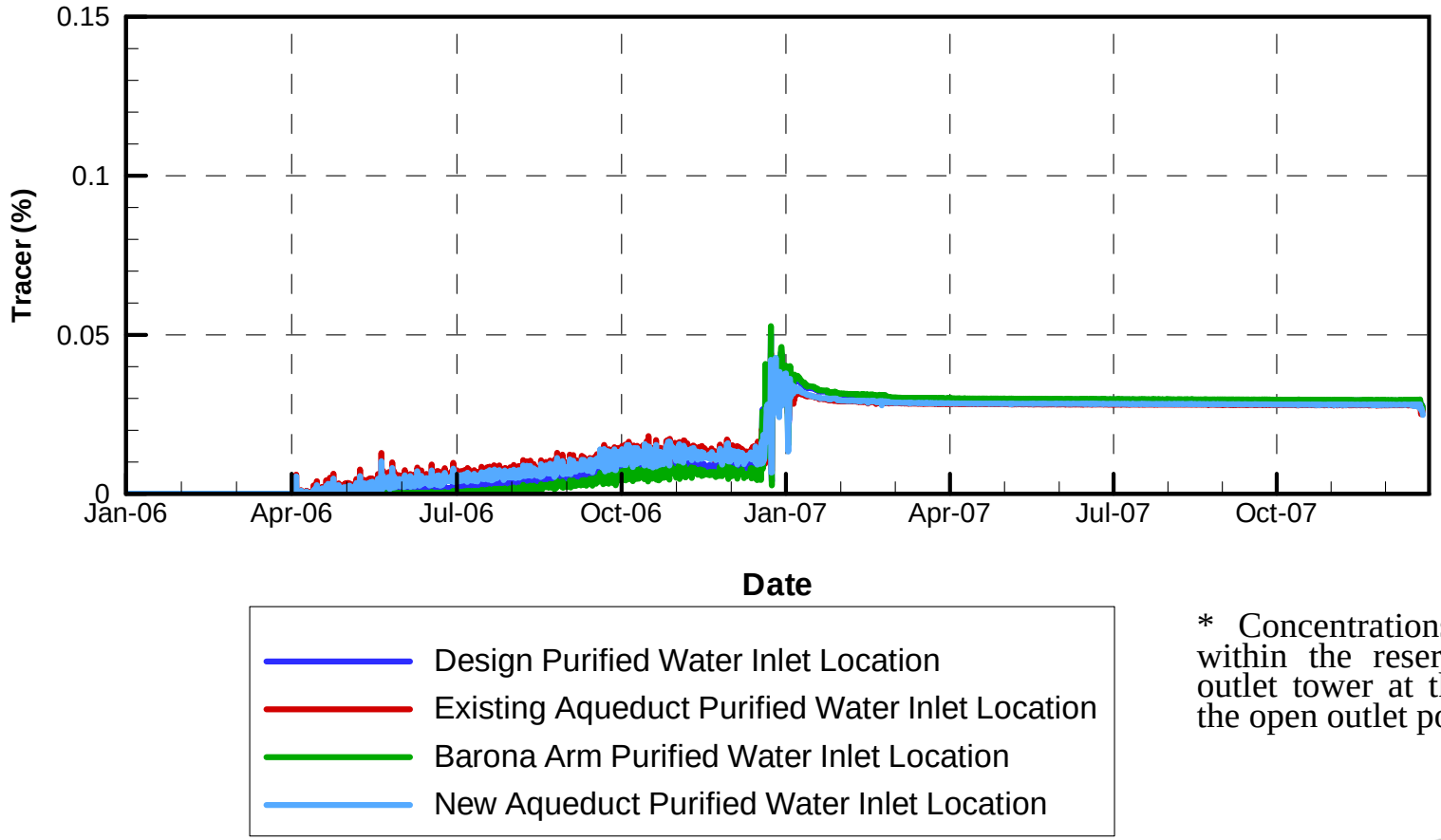

* Concentrations of tracer within the reservoir at the outlet tower at the depth of the open outlet port

Figure 26

FSI V094005
May 01, 2012

FLOW SCIENCE®

Comparison of Reservoir Outflow 24-hour Conservative Tracer Concentrations* from Different Purified Water Inlet Locations Under Base Case Operating Scenario

Tracer released on 7/1, Year 1 for 24 hours

(Open Port #2; Initial Inflow Concentration = 100%)

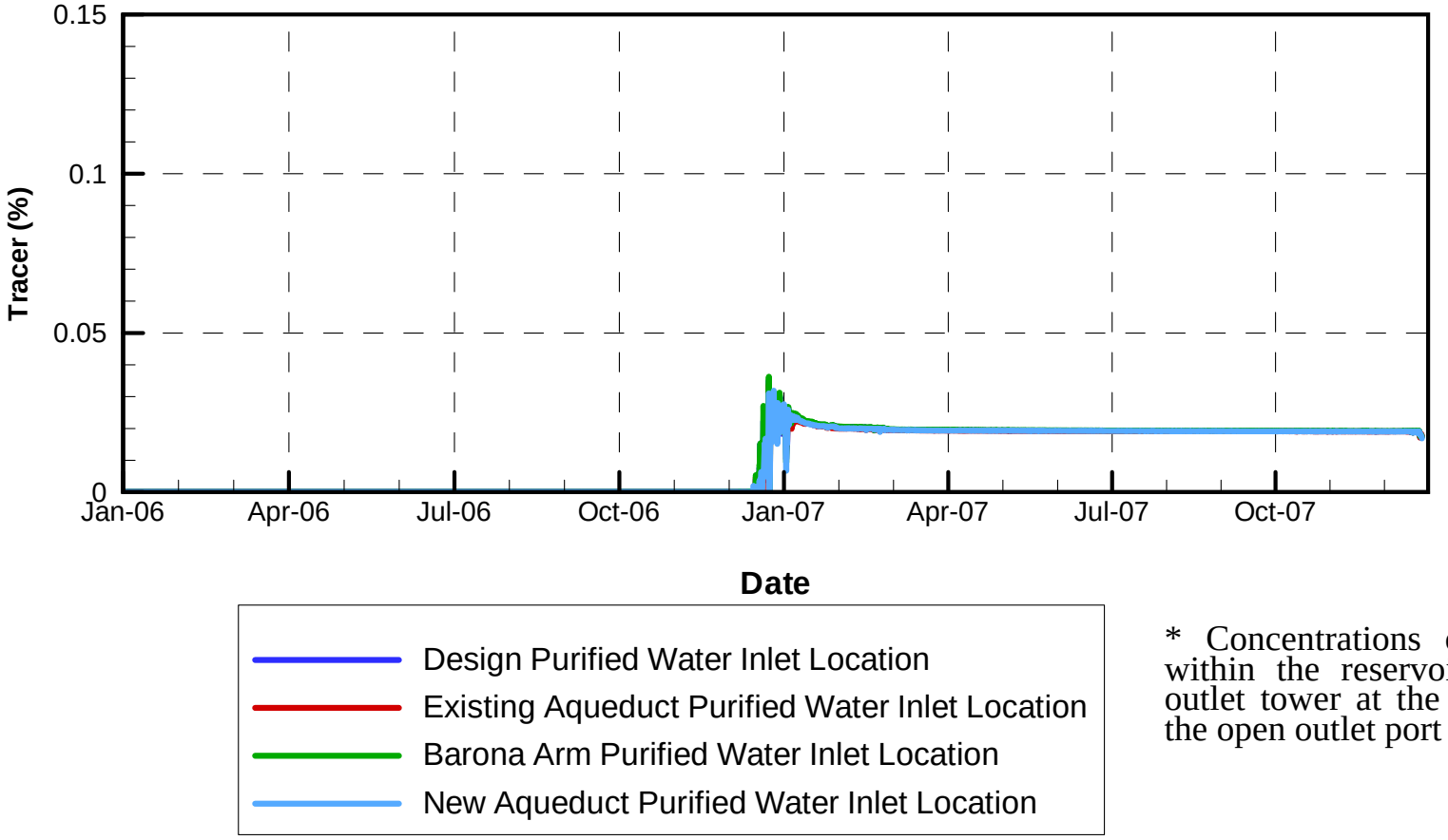

* Concentrations of tracer within the reservoir at the outlet tower at the depth of the open outlet port

FSI V094005
May 01, 2012

Figure 27

FLOW SCIENCE®

Comparison of Reservoir Outflow 24-hour Conservative Tracer Concentrations* from Different Purified Water Inlet Locations Under Base Case Operating Scenario

Tracer released on 10/1, Year 1 for 24 hours

(Open Port #2; Initial Inflow Concentration = 100%)

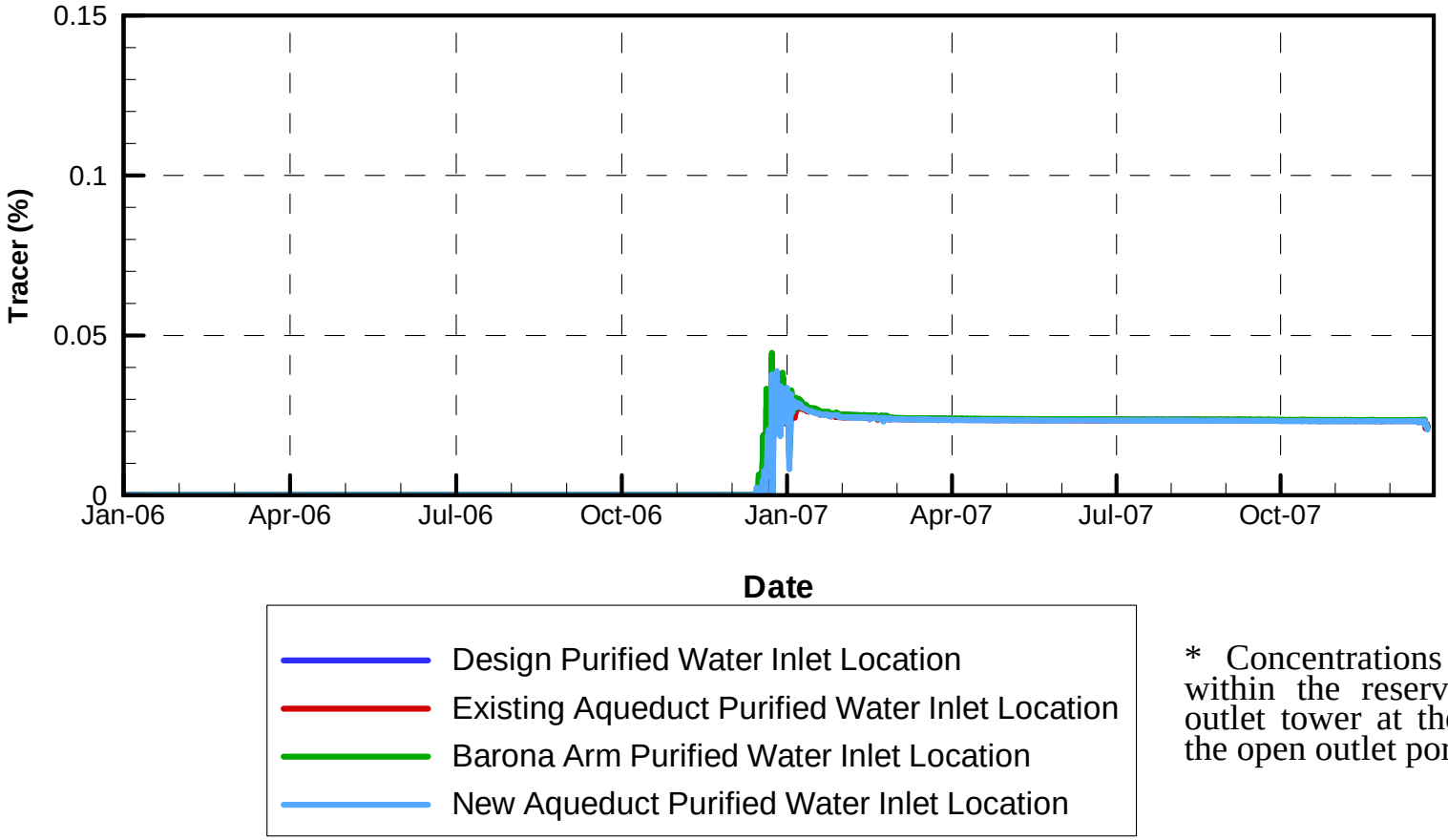

* Concentrations of tracer within the reservoir at the outlet tower at the depth of the open outlet port

FSI V094005
May 01, 2012

Figure 28

FLOW SCIENCE®

Comparison of Reservoir Outflow 24-hour Conservative Tracer Concentrations* from Different Purified Water Inlet Locations Under Base Case Operating Scenario

Tracer released on 1/5, Year 2 for 24 hours

(Open Port #2; Initial Inflow Concentration = 100%)

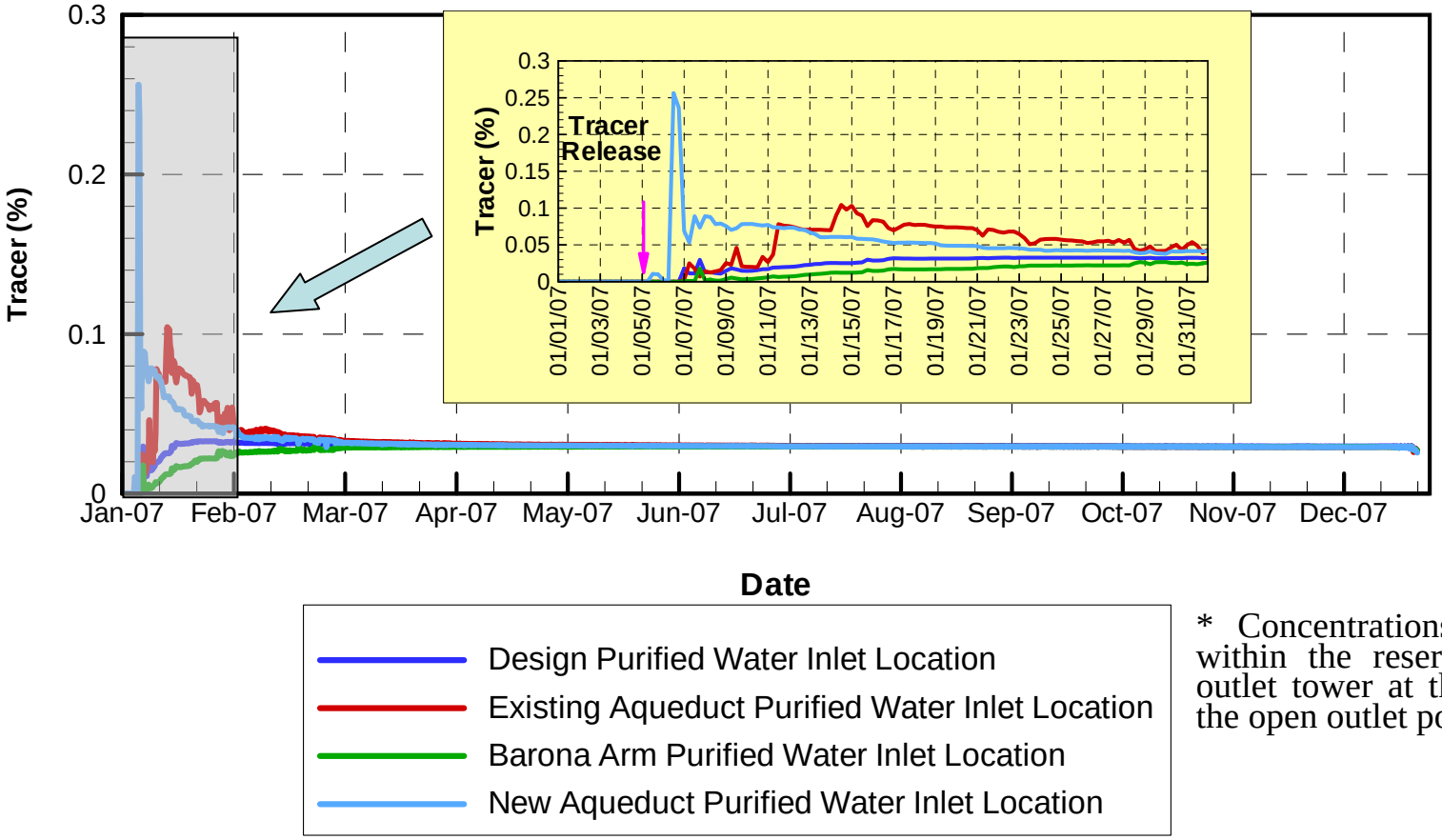

* Concentrations of tracer within the reservoir at the outlet tower at the depth of the open outlet port

Figure 29

FSI V094005
May 01, 2012

FLOW SCIENCE®

Comparison of Reservoir Outflow 24-hour Conservative Tracer Concentrations* from Different Purified Water Inlet Locations Under Base Case Operating Scenario

Tracer released on 1/15, Year 2 for 24 hours

(Open Port #2; Initial Inflow Concentration = 100%)

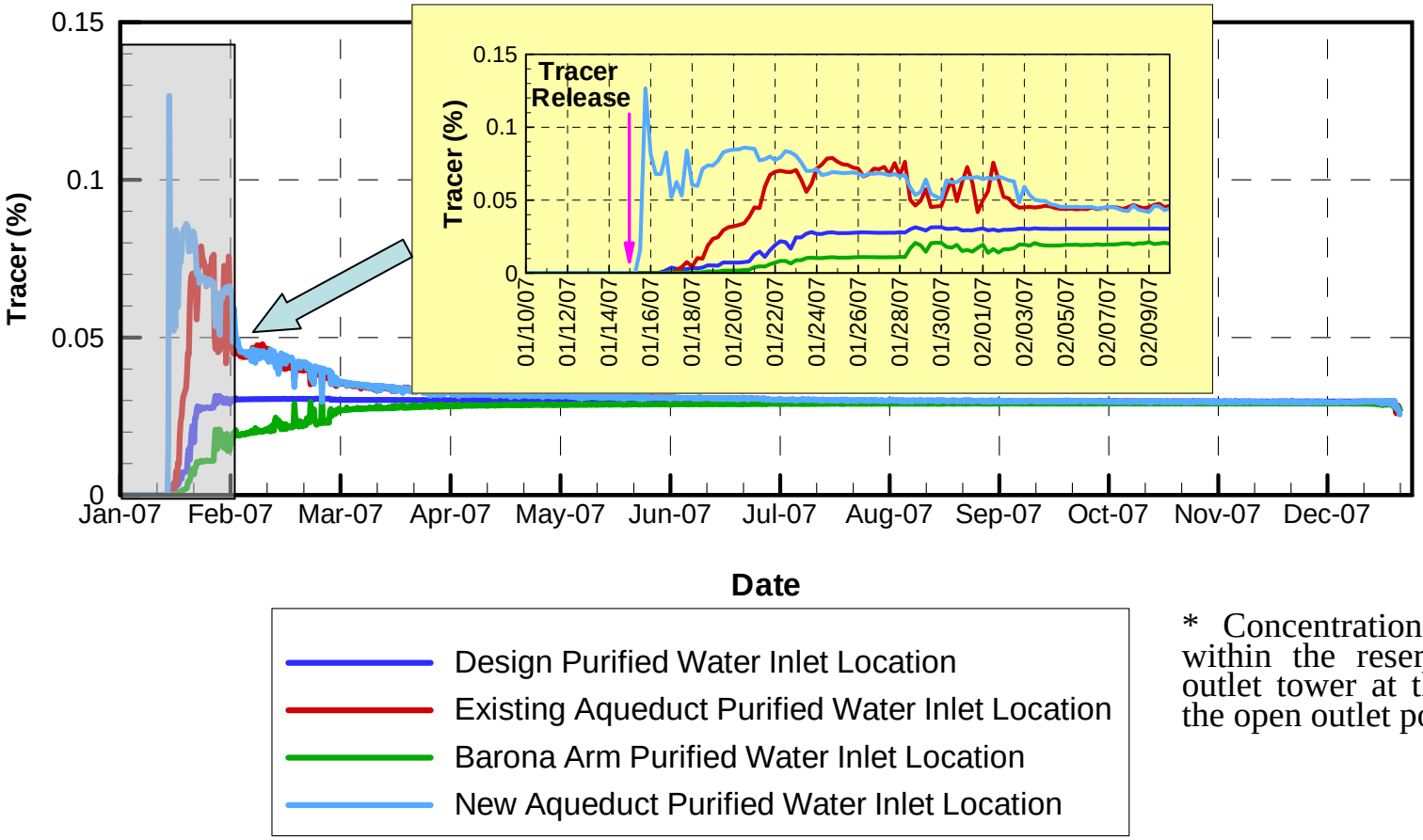

* Concentrations of tracer within the reservoir at the outlet tower at the depth of the open outlet port

Figure 30

FSI V094005
May 01, 2012

FLOW SCIENCE®

Comparison of Reservoir Outflow 24-hour Decaying Tracer Concentrations* from Different Purified Water Inlet Locations Under Extended Drought Scenario

(Open Port #2; Initial Inflow Concentration = 100%;
Decay Rate = One Log Reduction Per Month)

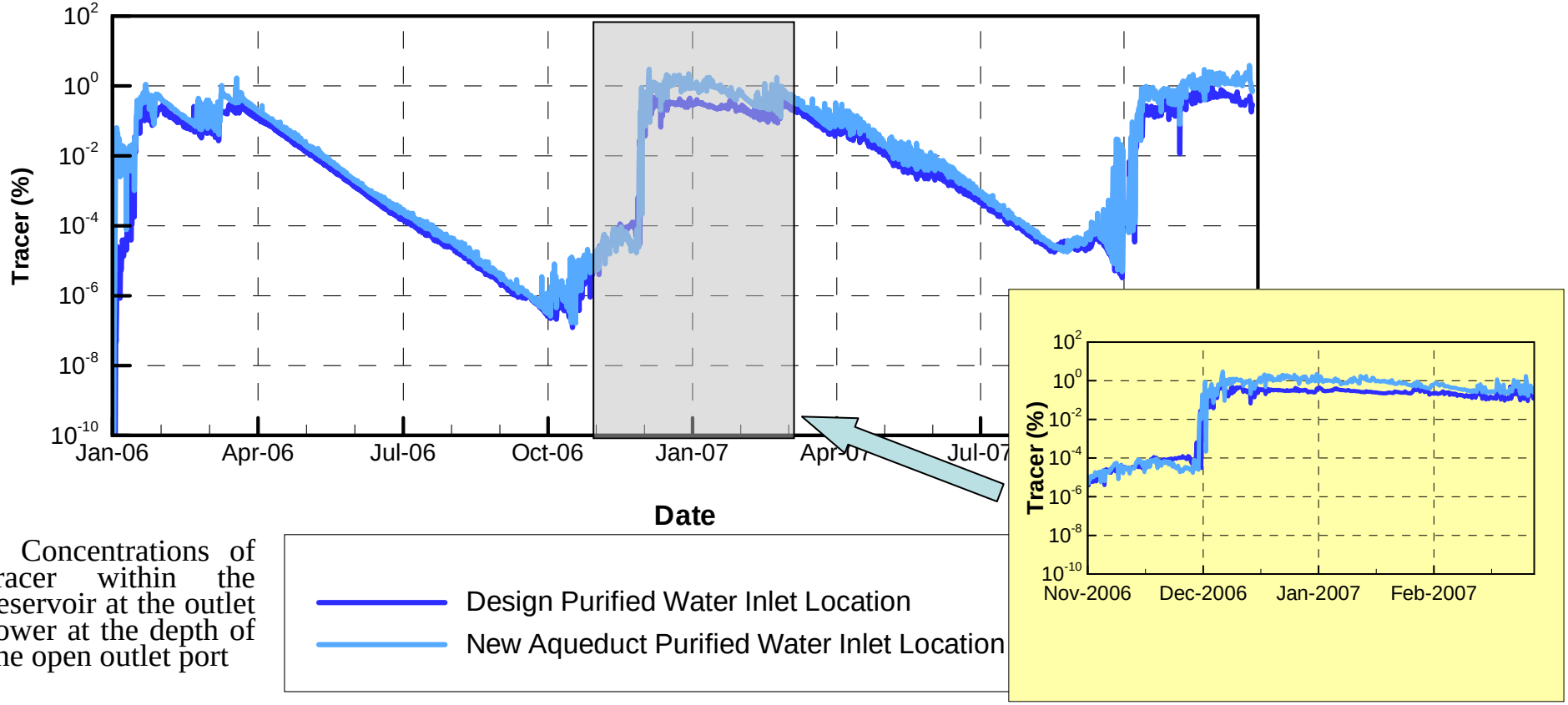

* Concentrations of tracer within the reservoir at the outlet tower at the depth of the open outlet port

FSI V094005
May 01, 2012

Figure 31

FLOW SCIENCE®

Comparison of Reservoir Outflow 24-hour Conservative Tracer Concentrations* from Different Purified Water Inlet Locations Under Extended Drought Scenario

Tracer Released on 12/2, Year 1 for 24 hours

(Open Port #2; Initial Inflow Concentration = 100%)

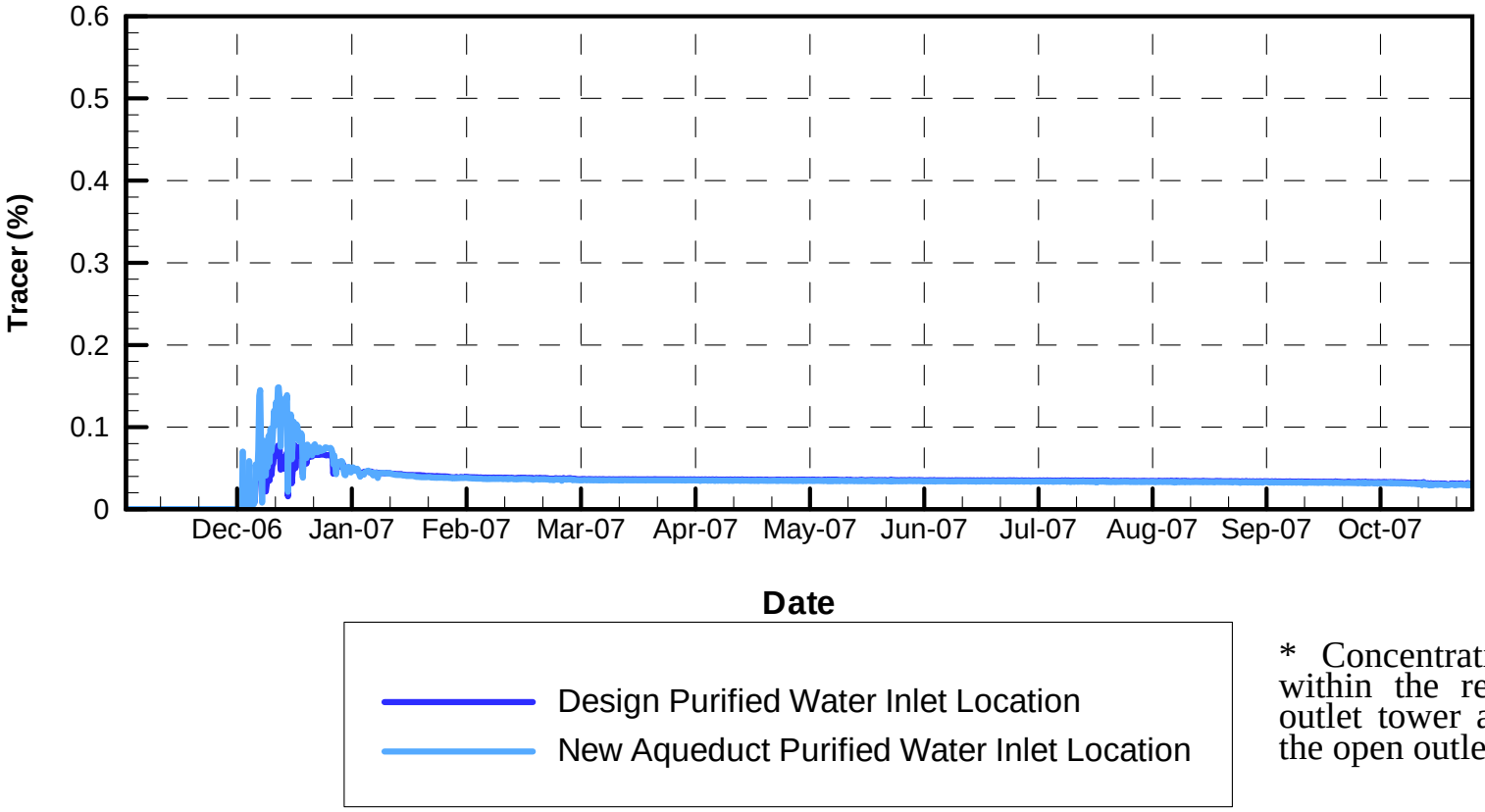

* Concentrations of tracer within the reservoir at the outlet tower at the depth of the open outlet port

FSI V094005
May 01, 2012

Figure 32

FLOW SCIENCE®

Comparison of Reservoir Outflow 24-hour Conservative Tracer Concentrations* from Different Purified Water Inlet Locations Under Extended Drought Scenario

Tracer Released on 1/6, Year 2 for 24 hours

(Open Port #2; Initial Inflow Concentration = 100%)

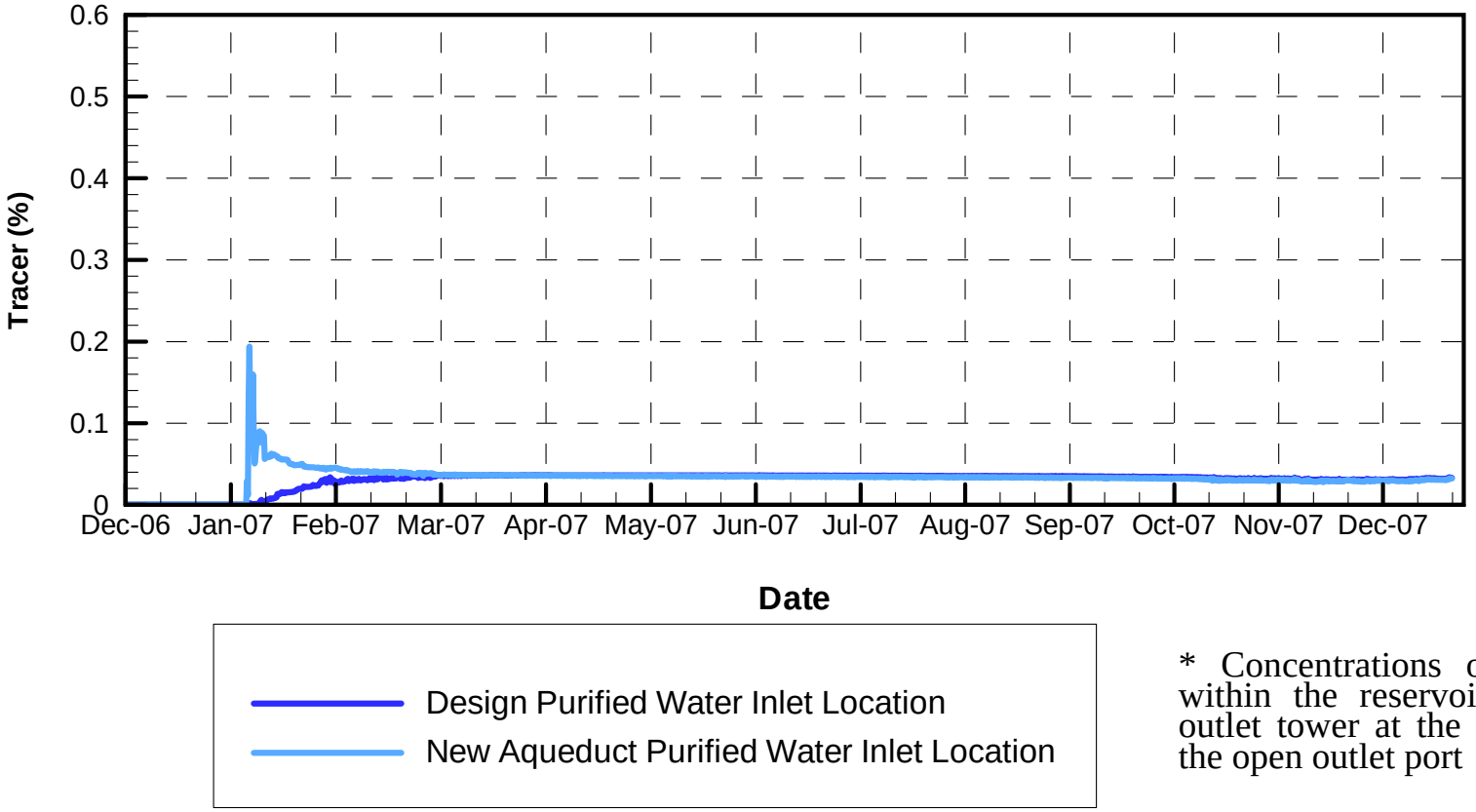

* Concentrations of tracer within the reservoir at the outlet tower at the depth of the open outlet port

FSI V094005
May 01, 2012

Figure 33

FLOW SCIENCE®

Comparison of Reservoir Outflow 24-hour Conservative Tracer Concentrations* from Different Purified Water Inlet Locations Under Extended Drought Scenario

Tracer Released on 1/14, Year 2 for 24 hours

(Open Port #2; Initial Inflow Concentration = 100%)

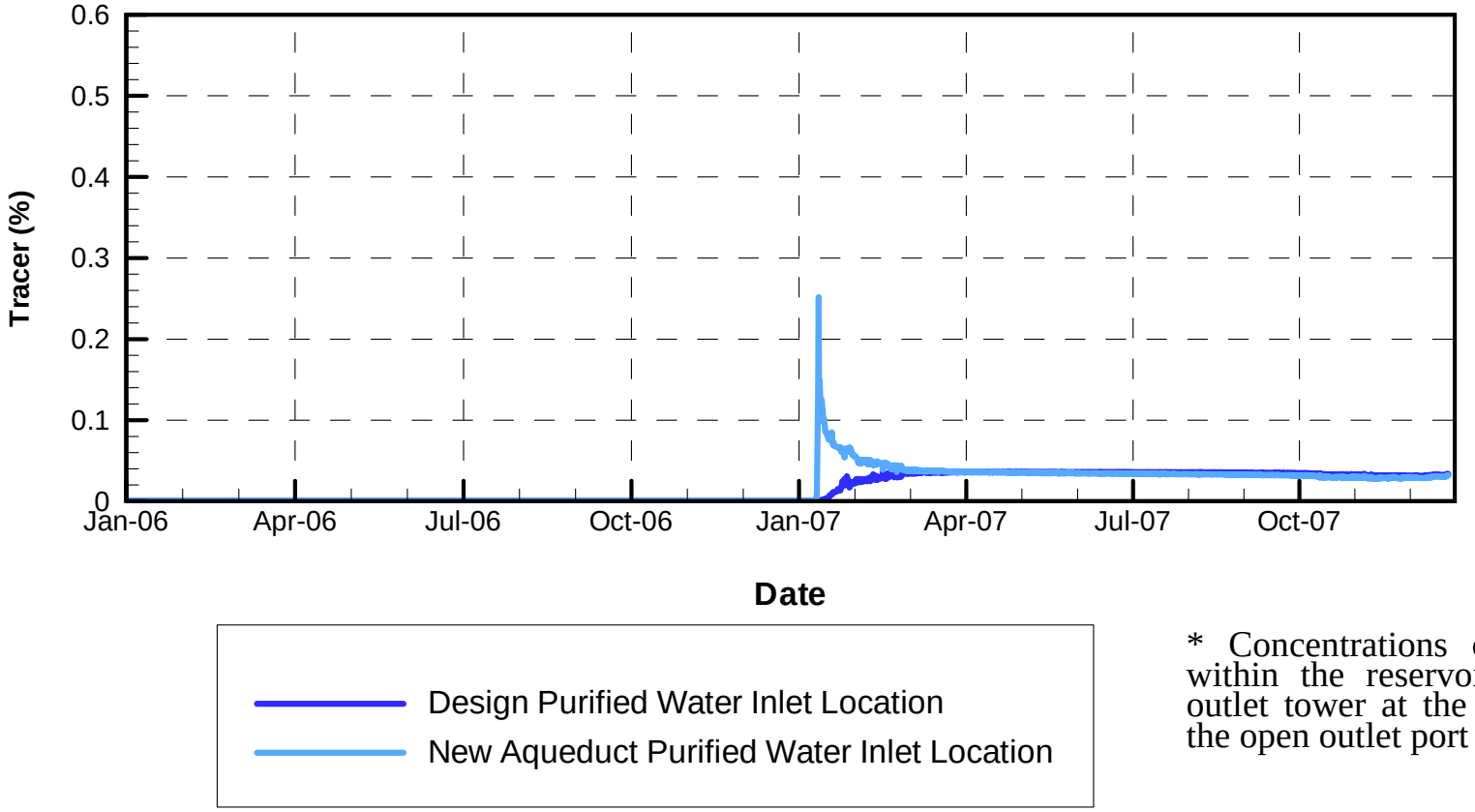

* Concentrations of tracer within the reservoir at the outlet tower at the depth of the open outlet port

FSI V094005
May 01, 2012

Figure 34

FLOW SCIENCE®

Comparison of Reservoir Outflow 24-hour Conservative Tracer Concentrations* from Different Purified Water Inlet Locations Under Extended Drought Scenario

Tracer Released on 1/21, Year 2 for 24 hours

(Open Port #2; Initial Inflow Concentration = 100%)

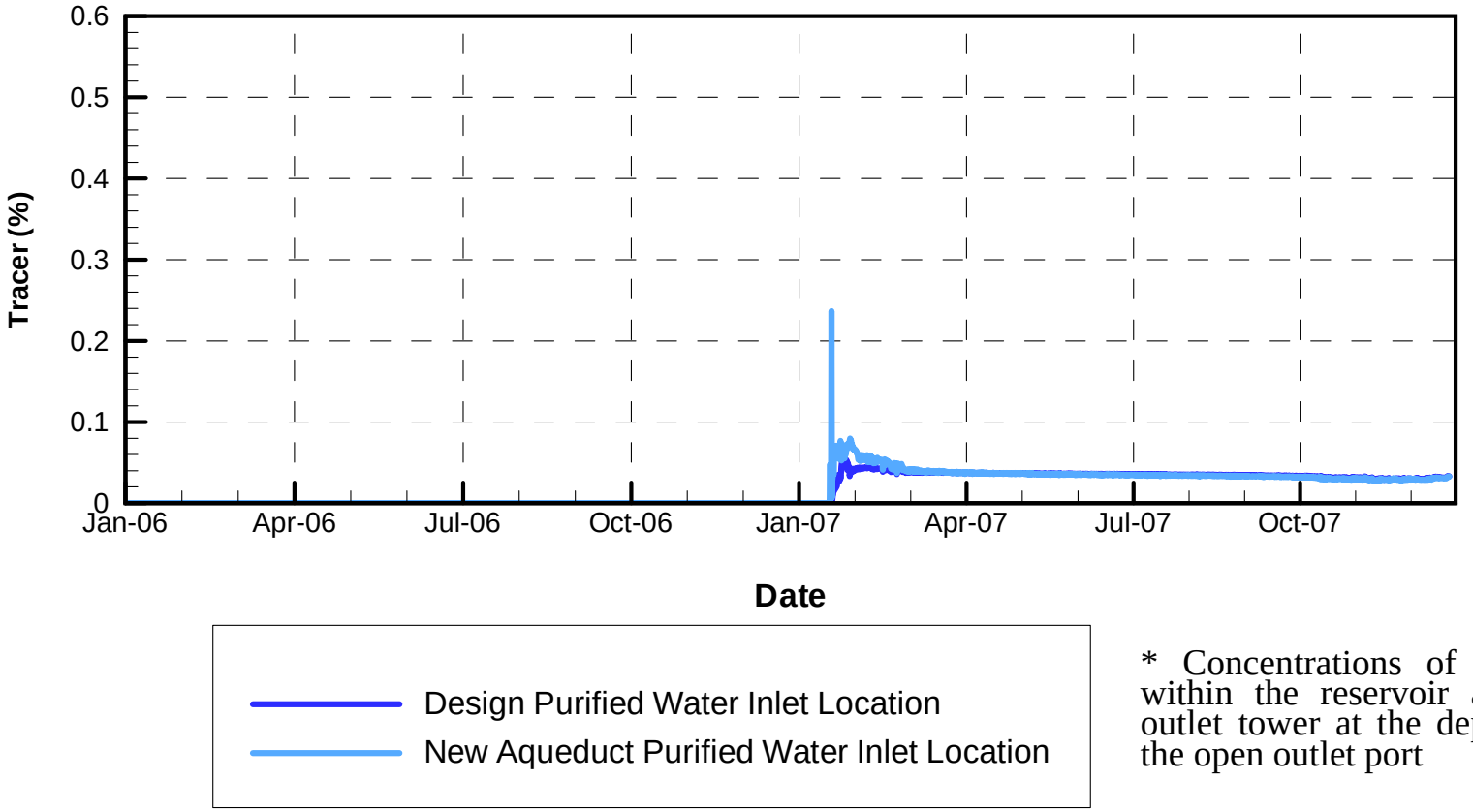

* Concentrations of tracer within the reservoir at the outlet tower at the depth of the open outlet port

FSI V094005
May 01, 2012

Figure 35

FLOW SCIENCE®

Comparison of Reservoir Outflow 24-hour Conservative Tracer Concentrations* from Different Purified Water Inlet Locations Under Extended Drought Scenario

Tracer Released on 11/29, Year 2 for 24 hours

(Open Port #2; Initial Inflow Concentration = 100%)

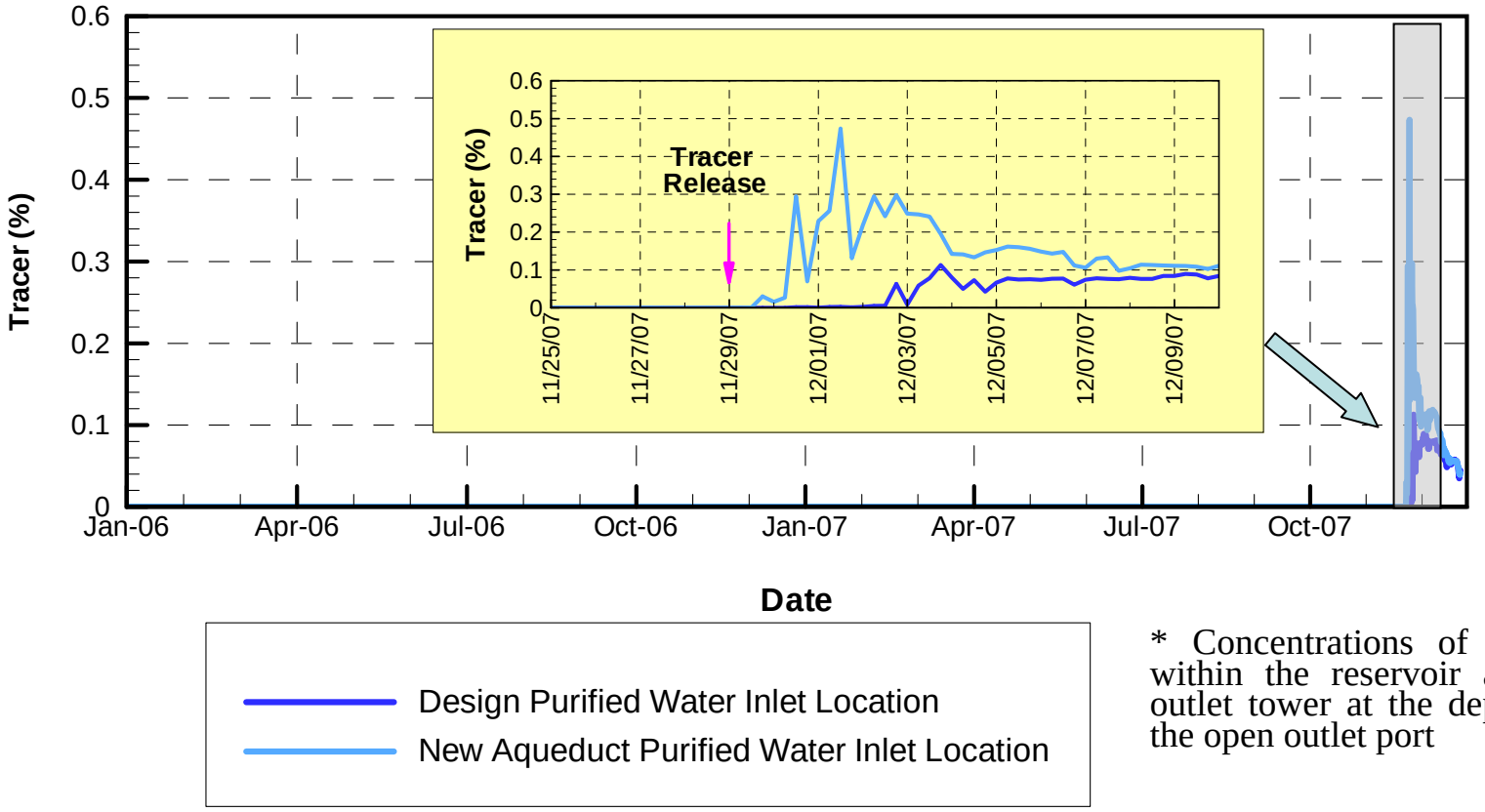

* Concentrations of tracer within the reservoir at the outlet tower at the depth of the open outlet port

FSI V094005
May 01, 2012

Figure 36

FLOW SCIENCE®

Comparison of Reservoir Outflow 24-hour Conservative Tracer Concentrations* from Different Purified Water Inlet Locations Under Extended Drought Scenario

Tracer Released on 12/2, Year 2 for 24 hours

(Open Port #2; Initial Inflow Concentration = 100%)

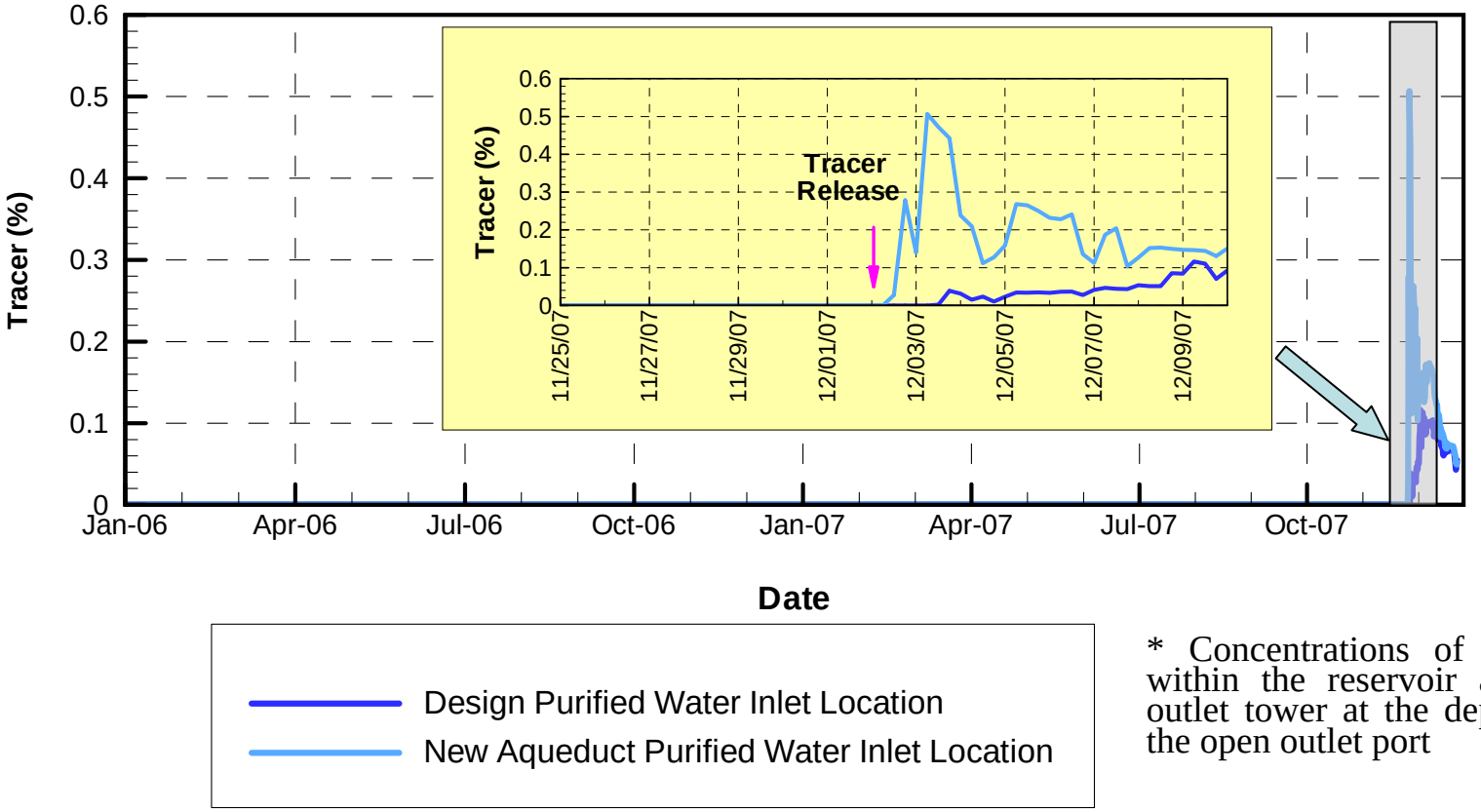

* Concentrations of tracer within the reservoir at the outlet tower at the depth of the open outlet port

FSI V094005
May 01, 2012

Figure 37

FLOW SCIENCE®

APPENDIX A

Description of ELCOM/CAEDYM/Visual Plumes Models and Evidence of Validation

DESCRIPTION OF ELCOM/CAEDYM MODELS AND EVIDENCE OF VALIDATION

The coupling of biogeochemical and hydrodynamic processes in numerical simulations is a fundamental tool for research and engineering studies of water quality in coastal oceans, estuaries, lakes, and rivers. A modeling system for aquatic ecosystems has been developed that combines a three-dimensional hydrodynamic simulation method with a suite of water quality modules that compute interactions between biological organisms and the chemistry of their nutrient cycles. This integrated approach allows for the feedback and coupling between biogeochemical and hydrodynamic systems so that a complete representation of all appropriate processes can be included in an analysis. The hydrodynamic simulation code is the Estuary Lake and Coastal Ocean Model (ELCOM) and the biogeochemical model is the Computational Aquatic Ecosystem Dynamics Model (CAEDYM).

The purpose of this appendix is to demonstrate that ELCOM and CAEDYM are accepted models that have been systematically tested and debugged, and then successfully validated in numerous applications. A history of the models is provided, followed by an outline of the general model methodology and evolution that emphasizes the basis of the ELCOM/ CAEDYM codes in previously validated models and research. Then the process of code development, testing, and validation of ELCOM/CAEDYM is detailed. Specific model applications are described to illustrate how the ELCOM/CAEDYM models have been applied to coastal oceans, estuaries, lakes, and rivers throughout the world and the results successfully validated against field data. Finally, a general description of the governing equations, numerical models, and processes used in the models is provided along with an extensive bibliography of supporting material.

A comprehensive description of the equations and methods used in the models is provided in the "Estuary Lake and Coastal Ocean Model: ELCOM v2.2 Science Manual" by Hodges and Dallimore (2006), "Estuary Lake and Coastal Ocean Model: ELCOM v2.2 User Manual" by Hodges and Dallimore (2007), "Computational Aquatic Ecosystem Dynamics Model: CAEDYM: v2.2 Science Manual" by Hipsey, Romero, Antenucci and Hamilton (2005), and the "Computational Aquatic Ecosystem Dynamics Model: CAEDYM: v2.2 User Manual" by Hipsey, Romero, Antenucci and Hamilton (2005).

A.1.1 MODEL HISTORY

The ELCOM/CAEDYM models were originally developed at the Centre for Water Research (CWR) at the University of Western Australia, although the hydrodynamics

code ELCOM is an outgrowth of a hydrodynamic model developed earlier by Professor Vincenzo Casulli in Italy and now in use at Stanford University under the name TRIM-3D. The CAEDYM model was essentially developed at CWR as an outgrowth of earlier water quality modules used in the one-dimensional model, Dynamic Reservoir Simulation Model - Water Quality (DYRESM-WQ, Hamilton and Schladow, 1997).

The original ELCOM/CAEDYM models, as developed by CWR, were implemented in Fortran 90 (with F95 extensions) on a UNIX computer system platform. In 2001, the codes for both models were ported to a personal computer (PC) platform through an extensive recompiling and debugging effort by Flow Science Incorporated (Flow Science) in Pasadena, California. Since then, Flow Science has updated the PC version of the code several times when new versions of the code have been released by CWR.

A.1.2 MODEL METHODOLOGY

ELCOM is a three-dimensional numerical simulation code designed for practical numerical simulation of hydrodynamics and thermodynamics for inland and coastal waters. The code links seamlessly with the CAEDYM biogeochemical model undergoing continuous development at CWR, as shown graphically in **Figure A.1**. The

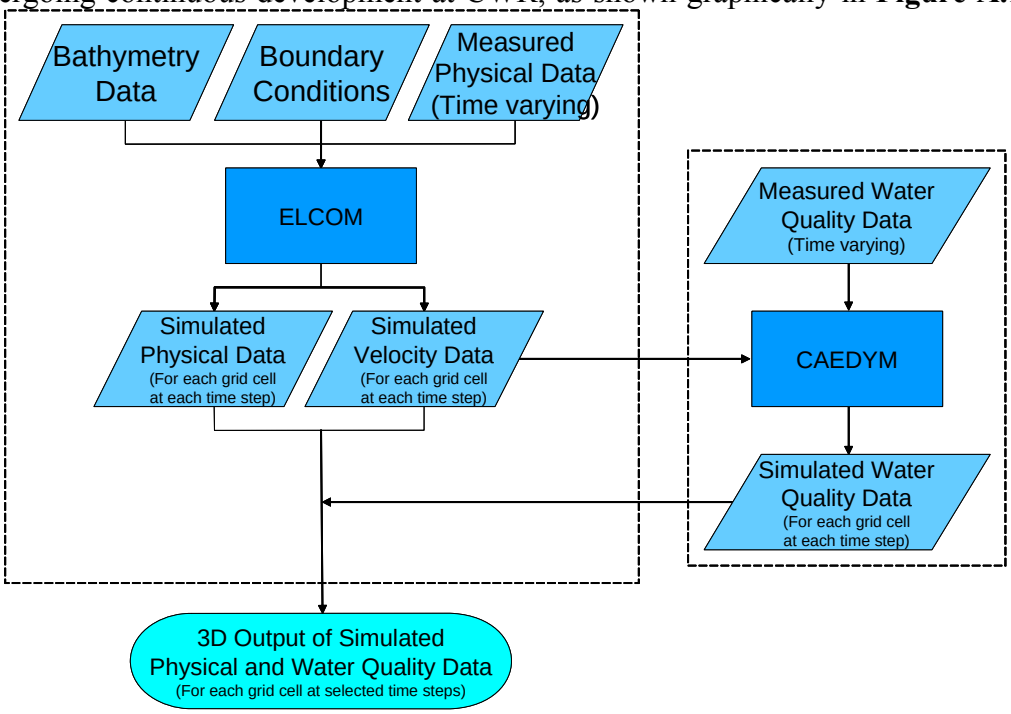

Figure A.1 Flow chart showing the integration of the linked ELCOM/CAEDYM models.

combination of the two codes provides three-dimensional simulation capability for examination of changes in water quality that arise from anthropogenic changes in either quality of inflows or reservoir operations.

The numerical method used in ELCOM is based on the TRIM-3D model scheme of Casulli and Cheng (1992) with adaptations made to improve accuracy, scalar conversion, numerical diffusion, and implementation of a mixed-layer model. The ELCOM model also extends the TRIM-3D scheme by including conservative advection of scalars. The unsteady Reynolds-averaged, Navier-Stokes equations, and the scalar transport equations serve as the basis of ELCOM. The pressure distribution is assumed hydrostatic and density changes do not impact the inertia of the fluid (the Boussinesq approximation), but are considered in the fluid body forces. There is an eddy-viscosity approximation for the horizontal turbulence correlations that represent the turbulent momentum transfer. Vertical momentum transfer is handled by a Richardson number-based diffusion coefficient. Since numerical diffusion generally dominates molecular processes, molecular diffusion in the vertical direction is neglected in ELCOM.

Both ELCOM and TRIM-3D are three-dimensional, computational fluid dynamics (CFD) models. CFD modeling is a validated and well-established approach to solving the equations of fluid motions in a variety of disciplines. Prior to the development of TRIM-3D, there were difficulties in modeling density-stratified flows and such flows required special numerical methods. With TRIM-3D, Casulli and Cheng (1992) developed the first such successful method to model density-stratified flows, such as occur in the natural environment. Since then, TRIM-3D has been validated by numerous publications. ELCOM is based on the same proven method, but incorporates additional improvements as described above. Furthermore, the ELCOM model is based on governing equations and numerical algorithms that have been used in the past (*e.g.,* in validated models such as TRIM-3D), and have been validated in refereed publications. For example:

- The hydrodynamic algorithms in ELCOM are based on the Euler-Lagrange method for advection of momentum with a conjugate gradient solution for the free-surface height (Casulli and Cheng, 1992).

- The free-surface evolution is governed by vertical integration of the continuity equation for incompressible flow applied to the kinematic boundary condition (*e.g.*, Kowalik and Murty, 1993).

- The numerical scheme is a semi-implicit solution of the hydrostatic Navier-Stokes equations with a quadratic Euler-Lagrange, or semi-Lagrangian (Staniforth and Côté, 1991).

- Passive and active scalars (*i.e.,* tracers, salinity, and temperature) are advected using a conservative ULTIMATE QUICKEST discretization (Leonard, 1991). The ULTIMATE QUICKEST approach has been implemented in two-dimensional format and demonstration of its effectiveness in estuarine flows has been documented by Lin and Falconer (1997).

- Heat exchange is governed by standard bulk transfer models found in the literature (*e.g.*, Smooch and DeVries, 1980; Imberger and Patterson, 1981; Jacquet, 1983).

- The vertical mixing model is based on an approach derived from the mixing energy budgets used in one-dimensional lake modeling as presented in Imberger and Patterson (1981), Spigel et al (1986), and Imberger and Patterson (1990). Furthermore, Hodges presents a summary of validation using laboratory experiments of Stevens and Imberger (1996). This validation exercise demonstrates the ability of the mixed-layer model to capture the correct momentum input to the mixed-layer and reproduce the correct basin-scale dynamics, even while boundary-induced mixing is not directly modeled.

- The wind momentum model is based on a mixed-layer model combined with a model for the distribution of momentum over depth (Imberger and Patterson, 1990).

The numerical approach and momentum and free surface discretization used in ELCOM are defined in more detail in Hodges, Imberger, Saggio, and Winters (1999). Similarly, the water quality processes and methodology used in CAEDYM are described in more detail in Hamilton and Schladow (1997). Further technical details on ELCOM and CAEDYM are provided in Sections 0 and 0 below.

A.1.3 VALIDATION AND APPLICATION OF ELCOM/CAEDYM

Since initial model development, testing and validation of ELCOM and/or CAEDYM have been performed and numerous papers on model applications have been presented, written, and/or published as described in more detail below. In summary:

- ELCOM solves the full three-dimensional flow equations with small approximations.

- ELCOM/CAEDYM was developed, tested, and validated over a variety of test cases and systems by CWR.

- Papers on ELCOM/CAEDYM algorithms, methodology, and applications have been published in peer reviewed journals such as the *Journal of Geophysical Research*, the *Journal of Fluid Mechanics*, the *Journal of Hydraulic Engineering*, the *International Journal for Numerical Methods in Fluids*, and *Limnology and Oceanography*.

- ELCOM/CAEDYM was applied by Flow Science to Lake Mead, Nevada. As part of this application, mass balances were verified and results were presented to a model review panel over a two-year period. The model review panel, the National Park Service, the United States Bureau of Reclamation, the Southern Nevada Water Authority, and the Clean Water Coalition (a consortium of water and wastewater operators in the Las Vegas, Nevada, region) all accepted the ELCOM/CAEDYM model use and validity.

- There are numerous applications of ELCOM/CAEDYM in the literature that compare the results to data, as summarized in Section 0.

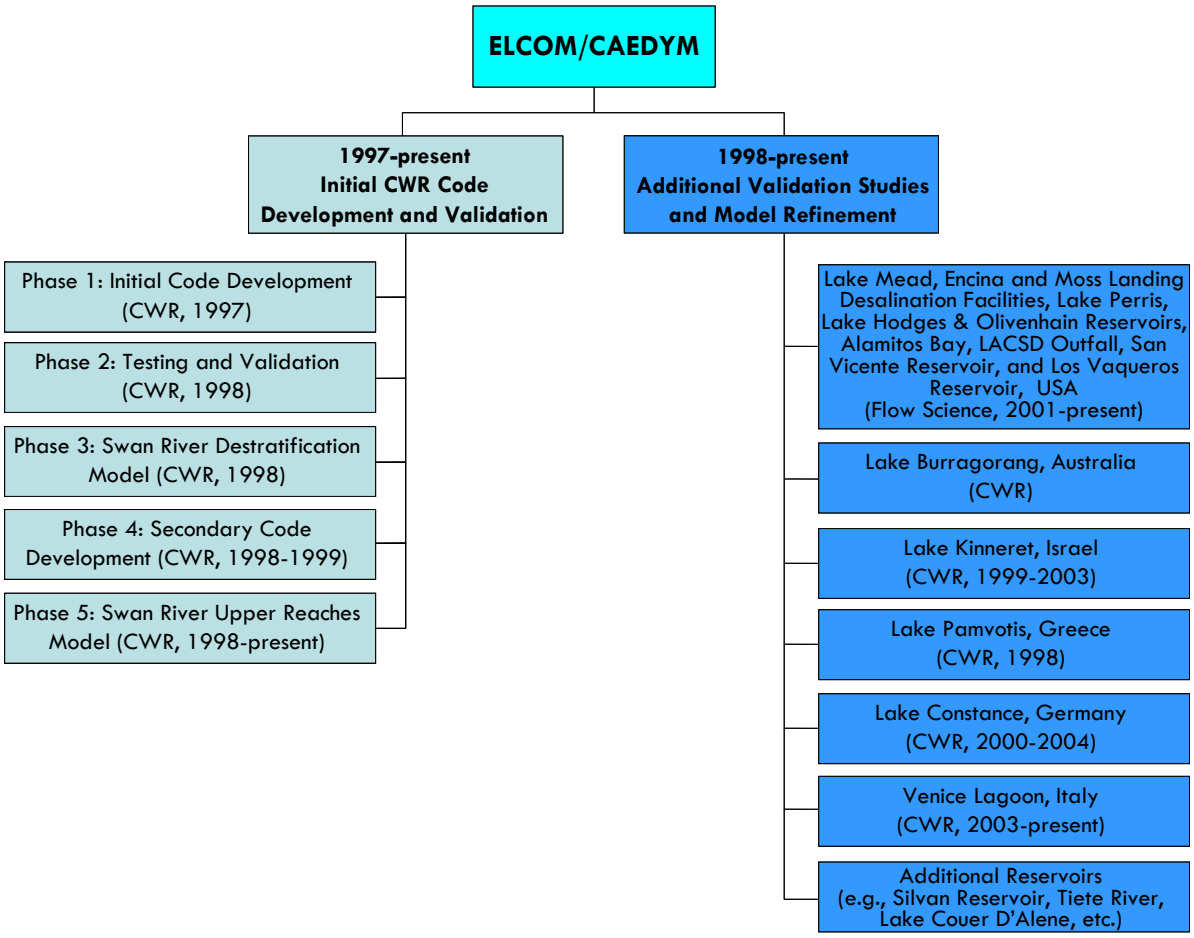

Figure A.2 ELCOM/CAEDYM code development, testing, validation, and applications by CWR and Flow Science Incorporated.

The process of code development, testing, and validation of ELCOM/CAEDYM by CWR, and the ongoing validation and refinement of the codes through further application of the models are detailed in the following subsections. The major components of the development, testing, and validation process are summarized in **Figure A.2**.

A.1.3.1 CWR Code Development, Testing, and Validation

Initial development of the code by CWR occurred from March through December 1997 (Phase 1), followed by a period of testing and validation from January through April 1998 (Phases 2 and 3). Secondary code development by CWR occurred from September 1998 through February 1999 (Phase 4). Testing and validation were

performed over a variety of test cases and systems to ensure that all facets of the code were tested. In addition, Phase 5 modeling of the Swan River since 1998 has been used to gain a better understanding of the requirements and limitations of the model (Hodges et al, 1999).

A.1.3.1.1 *Phase 1: Initial Code Development*

The ELCOM code was initially conceived by CWR as a Fortran 90/95 adaptation of the TRIM-3D model of Casulli and Cheng (1992) in order to: 1) link directly to the CAEDYM water quality module developed concurrently at CWR and 2) provide a basis for future development in a modern programming language. Although written in Fortran 77, TRIM-3D is considered a state-of-the-art numerical model for estuarine applications using a semi-implicit discretization of the Reynolds-averaged hydrostatic Navier-Stokes equations and an Euler-Lagrange method for momentum and scalar transport.

During development of ELCOM, it became clear that additional improvements to the TRIM-3D algorithm were required for accurate solution of density-stratified flows in estuaries. After the basic numerical algorithms were written in Fortran 90, subroutine-by-subroutine debugging was performed to ensure that each subroutine produced the expected results. Debugging and testing of the entire model used a series of test cases that exercised the individual processes in simplified geometries. This included test cases for the functioning of the open boundary condition (tidal forcing), surface wave propagation, internal wave propagation, scalar transport, surface thermodynamics, density underflows, wind-driven circulations, and flooding/drying of shoreline grid cells. Shortcomings identified in the base numerical algorithms were addressed during secondary code development (Phase 4).

Towards the end of the initial code development, ELCOM/CAEDYM were coupled and test simulations were run to calibrate the ability of the models to work together on some simplified problems. Results showing the density-driven currents induced by phytoplankton shading were presented at the Second International Symposium on Ecology and Engineering (Hodges and Herzfeld, 1997). Further details of modeling of density-driven currents due to combinations of topographic effects and phytoplankton shading were presented at a joint meeting of the American Geophysical Union (AGU) and the American Society of Limnology and Oceanography (ASLO) by Hodges et al. (1998), and at a special seminar at Stanford University (Hodges 1998). Additionally, presentations by Hamilton (1997), Herzfeld et al. (1997), and Herzfeld and Hamilton (1998) documented the concurrent development of the CAEDYM ecological model.

A.1.3.1.2*Phase 2: Testing and Validation*

The simplified geometry tests of Phase I revealed deficiencies in the TRIM-3D algorithm including the inability of the TRIM-3D Euler-Lagrange method (ELM) to provide conservative transport of scalar concentrations (e.g., salinity and temperature). Thus, a variety of alternate scalar transport methods were tested, with the best performance being a flux-conservative implementation of the ULTIMATE filter applied to third-order QUICKEST discretization based on the work of Leonard (1991).

Model testing and validation against simple test cases was again undertaken. In addition, a simulation of a winter underflow event in Lake Burragorang in New South Wales, Australia, was performed to examine the ability of the model to capture a density underflow in complex topography in comparison to field data taken during the inflow event. These tests showed that the ability to model underflows is severely constrained by the cross-channel grid resolution.

A.1.3.1.3*Phase 3: Swan River Destratification Model*

Phase 3 involved examining a linked ELCOM/CAEDYM destratification model of the Swan River system during a period of destratification in 1997 when intensive field monitoring had been conducted. The preliminary results of this work were presented at the Swan-Canning Estuary Conference (Hertzfeld *et al,* 1998). More comprehensive results were presented at the Western Australian Estuarine Research Foundation (WAERF) Community Forum (Imberger, 1998).

A.1.3.1.4*Phase 4: Secondary Code Development*

In conducting the Phase 3 Swan River destratification modeling, it became clear to CWR that long-term modeling of the salt-wedge propagation would require a better model for mixing dynamics than presently existed. Thus, the availability of an extensive field data set for Lake Kinneret, Israel, led to its use as a test case for development of an improved mixing algorithm for stratified flows (Hodges *et al*, 1999).

A further problem appeared in the poor resolution of momentum terms using the linear ELM discretization (i.e., as used in the original TRIM-3D method). Since the conservative ULTIMATE QUICKEST method (used for scalar transport, see Phase 1 above) does not lend itself to efficient use for discretization of momentum terms in a semi-implicit method, a quadratic ELM approach was developed for more accurate discretization of the velocities.

A.1.3.1.5 *Phase 5: Swan River Upper Reaches Model*

Phases 1-4 developed and refined the ELCOM code for accurate modeling of three-dimensional hydrodynamics where the physical domain is well resolved. Phase 5 is an ongoing process of model refinement that concentrates on developing a viable approach to modeling longer-term evolution hydrodynamics and water quality in the Swan River where fine-scale resolution of the domain is not practical. The Swan River application is also used for ongoing testing and calibration of the CAEDYM water quality module.

The Swan River estuary is located on the Swan Coastal Plain, Western Australia. It is subject to moderate to high nutrient loads associated with urban and agricultural runoff and suffered from *Microcystis aeruginosa* blooms in January 2000. In an effort to find a viable means of conducting seasonal to annual simulations of the Swan River that retain the fundamental along-river physics and the cross-channel variability in water quality parameters, CWR has developed and tested ELCOM/CAEDYM extensively. A progress report by Hodges et al (1999) indicates that ELCOM is capable of accurately reproducing the hydrodynamics of the Swan River over long time scales with a reasonable computational time.

Furthermore, studies conducted by Robson and Hamilton (2002) proved that ELCOM/CAEDYM accurately reproduced the unusual hydrodynamic circumstances that occurred in January 2000 after a record maximum rainfall, and predicted the magnitude and timing of the *Microcystis* bloom. These studies show that better identification and monitoring procedures for potentially harmful phytoplankton species could be established with ELCOM/CAEDYM and will assist in surveillance and warnings for the future.

A.1.3.2 Model Applications

In addition to the initial code development, testing, and validation by CWR, numerous other applications of ELCOM/CAEDYM have been developed by CWR and validated against field data. Additionally, Flow Science has applied ELCOM/CAEDYM extensively at Lake Mead (USA) and validated the results against measured data. The results of numerous ELCOM/CAEDYM model applications are presented below.

A.1.3.2.1 *Lake Mead (Nevada, USA)*

An ELCOM/CAEDYM model of Boulder Basin, Lake Mead near Las Vegas, Nevada, was used to evaluate alternative discharge scenarios for inclusion in an Environmental Impact Statement (EIS) for the Clean Water Coalition (CWC), a

consortium of water and wastewater operators in the Las Vegas region. **Figure A.3** is a cut-away of the three-dimensional model grid used for Boulder Basin, showing the varying grid spacing in the vertical direction.

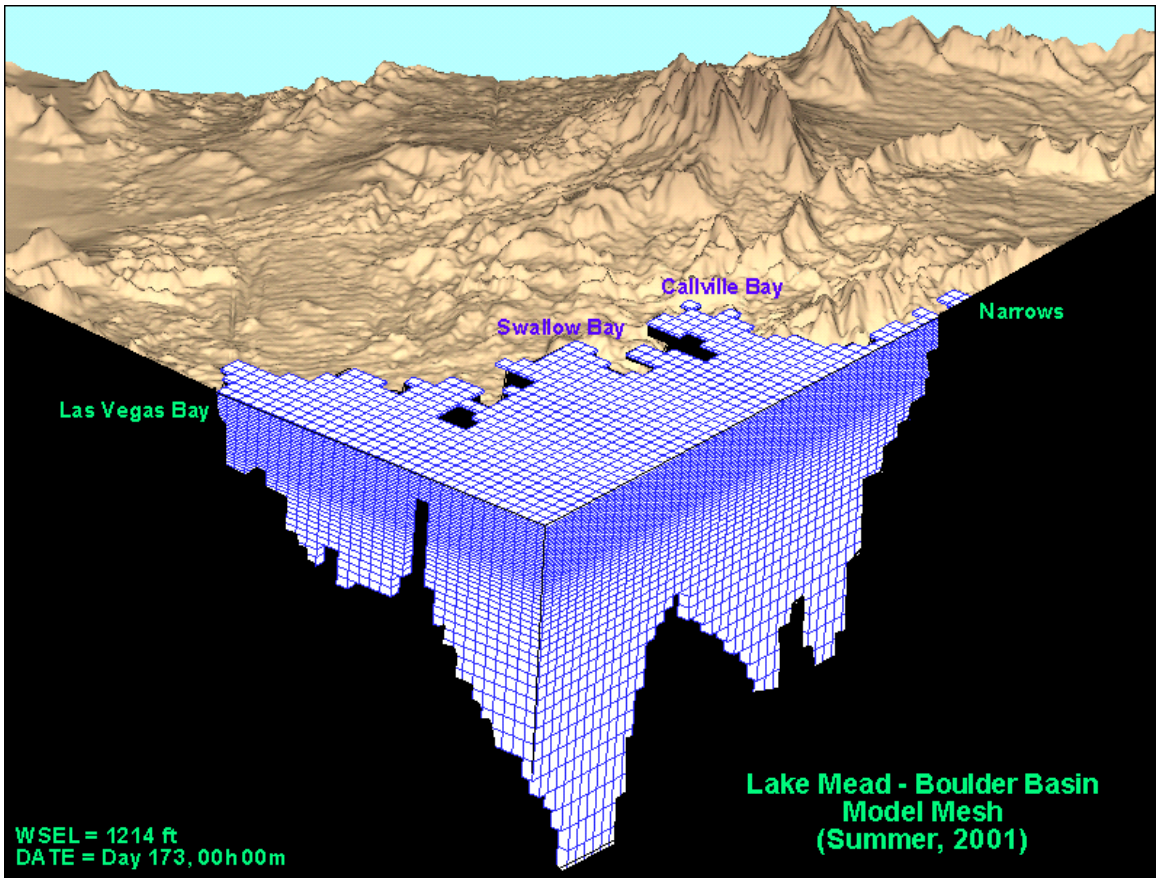

Figure A.3 Model grid for Lake Mead Boulder Basin model.

As part of the EIS process, a model review panel met monthly for two years to review the validation of the ELCOM/CAEDYM model, its calibration against field data, and its application. The modeling committee approved the use of the model. Subsequently, a scientific Water Quality Advisory Panel concluded that the ELCOM/CAEDYM model was applicable and acceptable. The members of the Water Quality Advisory Panel were diverse and included Jean Marie Boyer, Ph.D., P.E. (Water Quality Specialist/Modeler, Hydrosphere), Chris Holdren, Ph.D., CLM (Limnologist, United States Bureau of Reclamation), Alex Horne, Ph.D. (Ecological Engineer, University of California Berkeley), and Dale Robertson, Ph.D. (Research Hydrologist, United States Geological

Survey). More specifically, the Water Quality Advisory Panel agreed on the following findings:

- The ELCOM/CAEDYM model is appropriate for the project.
- There are few three-dimensional models available for reservoirs. ELCOM is one of the best hydrodynamic models and has had good success in the Boulder Basin of Lake Mead and other systems.
- The ELCOM model accurately simulates most physical processes.
- The algorithms used in CAEDYM are widely accepted (a biological consultant, Professor David Hamilton of The University of Waikato, New Zealand, was retained to review the CAEDYM coefficients and algorithms).

The Boulder Basin ELCOM/CAEDYM model was calibrated against four years of measured data for numerous physical and water quality parameters including temperature, salinity, conductivity, dissolved oxygen, pH, nutrients (nitrogen and phosphorus), chlorophyll *a*, perchlorate, chloride, sulfate, bromide, and total organic carbon. Detailed results of this calibration and the subsequent evaluation of alternative discharge scenarios were made available in late 2005 in the CWC EIS that was being prepared for this project. An example of the calibration results for chlorophyll *a* for 2002 is presented in **Figure A.4** below. In this figure, simulated concentrations are compared against field data measured in the lake by the United States Bureau of Reclamation (USBR) and the City of Las Vegas (COLV).

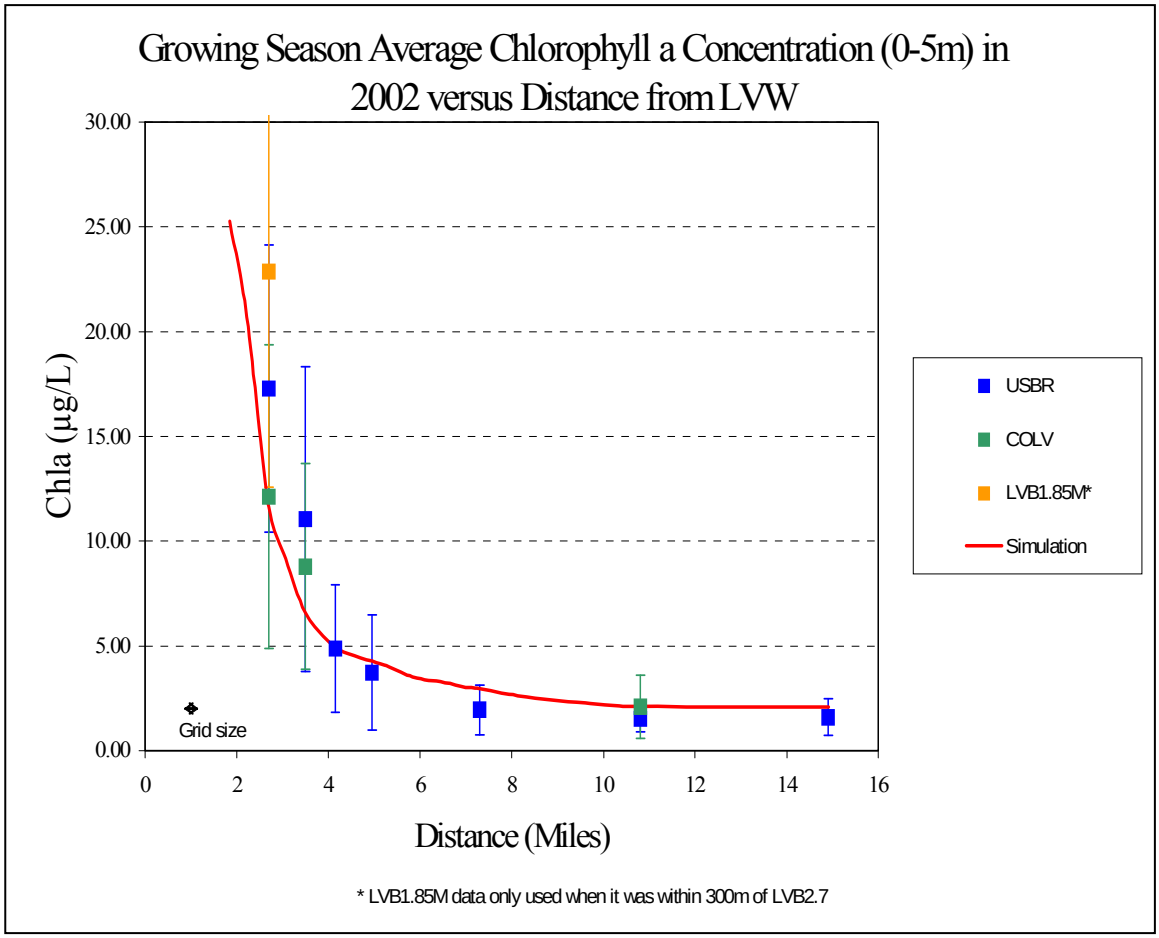

Figure A.4 ELCOM/CAEDYM calibration results for chlorophyll a in Boulder Basin for 2002 as a function of distance from the inflow at Las Vegas Wash.

Most recently, the original Boulder Basin model was extended to include all of Lake Mead, including the Overton Arm and Gregg Basin. The extended whole lake ELCOM/CAEDYM model has been calibrated against nine (9) years of data for use in informing design and operations management decisions. Specifically, the model has been used to simulate temperature (including stratification patterns), salinity, conductivity, dissolved oxygen, nutrients, chlorophyll *a* (as a surrogate for algae), perchlorate, total organic carbon, bromide, and suspended solids. **Figure A.5** below shows the extent of the expanded whole lake domain and the calibration results for conductivity for February 2005.

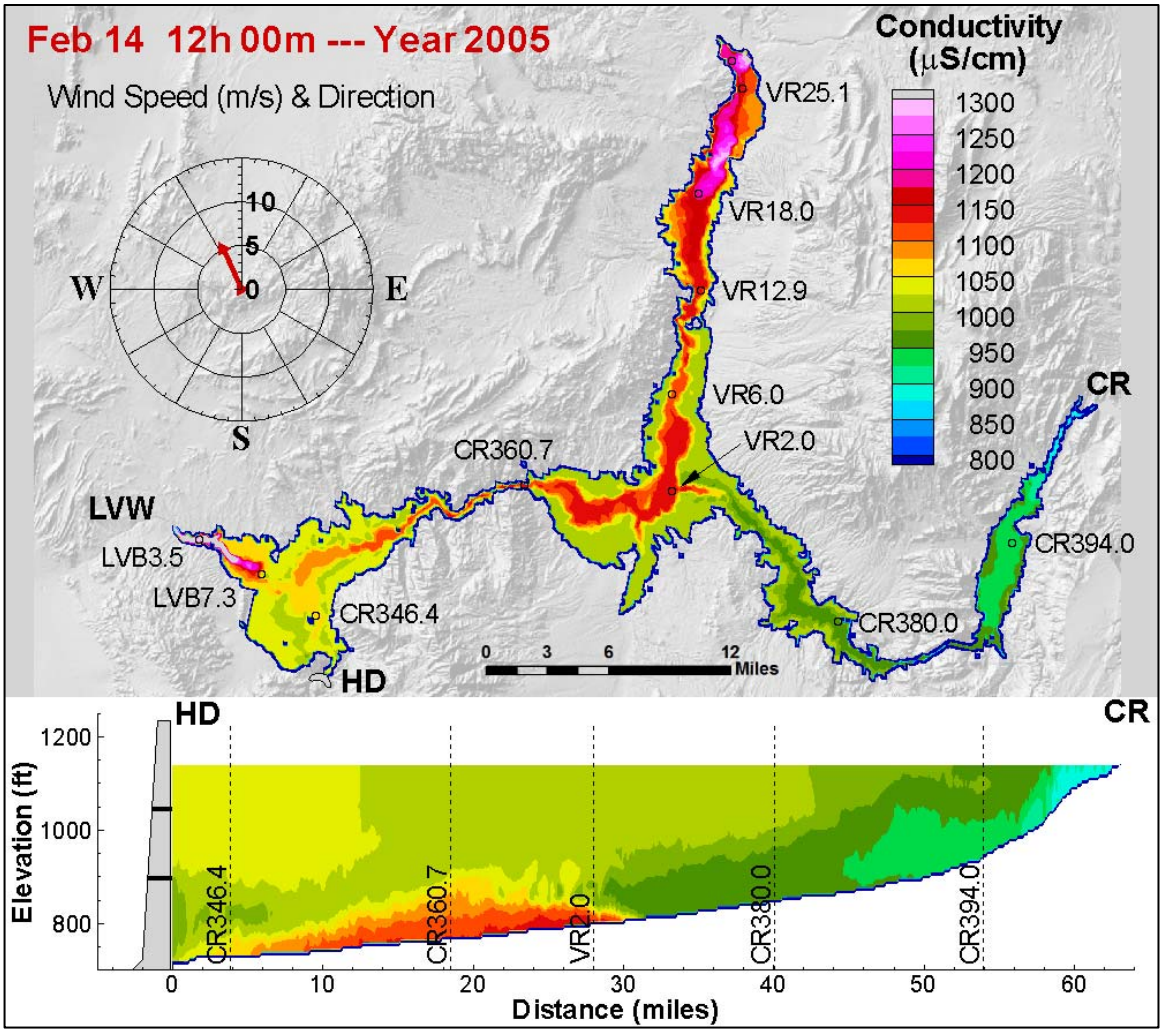

Figure A.5 ELCOM/CAEDYM calibration results for conductivity in the Lake Mead Whole Lake Model (including plan view of entire lake and cross-section from Hoover Dam to the mouth of the Colorado River).

ELCOM/CAEDYM model of the entire Lake Mead is being continually updated and calibrated on approximately a yearly basis, with funding having been provided by the CWC, the Southern Nevada Water Authority, and the National Park Service. These various stakeholders have demonstrated a long term commitment to maintaining the model because it has proven to be a worthy and successful tool. Additional funding for

ELCOM/CAEDYM modeling of the impacts of climate change on Lake Mead is being provided by the USBR under the WaterSMART grant program.

A.1.3.2.2*Lake Burragorang (New South Wales, Australia)*

ELCOM was applied and validated for Lake Burragorang in order to rapidly assess the potential impacts on water quality during an underflow event (CWR). Underflows usually occur during the winter when inflow water temperature is low compared to the reservoir. This causes the upheaval of hypolimnetic water at the dam wall, and as a result it transports nutrient rich waters into the euphotic zone.

The thermal dynamics during the underflow event were reproduced accurately by ELCOM for the case with idealized bathymetry data with coarse resolutions (straightened curves and rotating the lake in order to bypass the resolution problem), but not for the simulation with the complex, actual bathymetry. This is because the model tests showed that the ability to model underflows is severely constrained by the cross-channel grid resolution. When the cross-channel direction is poorly resolved at bends and curves, an underflow is unable to propagate downstream without a significant loss of momentum. Nevertheless, the simulations with the coarse idealized domain certainly can be used as aids and tools to visualize the behavior of reservoirs. Particularly, ELCOM was able to capture the traversal of the underflow down the length of Lake Burragorang and then had sufficient momentum to break against the wall causing the injection of underflow waters into the epilimnion near the dam. This simulated dynamic was in agreement with what was measured in the field.

A.1.3.2.3*Lake Kinneret (Israel)*

ELCOM was applied to model basin-scale internal waves that are seen in Lake Kinneret, Israel, since understanding of basin-scale internal waves behaviors provide valuable information on mixing and transport of nutrients below the wind-mixed layer in stratified lakes. In studies done by Hodges et al. (1999) and Laval et al (2003), the ELCOM simulation results were compared with field data under summer stratification conditions to identify and illustrate the spatial structure of the lowest-mode basin-scale Kelvin and Poincare waves that provide the largest two peaks in the internal wave energy spectra. The results demonstrated that while ELCOM showed quantitative differences in the amplitude and steepness of the waves as well as in the wave phases, the basin-scale waves were resolved very well by ELCOM. In particular, the model captures the qualitative nature of the peaks and troughs in the thermocline and the depth of the wind-mixed layer at relatively coarse vertical grid resolutions (Hodges et al, 1999).

A.1.3.2.4 *Lake Pamvotis (Greece)*

ELCOM/CAEDYM was applied to Lake Pamvotis, a moderately sized (22 km^2), shallow (4 m average depth) lake located in northwest Greece. Since the lake has undergone eutrophication over the past 40 years, many efforts are directed at understanding the characteristics of the lake and developing watershed management and restoration plans.

Romero and Imberger (1999) simulated Lake Pamvotis over a one month period during May to June, 1998, and compared the simulated thermal and advective dynamics of the lake with data obtained from a series of field experiments. The simulation results over-predicted heating; however, diurnal fluctuations in thermal structures were similar to those measured. Since the meteorological site was sheltered from the winds, the wind data used in the simulation was believed to be too low, causing insufficient evaporative heat-loss and subsequent over-heating by ELCOM. An increase in the wind speed by a factor of three gave temperature profiles in agreement with the field data. Moreover, the study demonstrated that the model is capable of predicting the substantial diurnal variations in the intensity and direction of both vertical and horizontal velocities. Romero and Imberger were also able to illustrate the functionality of ELCOM when coupled to the water quality model, CAEDYM, and confirmed that the model could be used to evaluate the effect of various strategies to improve poor water quality in localized areas in the lake.

A.1.3.2.5 *Lake Constance (Germany, Austria, Switzerland)*

Appt (2000) and Appt et al. (2004) applied ELCOM to characterize the internal wave structures and motions in Lake Constance [Bodensee] since internal waves are a key factor in understanding the transport mechanisms for chemical and biological processes in a stratified lake such as Lake Constance. Lake Constance is an important source of drinking water and a major tourism destination for its three surrounding countries of Germany, Austria, and Switzerland. Due to anthropogenic activities and climatic changes, Lake Constance water quality has deteriorated and its ecosystem has changed.

It was shown that ELCOM was able to reproduce the dominant internal wave and major hydrodynamic processes occurring in Lake Constance. For instance, three types of basin-scale waves were found to dominate the wave motion: the vertical mode-one Kelvin wave, the vertical mode-one Poincare waves, and a vertical mode-two Poincare wave. Moreover, an upwelling event was also reproduced by ELCOM suggesting that the width and length ratio of the basin, spatial variations in the wind, and Coriolis effects play critical roles in the details of the upwelling event. This on-going research has shown

that ELCOM can be used as a tool to predict and understand hydrodynamics and water quality in lakes.

A.1.3.2.6 *Venice Lagoon (Italy)*

ELCOM/CAEDYM is being used to develop a hydrodynamic and sediment transport model of Venice Lagoon, Italy, since future gate closures at the mouth of the lagoon are likely to impact flushing patterns. This project is an integral part of the Venice Gate Projects in Italy that was launched in May 2003 to prevent flooding.

ELCOM was validated for the tidal amplitude and phase using the data obtained from 12 tidal stations located throughout the lagoon (Yeates, 2004). Remaining tasks include model validation of temperature, salinity, and velocity against measurements made in the major channels of the lagoon.

A.1.3.2.7 *Silvan Reservoir (Australia)*

ELCOM is currently being applied to reproduce the circulation patterns observed in Silvan Reservoir, Australia, during a field experiment that was conducted in March 2004 to determine the transport pathways in the lake. This experiment confirmed the upwelling behavior of the lake and the strong role of the inflows in creating hydraulic flows in the reservoir (Antenucci, 2004).

A.1.3.2.8 *Billings and Barra Bonita Reservoirs (Brazil)*

ELCOM/CAEDYM is being applied to Billings and Barra Bonita Reservoirs in Brazil. Billings Reservoir is an upstream reservoir that feeds Barra Bonita via the Tiete River. The objective of the project is to develop an integrated management tool for these reservoirs and river reaches for use in the future planning of water resource utilization in Sao Paulo, Brazil (Romero and Antenucci, 2004).

A.1.3.2.9 *Lake Coeur D'Alene (Idaho, USA)*

ELCOM/CAEDYM is being applied to investigate the trade-off between reducing heavy metal concentrations and a potential increase in eutrophication due to remediation procedures in Lake Coeur D'Alene, Idaho. In order to investigate heavy metal fate and transport, CAEDYM is being improved further to include heavy metals and a feedback loop to phytoplankton based on metal toxicity (Antenucci, 2004).

A.1.3.2.10 *Seawater Desalination at Encina (California, USA)*

Flow Science conducted ELCOM modeling in 2004-2006 for a proposed desalination facility to be sited adjacent to the Encina Power Plant in Carlsbad, California. The proposed Encina facility involved source water taken from inside Agua Hedionda Lagoon and discharge of brines with the power plant cooling water via a surface channel across the beach south of the lagoon mouth. Flow Science used both a fine grid model to simulate water quality and dilution local to the intake and outfall and a larger grid model to simulate the effect of treated wastewater discharges and ocean currents and tides in the ocean near the lagoon. For the Encina study, Flow Science also used ELCOM to predict mixing in the vicinity of the plant discharge. The study area encompassed about 100 square miles of the ocean and also included some inland lagoons. The model resolved various tidal conditions and plant operating scenarios. The model compared favorably to existing oceanic data in the vicinity of the discharge.

A.1.3.2.11 *Moss Landing Desalination Project (California, USA)*

Flow Science applied ELCOM to simulate the flow and mixing in the entire Monterey Bay, including Elkhorn Slough. The purpose of the modeling was to evaluate the impacts of the proposed Moss Landing Desalination facility on receiving waters. The desalination facility was proposed to utilize a nearby existing power plant intake in Moss Landing Harbor and discharge to the ocean via the power plant's existing outfall, which is a submerged outfall located in Monterey Bay offshore of the harbor entrance. The ELCOM model resolved the details of the mixing in the vicinity of the power plant/desalination facility combined discharge. The model results compared favorably to existing measured water quality parameters. The results were used to determine compliance with water quality regulations for the combined outfall. The study was performed in 2004-2006.

A.1.3.2.12 *Lake Perris (California, USA)*

In 2005, ELCOM was applied to Lake Perris in order to compare the impacts of several recreational use strategies on measured fecal coliform concentrations at the reservoir outlet tower. The physical results of the simulation were validated against measured temperature and salinity data over a one-year period. The comparison of fecal coliform concentrations against measured data was fair due to a lack of data describing the timing and magnitude of loading and the settling and re-suspension of fecal matter.

The ELCOM model was expanded in 2006-2007 to include CAEDYM in order to evaluate the performance of a proposed hypolimnetic oxygenation system and observed

water quality benefits. The model was calibrated against two years of historical data and used to assess the magnitude and extent of oxygenation in the hypolimnion as a result of system operation. Impacts on dissolved oxygen concentrations and nutrient dynamics and algal production potential (as represented by chlorophyll *a*) were also evaluated, and recommendations were provided for final design of the system. The project has not yet been constructed due to seismic safety risks with the dam that must first be addressed.

A.1.3.2.13 *Lake Hodges and Olivenhain Reservoir (California, USA)*

The San Diego County Water Authority (SDCWA) is planning a tunnel connection between Lake Hodges and Olivenhain Reservoir. The tunnel and an associated hydroelectric turbine will allow for operation of the two reservoirs as part of a pumped storage project. Due to the difference in water quality between the two reservoirs, the SDCWA was concerned that the planned pumped storage project could adversely impact water quality in Olivenhain Reservoir. In order to evaluate the water quality impacts of the planned pumped storage operations on Olivenhain Reservoir, Flow Science developed a coupled ELCOM model of the two reservoirs in 2007-2008 to simulate temperature and salinity and several tracers in order to characterize the extent of mixing of the pumped storage inflow water from Lake Hodges within Olivenhain Reservoir and the percentages of Lake Hodges and Olivenhain Reservoir water throughout each reservoir due to the pumped storage operations and subsequent mixing.

A.1.3.2.14 *Lower San Gabriel River, Intake Channel, and Alamitos Bay (California, USA)*

The Los Angeles Department of Water and Power (LADWP) Haynes Generating Station (HnGS) and AES Generating Station (AES) each utilize three outfalls located on the east and west bank of the Lower San Gabriel River, respectively, and discharge cooling water to the Lower San Gabriel River Flood Control Channel (LSGR). Flow Science conducted ELCOM modeling from 2003-2010 to evaluate the mixing of flows within the river channel and found that, under typical operating conditions, the cooling water discharges form a "barrier" between freshwater from the upstream river channel and ocean water downstream of the LSGR. Both modeling and field work (conducted by others) confirmed that the net direction of flow downstream of HnGS and AES is downstream, even during flood tide conditions. Flow Science's modeling also evaluated temperature, salinity, and mixing in the LSGR for a wide range of potential future conditions and for hypothetical conditions in which both HnGS and AES cooling water flows are removed from the LSGR. Water quality in the adjacent Alamitos Bay, which is strongly influenced by flushing induced by cooling water flows from HnGS and AES, was also evaluated using ELCOM. In addition, Flow Science used CAEDYM to evaluate

nutrient concentrations, algae, and dissolved oxygen within the Bay for a range of actual and potential future operating conditions. The HnGS Intake Channel (which connects Alamitos Bay to HnGS) was also evaluated with ELCOM/CAEDYM.

Results of the Flow Science analyses have been used by LADWP in NPDES permit discussions with the Regional Water Board, in CEQA evaluations supporting the potential future repowering of HnGS Units 5 and 6, and in comments on the State's draft Once-Through Cooling (OTC) policy.

A.1.3.2.15 *Joint Water Pollution Control Plant Outfall Evaluation (California, USA)*

The Sanitation Districts of Los Angeles County (LACSD) are conducting a detailed study to evaluate the feasibility of a proposed new ocean outfall to carry treated wastewater from the Joint Water Pollution Control Plant (JWPCP) in Carson, California, to an ocean discharge location off the southern California coast near the Palos Verdes and San Pedro Shelves. As part of the Feasibility Study, Flow Science developed an ELCOM model in 2007 to evaluate the impact of this proposed ocean outfall. The near-field effluent discharge model, NRFIELD2, coupled with the far field hydrodynamic model, ELCOM, was used to simulate the mixing and determine the concentrations of a conservative effluent tracer and various indicator bacteria (assuming no chlorination). The coupled model was validated using measured current and temperature data in the vicinity of the potential discharge sites. The water quality impacts of five proposed diffuser discharge sites were evaluated, and the modeling results will be used by LACSD to estimate concentrations of indicator bacteria at selected locations at the shore and inshore regions that would result from a discharge without chlorination. Ongoing ELCOM modeling will be performed to assist LACSD in selecting a preferred diffuser location. An example of the simulated effluent tracer concentrations during summer for one of the potential diffuser sites is presented in **Figure A.6** below.

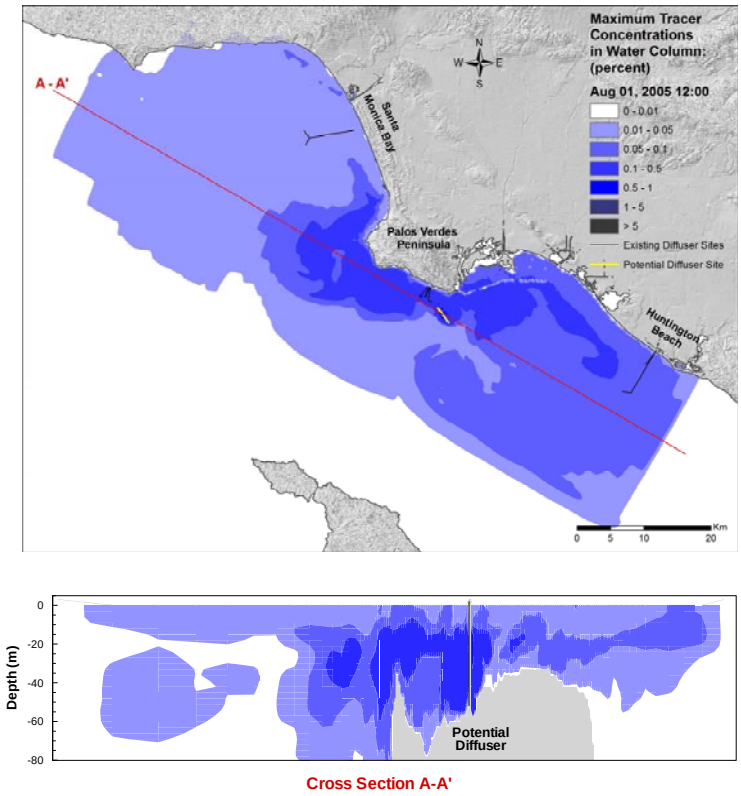

Figure A.6 Plan and section views of ELCOM simulated effluent tracer concentrations from proposed diffuser Site 1 in summer (August 1, 2005).

A.1.3.2.16 *San Vicente Reservoir (California, USA)*

Flow Science is assisting the City of San Diego in assessing the mixing and dilution potential resulting from the potential injection of highly treated effluent into San Vicente Reservoir. In 2010, Flow Science developed an ELCOM/CAEDYM model to assess the mixing and dispersion properties in San Vicente Reservoir as well as a field program to validate the modeling. The ELCOM/CAEDYM model includes temperature, salinity, conductivity, dissolved oxygen, nutrients, chlorophyll *a* (as a surrogate for algae), and multiple tracers. The model provides an accurate three-dimensional representation of water quality within the reservoir. The model was calibrated for the reservoir at its

current capacity against two years of historical data. The calibrated model has since been applied to the expanded reservoir to evaluate the impacts of the advanced water treatment (AWT) water. The model is being used to predict water quality conditions in the future enlarged reservoir and will also be used to help manage water quality in the enlarged reservoir once it is filled. The work is being reviewed by an expert panel being overseen by the National Water Research Institute. The panel is expected to complete its review and accept the use of the modeling.

A.1.3.2.17 *Los Vaqueros Reservoir (California, USA)*

In conjunction with the Contra Costa Water District (CCWD), Flow Science developed a three-dimensional ELCOM/CAEDYM model of Los Vaqueros Reservoir beginning in 2006 that is capable of providing an accurate, three-dimensional representation of water quality including temperature, salinity/TDS, nutrients and algae. The ELCOM model was calibrated against two years of historical data and validated against four years of data, while the CAEDYM model was calibrated for four years of historical data. **Figure A.7** shows a comparison of the measured versus simulated annual and growing season average chlorophyll *a* concentrations which show very good agreement. In ongoing work, Flow Science is using the ELCOM/CAEDYM model to evaluate the water quality of the reservoir under future conditions where the impounding dam is raised. This will expand the capacity of the reservoir from 100,000 acre-ft to 160,000 acre ft. The water quality model is being used to determine the changes in outflow water quality resulting from the expansion and to provide preliminary design recommendations for the inlet/outlet facilities with respect to improving water quality.

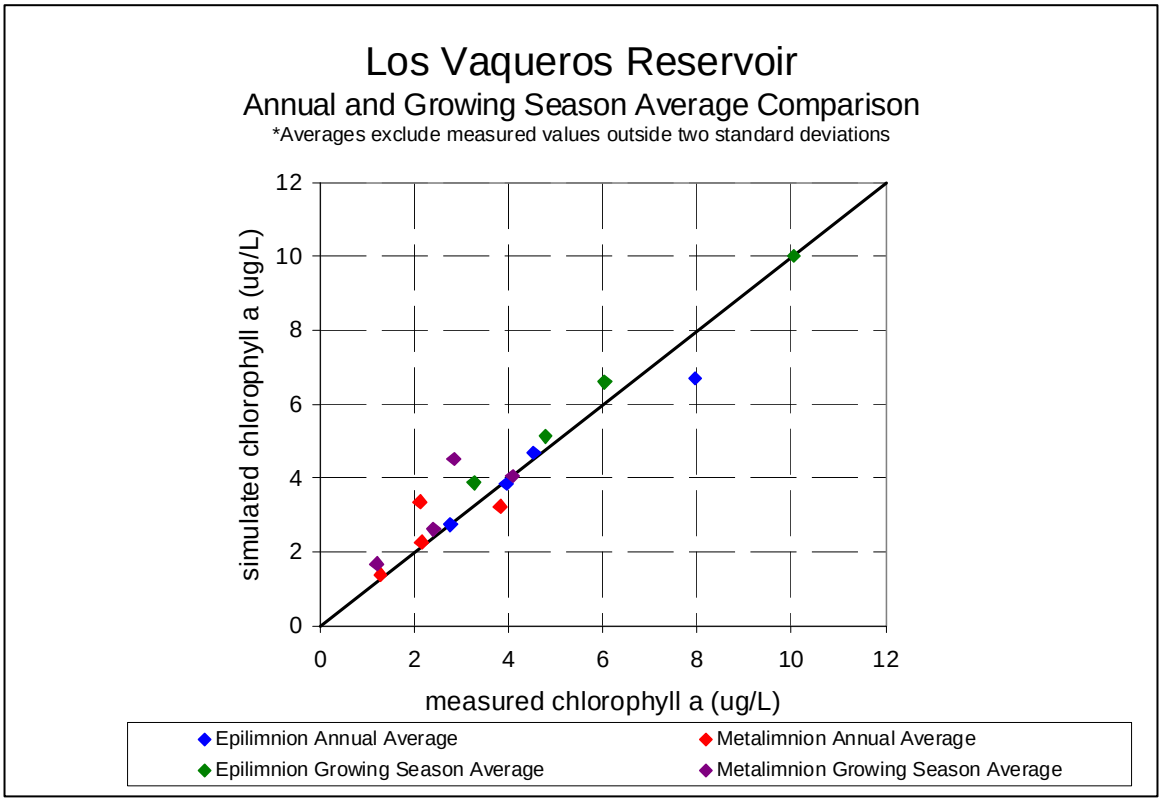

Figure A.7 Comparison of simulated ELCOM/CAEDYM results and measured chlorophyll *a* data for 2006-2009.

A.1.3.2.18 *Other Applications*

Other ELCOM/CAEDYM applications and development in on-going research at CWR include:

- Plume dynamics and horizontal dispersion (Marmion Marine Park, Australia).
- Inflow and pathogen dynamics (Helena, Myponga and Sugarloaf Reservoirs, Australia).
- Mixing and dissipation in stratified environments (Tone River, Japan, and Brownlee Reservoir, USA).

- Tidally forced estuaries and coastal lagoons (Marmion Marine Park and Barbamarco Lagoon, Italy).

- Three-dimensional circulation induced by wind and convective exchange (San Roque Reservoir, Argentina, and Prospect Reservoir, Australia).

- Sea-surface temperature fluctuation and horizontal circulation (Adriatic Sea).

- Response of bivalve mollusks to tidal forcing (Barbamarco Lagoon, Italy).

A.1.4 TECHNICAL DESCRIPTION OF ELCOM

As outlined above, ELCOM solves the unsteady, viscous Navier-Stokes equations for incompressible flow using the hydrostatic assumption for pressure. ELCOM can simulate the hydrodynamics and thermodynamics of a stratified system, including baroclinic effects, tidal forcing, wind stresses, heat budget, inflows, outflows, and transport of salt, heat and passive scalars. Through coupling with the CAEDYM water quality module, ELCOM can be used to simulate three-dimensional transport and interactions of flow physics, biology, and chemistry. The hydrodynamic algorithms in ELCOM are based upon the proven semi-Lagrangian method for advection of momentum with a conjugate-gradient solution for the free-surface height (Casulli and Cheng, 1992) and a conservative ULTIMATE QUICKEST transport of scalars (Leonard, 1991). This approach is advantageous for geophysical-scale simulations since the time step can be allowed to exceed the Courant-Friedrichs-Lewy (CFL) condition for the velocity without producing instability or requiring a fully-implicit discretization of the Navier-Stokes equations.

A.1.4.1 Governing Equations

Significant governing equations and approaches used in ELCOM include:

- Three-dimensional simulation of hydrodynamics (unsteady Reynolds-averaged Navier-Stokes equations).

- Advection and diffusion of momentum, salinity, temperature, tracers, and water quality variables.

- Hydrostatic approximation for pressure.

- Boussinesq approximation for density effects.

- Surface thermodynamics module accounts for heat transfer across free surface.
- Wind stress applied at the free surface.
- Dirichlet boundary conditions on the bottom and sides.

A.1.4.2Numerical Method

Significant numerical methods used in ELCOM include:

- Finite-difference solution on staggered-mesh Cartesian grid.
- Implicit volume-conservative solution for free-surface position.
- Semi-Lagrangian advection of momentum allows time steps with CFL > 1.0.
- Conservative ULTIMATE QUICKEST advection of temperature, salinity, and tracers.
- User-selectable advection methods for water quality scalars using upwind, QUICKEST, or semi-Lagrangian to allow trade-offs between accuracy and computational speed.
- Solution mesh is Cartesian and allows non-uniformity (i.e. stretching) in horizontal and vertical directions.

The implementation of the semi-Lagrangian method in Fortran 90 includes sparse-grid mapping of three-dimensional space into a single vector for fast operation using array-processing techniques. Only the computational cells that contain water are represented in the single vector so that memory usage is minimized. This allows Fortran 90 compiler parallelization and vectorization without platform-specific modification of the code. A future extension of ELCOM will include dynamic pressure effects to account for nonlinear dynamics of internal waves that may be lost due to the hydrostatic approximation.

Because the spatial scales in a turbulent geophysical flow may range from the order of millimeters to kilometers, it is presently impossible to conduct a Direct Navier-Stokes (DNS) solution of the equations of motion (i.e. an exact solution of the equations). Application of a numerical grid and a discrete time step to a simulation of a geophysical domain is implicitly a filtering operation that limits the resolution of the equations.

Numerical models (or closure schemes) are required to account for effects that cannot be resolved for a particular grid or time step. There are four areas of modeling in the flow physics: (l) turbulence and mixing, (2) heat budgets, (3) hydrodynamic boundary conditions, and (4) sediment transport.

A.1.4.3 Turbulence Modeling and Mixing

ELCOM presently uses uniform fixed eddy viscosity as the turbulence closure scheme in the horizontal plane (in future versions a Smagorinsky 1963 closure scheme will be implemented to represent subgrid-scale turbulence effects as a function of the resolves large-scale strain-rates). These methods are the classic "eddy viscosity" turbulence closure. With the implementation of the Smagorinsky closure, future extensions will allow the eddy-viscosity to be computed on a local basis to allow improvements in modeling local turbulent events and flow effects of biological organisms (e.g., drag induced by macroalgae or seagrass).

In the present code, the user has the option to extend the eddy-viscosity approach to the vertical direction by setting different vertical eddy-viscosity coefficients for each grid layer. However, in a stratified system, this does not adequately account for vertical turbulent mixing that may be suppressed or enhanced by the stratification (depending on the stability of the density field and the magnitude of the shear stress). To model the effect of density stratification on turbulent mixing the CWR has developed a closure model based on computation of a local Richardson number to scale. The latter is generally smaller than the time step used in geophysical simulations, so the mixing is computed in a series of partial time steps. When the mixing time-scale is larger than the simulation time step, the mixing ratio is reduced to account for the inability to obtain mixing on very short time scales. This model has the advantage of computing consistent mixing effects without regard to the size of the simulation time-step (i.e. the model produces mixing between cells that is purely a function of the physics and not the numerical step size).

A.1.4.4 Heat Budget

The heat balance at the surface is divided into short-wave (penetrative) radiation and a heat budget for surface heat transfer effects. The surface heat budget requires user input of the net loss or gain through conduction, convection, and long wave radiation in the first grid layer beneath the free surface. The short wave range is modeled using a user-prescribed input of solar radiation and an exponential decay with depth that is a function of a bulk extinction coefficient (a Beer's law formulation for radiation absorption). This coefficient is the sum of individual coefficients for the dissolved

organics ("gilvin"), phytoplankton biomass concentration, suspended solids, and the water itself. The extinction coefficients can either be computed in the water quality module (CAEDYM) or provided as separate user input.

A.1.4.5 Hydrodynamic Boundary Conditions

The hydrodynamic solution requires that boundary conditions on the velocity must be specified at each boundary. There are six types of boundary conditions: (1) free surface, (2) open edge, (3) inflow-outflow, (4) no-slip, (5) free-slip, and (6) a Chezy-Manning boundary stress model (the latter is presently not fully implemented). For the free surface, the stress due to wind and waves is required. The user can either input the wind/wave stress directly, or use a model that relates the surface stress to the local wind speed and direction *via* a bulk aerodynamic drag coefficient. Open boundaries (e.g. tidal inflow boundaries for estuaries) require the user to supply the tidal signature to drive the surface elevation. Transport across open boundaries is modeled by enforcing a Dirichlet condition on the free-surface height and allowing the inflow to be computed from the barotropic gradient at the boundary. Inflow-outflow boundary conditions (e.g. river inflows) are Dirichlet conditions that specify the flow either at a particular boundary location *or inside the domain*. Allowing an inflow-outflow boundary condition to be specified for an interior position (i.e. as a source or sink) allows the model to be used for sewage outfalls or water outlets that may not be located on a land boundary. Land boundaries can be considered zero velocity (no-slip), zero-flux (free-slip) or, using a Chezy-Manning model, assigned a computed stress.

A.1.4.6 Sediment Transport

While sediment transport is fundamentally an issue of flow physics, the algorithms for the sediment transport are more conveniently grouped with the water quality algorithms in CAEDYM. Settling of suspended particulate matter is computed using Stokes law to obtain settling velocities for the top and bottom of each affected grid cell. This allows the net settling flux in each cell to be computed. A two-layer sediment model has been developed that computes resuspension, deposition, flocculation, and consolidation of sediment based on (1) the shear stress at the water/sediment interface, (2) the type of sediment (cohesive/non-cohesive), and (3) the thickness of the sediment layer. Determination of the shear stress at the water/sediment interface requires the computation of bottom shear due to current, wind, and waves. A model has been developed to account for the effects of small-scale surface waves that cannot be resolved on a geophysical-scale grid. This model computes the theoretical wave height and period for small-scale surface waves from the wind velocity, water depth, and domain fetch. From these, the wavelength and orbital velocities are calculated. The wave-induced shear

stress at the bottom boundary resulting from the wave orbital velocities is combined with a model for the current-induced shear stress to obtain the total bottom shear that effects sediment resuspension. The cohesiveness of the sediment determines the critical shear stresses that are necessary to resuspend or deposit the sediments. A model of consolidation of the sediments is used to remove lower sediment layers from the maximum mass that may be resuspended.

A.1.5 TECHNICAL DESCRIPTION OF CAEDYM

CAEDYM is an outgrowth of previous CWR water quality modules in DYRESM-WQ and the Estuary Lake Model - Water Quality (ELMO-WQ) codes. CAEDYM is designed as a set of subroutine modules that can be directly coupled with one, two, or three-dimensional hydrodynamic "drivers", catchment surface hydrological models, or groundwater models. Additionally, it can be used in an uncoupled capacity with specification of velocity, temperature, and salinity distributions provided as input files rather than as part of a coupled computation. The user can specify the level of complexity in biogeochemical process representation so both simple and complex interactions can be studied. Direct coupling to a hydrodynamic driver (e.g. ELCOM) allows CAEDYM to operate on the same spatial and temporal scales as the hydrodynamics. This permits feedbacks from CAEDYM into ELCOM for water quality effects such as changes in light attenuation or effects of macroalgae accumulation on bottom currents. **Figure A.8** shows an illustration of the interactions of modeled parameters in CAEDYM. Being an “N-P-Z” (nutrient-phytoplankton-zooplankton) model, CAEDYM can be used to assess eutrophication. Unlike the traditional general ecosystem model, CAEDYM serves as a species- or group-specific model (i.e. resolves various phytoplankton species). Furthermore, oxygen dynamics and several other state variables are included in CAEDYM.

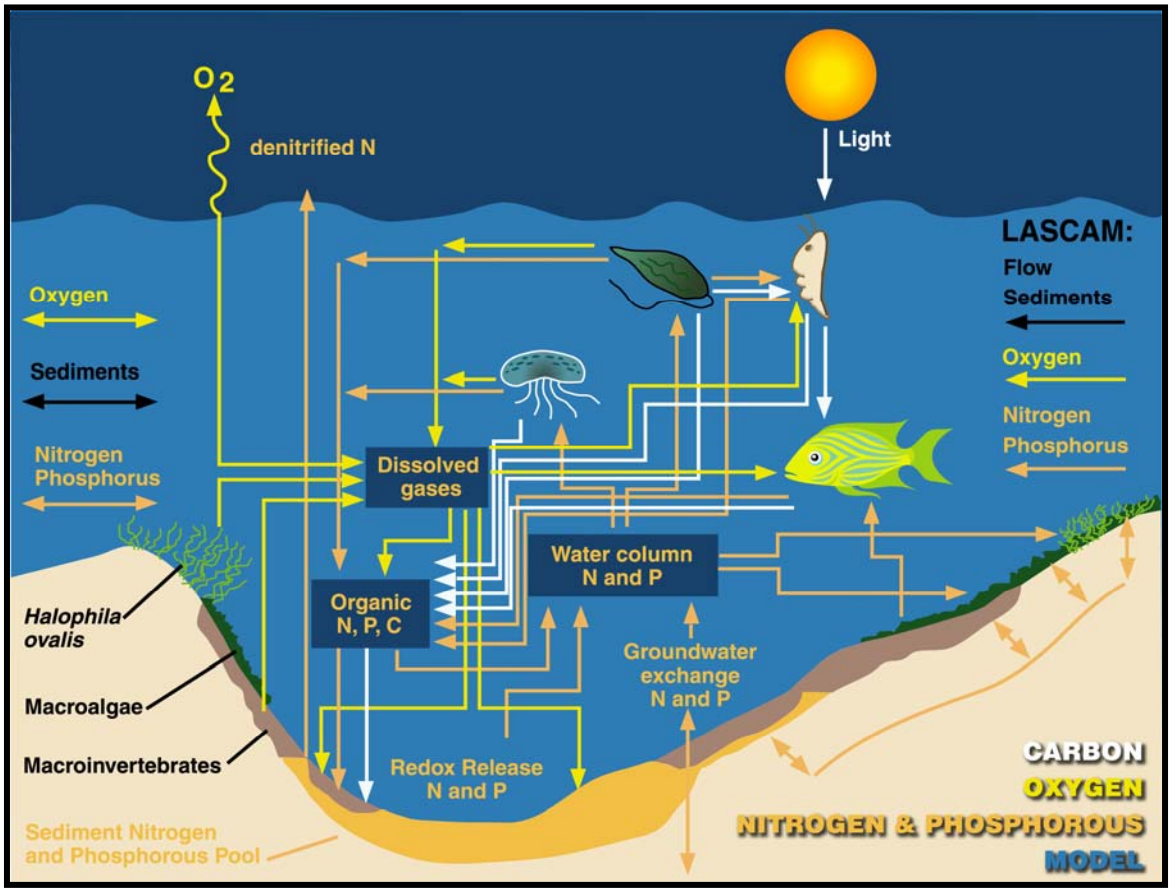

Figure A.8 Illustration of interactions of modeled parameters in CAEDYM.

The representation of biogeochemical processes in ecological models has, historically, been treated in a simple manner. In fact, the pioneering work on modeling marine ecosystems (Riley et al, 1949; Steel, 1962) is still used as a template for many of the models that are currently used (Hamilton and Schladow, 1997). The level of sophistication and process representation included in CAEDYM is of a level hitherto unseen in any previous aquatic ecosystem model. This enables many different components of the system to be examined, as well as providing a better representation of the dynamic response of the ecology to major perturbations to the system (e.g. the response to various management strategies). **Figure A.9** shows the major state variables included in the CAEDYM model. Using CAEDYM to aid in management decisions and system understanding requires (1) a high level of process representation, (2) process

interactions and species differentiation of several state variables, and (3) applicability over a spectrum of spatial and temporal scales. The spectrum of scales relates to the need for managers to assess the effects of temporary events, such as anoxia at specific

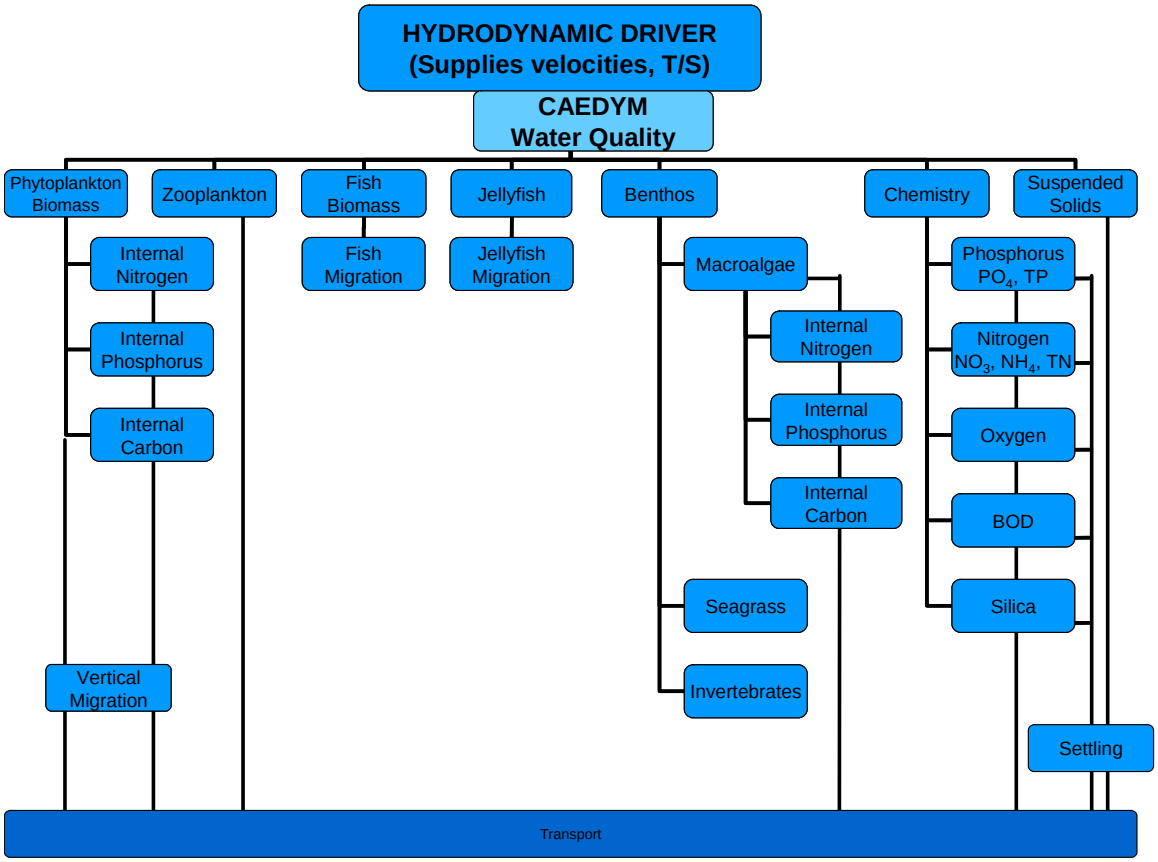

Figure A.9 Major state variables included in the CAEDYM model.

locations, through to understanding long-term changes that may occur over seasons or years. There is considerable flexibility in the time step used for the ecological component. Long time steps (relative to the hydrodynamic advective scale) may be used to reduce the frequency of links to ELCOM when long-term (i.e. seasonal or annual) simulations are run.

A.1.5.1 Biological Model

The biological model used in CAEDYM consists of seven phytoplankton groups, five zooplankton groups, six fish groups, four macroalgae groups and three invertebrate groups, as well as models of seagrass and jellyfish. This set will be expanded as biological models are developed, tested, and calibrated to field data. There is flexibility for the user in choosing which species to include in a simulation. Vertical migration is simulated for motile and non-motile phytoplankton, and fish are migrated throughout the model domain according to a migration function based on their mortality. A weighted grazing function is included for zooplankton feeding on phytoplankton and fish feeding on zooplankton. The biomass grazed is related to both food availability and preference of the consumer for its food supply. Improved temperature, respiration and light limitation functions have been developed to represent the environmental response of the organisms. The benthic processes included a self-shading component and beach wrack function for macroalgae, sediment bioturbation and nutrient cycling by polychaetes, and effects of seagrass on sediment oxygen status.

In particular, the seven phytoplankton groups modeled are dinoflagellates, freshwater diatoms, marine/estuarine diatoms, freshwater cyanobacteria, marine estuarine cyanobacteria, chlorophytes, and cryptophytes. Phytoplankton biomass is represented in terms of chlorophyll *a*. Phytoplankton concentrations are affected by the following processes:

- Temperature growth function
- Light limitation
- Nutrient limitation by phosphorus and nitrogen (and when diatoms are considered, silica)
- Loss due to respiration, natural mortality, excretion, and grazing
- Salinity response
- Vertical migration and settling

A.1.5.2 Nutrients, Metals, and Oxygen Dynamics

The transport and chemical cycling of nutrients is an important part of simulating the interaction of biological organisms in an ecosystem. CAEDYM includes as state variables the following:

- Nutrients (dissolved inorganic phosphorus, total phosphorus, total nitrogen, ammonium nitrate, and silica).
- Dissolved oxygen and biochemical oxygen demand.
- Metals (dissolved and particulate forms of iron and manganese).
- Suspended sediment (the particulate and colloidal fractions).
- pH

The model incorporates oxygen dynamics and nutrient cycling in both the sediments and water column. A sediment pool of organic detritus and inorganic sediments, both of which may be resuspended into the water column, is included. Redox-mediated release of dissolved nutrients is simulated from the sediments to the water column.

Processes included in the water and sediment oxygen dynamics include:

- Atmospheric exchange (Wanninkhof, 1992).
- Oxygen production and consumption through phytoplankton, macroalgae, and seagrass/macrophyte photosynthesis and respiration, respectively.
- Utilization of dissolved oxygen due to respiration of higher organisms such as zooplankton and fish and due to photosynthesis and respiration in jellyfish
- Water column consumption of oxygen during nitrification.
- Biochemical oxygen demand due to mineralization of organic matter in the water column and in the sediments.

Oxygen flux from the water column to the sediments, sediment oxygen demand (SOD), as developed from Fick's law of diffusion.

The last two processes are used together with a sediment porosity and diffusion coefficient (Ullman and Aller, 1982) in order to define the depth of the toxic layer in the sediments.

Nutrient processes included in the sediment and water column dynamics include:

- Phytoplankton nutrient uptake, with provision for luxury storage of nutrients.
- Release of dissolved inorganic nutrients from phytoplankton excretion.
- Excretion of nutrients as fecal material by zooplankton.
- Nitrification and denitrification by bacterial mediated action.
- Generation of inorganic nutrients from organic detritus.
- Transfer of nutrients through the food chain (e.g. phytoplankton--zooplankton--fish).
- Uptake of nutrients by macroalgae and seagrasses.
- Adsorption/desorption of nutrients from inorganic suspended sediments.
- Sediment/water transfer of nutrients (*via* such processes as sediment resuspension, sedimentation, redox-mediated nutrient release, and bioturbation).

In essence, CAEDYM represents the type of interactive processes that occur amongst the ecological and chemical components in the aquatic ecosystem. As a broad generalization, one component of the system cannot be manipulated or changed within the model without affecting other components of the system. Similarly in nature, changing an integral component in the aquatic system will have wide-ranging and follow-on effects on many of the other system components. CAEDYM is designed to have the complexity and flexibility to be able to handle the continuum of responses that will be elicited as components of a system that are manipulated. Thus, the model represents a valuable tool to examine responses under changed conditions, as for example, when new approaches to managing an ecosystem are adopted.

A.2 DESCRIPTION OF ELCOM/CAEDYM/VISUAL PLUMES (ECP)

A.2.1 INTRODUCTION

Outfalls are commonly used to discharge treated effluent into open waters. The hydrodynamics of an effluent discharged through an outfall can be conceptualized as a mixing process occurring in two separate regions: a near-field region and a far-field region. In the near-field region the effluent generally experiences a significant amount of mixing, and dilution occurs very rapidly. In this region, the initial jet characteristics of momentum flux, buoyancy flux, flow rate, as well as outfall geometry greatly influence the effluent trajectory and degree of mixing (Fischer et al, 1979). As the effluent plume travels further away from the source, the source characteristics become less important and the far-field region is attained. Mixing of the effluent plume in this region is caused by spatial and temporal variations of ambient velocity fields and dilution generally occurs slowly over a long distance, but may be rapid if there is a high degree of turbulence in the environment.

Due to different dominant temporal and spatial scales of flow velocity and effluent concentration in the near and far field region, a complete model that accounts for all important spatial and temporal scales in both the near-field and far-field regions is not feasible. Instead, these two regions are usually treated by separate models termed the near-field model and the far-field model respectively.

The near-field model has been under intensive study from the 1950s through the early 1990s. Thorough reviews of these studies are provided by Fischer et al. (1979), Baumgartner et al. (1994), and Roberts et al. (1989 a, b, c). These studies have produced a number of near-field models that were verified by both field and laboratory data. Among them, Visual Plumes (VP or PLUMES), endorsed by the U.S. Environmental Protection Agency (USEPA), is the most popular model and has been widely used by regulatory agencies and outfall designers to estimate the near-field dilution.

A variety of models can be used to model far-field mixing processes. These include ELCOM/ CAEDYM, Princeton Ocean Model (POM), and MIT General Circulation Model (MITGCM). All of these models obtain a velocity field from the numerical calculation of the equations of motion and account for influences by tide, wind stress, and pressure gradient due to free surface gradients (barotropic) or density gradients (baroclinic). Given the velocity field, the pollutant concentration field is

typically obtained by solving the Eulerian advective diffusion equation in three dimensions or by using the Lagrangian particle-tracking method.

In simple water bodies with well-defined uni-directional current regimes, the use of near-field models alone may suffice to evaluate a design of an outfall discharge that meets regulations. However, in regions with multiple current regimes (inertial, tide, wind, and buoyancy driven) and with large pollutant loadings, especially where several sources may interact, near-field models must be supplemented by far-field transport and water quality models. The latter are capable of prediction, over a greater distance in the water body, of the concentration distributions for different pollutants, nutrients, and other bio-chemical parameters. They do not, however, have the high spatial resolution that is required to predict near-field mixing processes. Thus, a coupled approach is necessary. In the following sections, a method of coupling the near-field model PLUMES and the far-field model ELCOM/CAEDYM is discussed. The coupled code is referred to as ELCOM/CAEDYM/PLUMES (ECP). Note that there is no standard procedure for the coupling of near and far field models and the coupling procedure varies from code to code mainly because of the different code structures among all of the near-field and far-field models.

A.2.2 NEAR-FIELD MODEL – PLUMES

PLUMES is an interface program that contains the near-field models such as the Roberts, Snyder, and Baumgartner model (RSB) and UM and CORnell MIXing Zone Expert System (CORMIX) (Baumgartner et al., 1994). In ECP, the UM model is chosen to simulate near-field dilution. The UM model is an integral near-field model that uses one-dimensional conservation equations for mass, momentum, salinity and temperature, to model the growth of the plume once the effluent has left the port. Assumptions are made about the shape of the plume and the distribution of pollutant concentration within the plume. Several mechanisms of entrainment such as aspirated, forced, and turbulent diffusion are considered. Both positively and negatively buoyant plumes, single source and multi-port diffuser configurations can be modeled. Model outputs include average dilution, centerline dilution, and horizontal distance of the effluent plume. The major limitation of UM lies in the assumption of an infinite receiving water body, similar to all other available integral-type models (e.g. RSB model). Thus, UM should only be used for deep-water outfalls without boundary interactions. More details on UM and PLUMES can be found in Baumgartner et al. (1994).

A.2.3 FAR-FIELD MODEL – ELCOM/CAEDYM

ELCOM is a three-dimensional hydrodynamic model for lakes and reservoirs and is used to predict the velocity, temperature, and salinity distribution in natural water bodies subjected to external environmental forcing, such as wind stress, surface heating, or cooling. Through coupling with the CAEDYM water quality module, ELCOM can be used to simulate three dimensional transport and interactions of flow physics, biology, and chemistry. ELCOM/CAEDYM is the chosen far-field model in ECP.

A.2.4 COUPLING PLUMES AND ELCOM/CAEDYM

The adopted coupling procedure is based on four steps: ambient conditions modeling, near-field modeling, coupling of near-field and far-field models, and far-field modeling.

1. Ambient conditions modeling

   The near-field model, UM, needs the input of ambient conditions such as the prevailing velocity, temperature, and salinity profiles in the vicinity of the outfall. These profiles are extracted from the ELCOM/CAEDYM simulation at the beginning of a time step at a vertical column of grid cells containing or overlapping the diffuser (the "Diffuser Cell Column" in **Figure A.10**). The depth of the diffuser is also updated based on the surface elevation at that time step.

2. Near-field modeling

   The UM model is applied at each time step using the ambient conditions extracted from ELCOM/CAEDYM. Furthermore, effluent data is obtained from input files for ELCOM/CAEDYM, and the diffuser geometry is specified in the input file called "diffuser_config.dat." The UM model is modified to consider the trapping or surfacing of the plume as the end of the near-field region. The computed average dilution along the trajectory of the plume is then stored for the following coupling step.

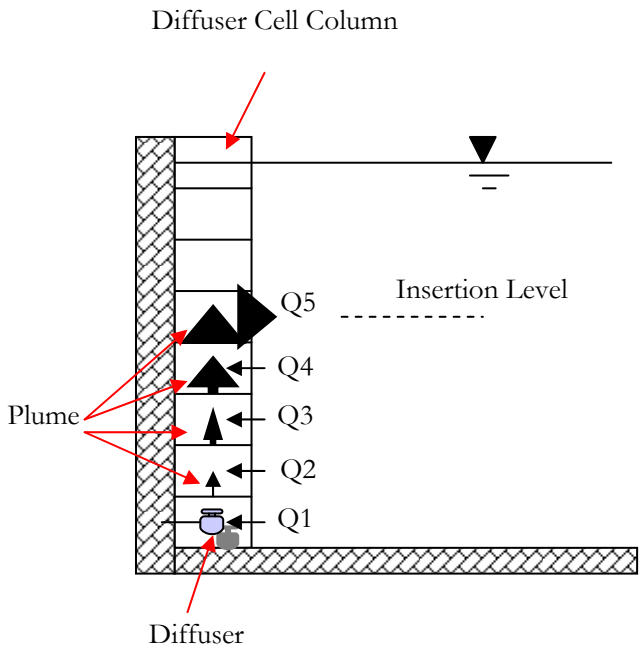

Figure A.10 Schematic of coupling procedure for near-field and far-field models.

3. Coupling of near-field and far-field models

After identifying the "Diffuser Cell Column" (**Figure A.10**), the dilution in each of the cells along this column can be calculated from the linear interpolation of results from UM. Water is then withdrawn from each of these cells based on the dilution occurring in the cell. This withdrawn water is then mixed with the effluent to form the effluent plume and passed to the cell above. Finally, the diluted effluent is then inserted into the cell where the UM model indicates the occurrence of trapping or surfacing (**Figure A.10**). Flow rate, temperature, salinity, and tracer concentrations within this inserted inflow are determined by mass conservation.

4. Far-field modeling

ELCOM/CAEDYM treats the previous coupling process as a series of outflows and inflows along the "Diffuser Cell Column" and proceeds with its time-marching far-field simulation for the time step. Steps 1 - 4 are then repeated for the next time step until the simulation ends.

A.2.5 VERIFICATION OF ECP

The UM model was originally written in TURBO PASCAL and was converted into FORTRAN and included in ECP. The comparison between the results from UM of PLUMES and UM of ECP shows an exact match (**Figure A.11**) and the conversion of the UM model is verified.

Output from UM Model of PLUMES

depth (m)	dilution (m)	horiz dis	
50.000	1.000	0.000	
49.761	1.971	0.005	
49.311	3.913	0.035	
48.585	7.797	0.127	
47.525	15.566	0.327	
46.035	31.104	0.696	
45.928	32.424	0.725	merging
43.228	62.180	1.529	
37.335	124.335	3.385	
25.609	248.651	7.517	
22.323	285.625	8.893	trap level
15.436	395.624	12.750	begin overlap, dilution
	overestimated		
14.308	442.027	13.760	surface hit

Output from UM Model of ECP

depth (m)	dilution (m)	horiz dis	
50.000	1.000	0.000	
49.761	1.971	0.005	
49.311	3.913	0.035	
48.585	7.797	0.127	
47.525	15.566	0.327	
46.035	31.104	0.696	
45.928	32.424	0.725	merging
43.228	62.180	1.529	
37.335	124.335	3.385	
25.609	248.651	7.517	
22.323	285.625	8.893	trap level
15.436	395.624	12.750	begin overlap, dilution
	overestimated		
14.308	442.027	13.760	surface hit

Figure A.11 Comparison of outputs from UM of PLUMES and ECP

Mass conservation within ECP was tested by simulating an idealized lake with a single outfall (inflow) and no outflow. Total mass of both a conservative tracer and total phosphorus (TP) in the lake was calculated at each time step and compared with a similar simulation using ELCOM/CAEDYM (where the outfall was treated as a single inflow). Less than 0.1% difference was found for the conservative tracer and less than 1% difference was found for TP at the end of a one-year simulation. These small differences indicate that mass conservation within the ECP code is comparable to that of ELCOM/CAEDYM.

The accuracy of ECP can also be qualitatively evaluated by simulating the behavior of a plume under stratified and unstratified ambient conditions. **Figure A.12** shows that ECP correctly predicts surfacing of the plume under unstratified conditions and the level of insertion of the plume under stratified conditions.

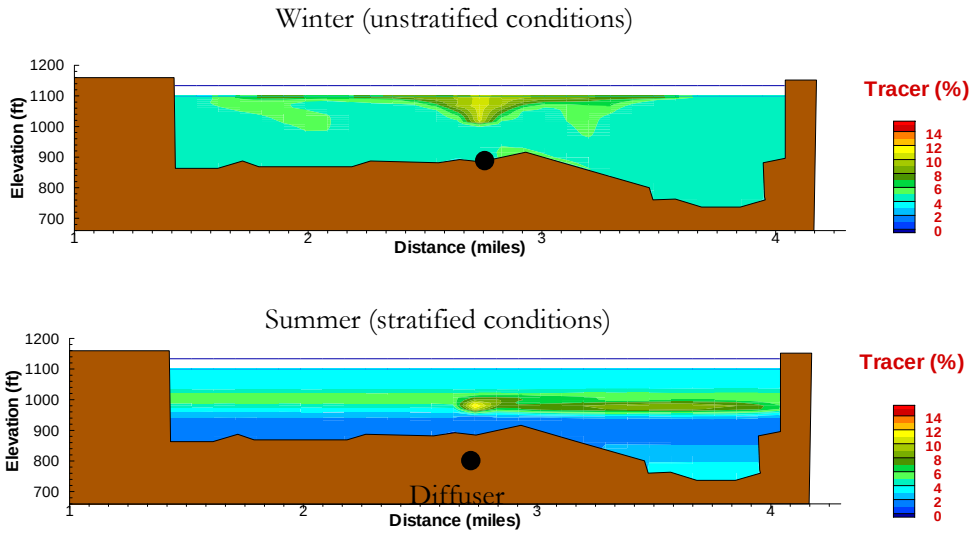

Figure A.12 Comparison of tracer concentrations released from an outfall under stratified and unstratified conditions using ECP.

A.3 BIBLIOGRAPHY

A.3.1 REFERENCED IN TEXT

Amorocho, J. and DeVries, J.J. (1980). "A new evaluation of the wind stress coefficient over water surfaces," Journal of Geophysical Research, 85:433-442.

Antenucci, Jason (2004). "Tracing Short-Circuiting Potential," from CWR Models: Bytes and Nybbles, Autumn 2004, Issue 10, page 2.

Antenucci, Jason (2004). "New Metals Model for CAEDYM," from CWR Services: Bytes and Nybbles, December 2004, Issue 11, page 1.

Appt, Jochen (January 2000), "Review on the modeling of short period internal waves in lakes with focus on Lake Constance," Pfaffenwaldring 61, D-70550 Stuttgart, Universität Stuttgart, Institut für Hydraulik und Grandmaster, Stuttgart.

Appt, J., Imberger, J., Kobus, H. (2004), "Basin-scale motion in stratified Upper Lake Constance," Limnology and Oceanography, 49(4), 919-933

Baumgartner, D. J., Frick, W. E. & Roberts, P. J. W. (1994), Dilution Models for Effluent Discharges (3rd ed.), *United States Environmental Protection Agency (EPA/600/R-94/086).*

Casulli, Vincenzo and Cheng, Ralph T. (1992), "Semi-implicit finite difference methods for three-dimensional shallow water flow," *International Journal for Numerical Methods in Fluids*, **15**, 629-48.

CWR, "Limnological Study of Lake Burragorang," Centre For Water Research, The University of Western Australia, Chapter 4 excerpt from report, pp. 104-126.

Fischer, H.B., List, E.J., Koh, R.C.Y., Imberger, J. & Brooks, N.H. (1979), Mixing in Inland and Coastal Waters, *Academic Press, New York*

Hamilton, D. (1997). "An integrated ecological model for catchment hydrology and water quality for the Swan and Canning Rivers," presented at the 2nd International Symposium on Ecology and Engineering, 10-12 November 1997, Freemantle, Australia. IAHR Eco-Hydraulics section.

Hamilton, D.P. and S.G. Schladow (1997), "Prediction of water quality in lakes and reservoirs: Part I: Model description," *Ecological Modelling, 96*, 91-110.

Herzfeld, M. and Hamilton, D. (1998), "A computational aquatic ecosystem dynamics model for the Swan River," *EOS Trans. AGU*, **79**(1), Ocean Sciences Meet. Suppl. OS11P-02.

Herzfeld, M.; Hodges, B.R.; and Hamilton, D. (1998), "Modelling the Swan River on small temporal and spatial scales," The Swan Canning Estuary conference, York, Australia, Apr., 1998.

Herzfeld, M.; Hamilton, D.; and Hodges, B.R. (1997), "Reality vs. management: The role of ecological numerical models," *2nd International Symposium on Ecology and Engineering*, 10-12 November 1997, Fremantle, Australia, IAHR Eco-Hydraulics section.

Hipsey, M.R., Romero, J.R., Antenucci, J.P. and Hamilton, D. (2005) "Computational Aquatic Ecosystem Dynamics Model: CAEDYM: v2.2 Science Manual", Centre for Water Research, The University of Western Australia.

Hipsey, M.R., Romero, J.R., Antenucci, J.P. and Hamilton, D. (2005) "Computational Aquatic Ecosystem Dynamics Model: CAEDYM: v2.2 User Manual", Centre for Water Research, The University of Western Australia.

Hodges, B.R. (1998), "Hydrodynamics of differential heat absorption," *Environmental Mechanics Laboratory Seminar*, Dept. of Civil Eng., Stanford University, Feb. 1998.

Hodges, B.R. and Dallimore C (2006), "Estuary Lake and Coastal Ocean Model: ELCOM v2.2 Science Manual", Centre for Water Research, The University of Western Australia.

Hodges, B.R. and Dallimore C (2007), "Estuary Lake and Coastal Ocean Model: ELCOM v2.2 User Manual", Centre for Water Research, The University of Western Australia.

Hodges, B.R. and Herzfeld, M. (1997), "Coupling of hydrodynamics and water quality for numerical simulations of Swan River," *2nd International Symposium on Ecology and Engineering*, 10-12 November, Fremantle, Australia, IAHR Eco-Hydraulics section.

Hodges, B.R.; Herzfeld, M.; Winters, K.; and Hamilton, D. (1998), "Coupling of hydrodynamics and water quality in numerical simulations," *EOS Trans. AGU*, **79**(1), Ocean Sciences Meet. Suppl. OS11P-01.

Hodges, B.R., Imberger, J., Saggio, A., and K. Winters (1999), "Modeling basin-scale internal waves in a stratified lake," *Limnology and Oceanography*), **45**(7), 1603-20.

Hodges, B.R., Yue, N., and Bruce, L. (May 27, 1999), "Swan River hydrodynamic model progress report," Centre For Water Research, The University of Western Australia, 14pp.

Jacquet, J. (1983). "Simulation of the thermal regime of rivers," In Orlob, G.T., editor, Mathematical Modeling of Water Quality: Streams, Lakes and Reservoirs, pages 150-176. Wiley-Interscience.

Kowalik, Z. and Murty, T.S. (1993). "Numerical Modeling of Ocean Dynamics," World Scientific.

Laval, B., Imberger, J., Hodges, B.R., and Stocker, R. (2003), "Modeling circulation in lakes: spatial and temporal variations," Limnology and Oceanography 48(3), 983-994.

Leonard, B.P. (1991), "The ULTIMATE conservative difference scheme applied to unsteady one-dimensional advection," *Computational Methods in Applied Mechanics and Engineering*, **88**, 17-74.

Lin, B. and Falconer, R.A. (1997). "Tidal flow and transport modeling using ULTIMATE QUICKEST," Journal of Hydraulic Engineering, 123:303-314.

Roberts, P.J.W., Snyder, W.H. & Baumgartner, D.J. (1989a), Ocean Outfalls I, Submerged wastefield formation, *J. Hydraulic Engineering*, **115**, 1-25

Roberts, P.J.W., Snyder, W.H. & Baumgartner, D.J. (1989b), Ocean Outfalls II, Spatial evolution of submerged wastefield, *J. Hydraulic Engineering*, **115**, 26-48

Roberts, P.J.W., Snyder, W.H. & Baumgartner, D.J. (1989c), Ocean Outfalls III, Effect of diffuser design on submerged wastefield, *J. Hydraulic Engineering*, **115**, 49-70

Robson, B.J. and Hamilton, D. P. (2002). "Three-Dimensional Modeling of a Microcystis bloom event in a Western Australian Estuary." Centre For Water Research, The University of Western Australia, 491- 496 pp.

Romero, J.R. and Antenucci, J. (2004). "The Tiete River: Supply for Sao Paolo, Brazil," from CWR Models: Bytes and Nybbles, Autumn 2004, Issue 10, page 4.

Romero, J.R. and Imberger, J. (1999). "Lake Pamvotis Project-Final report", ED report WP 1364 JR, Centre for Water Research, Crawley, Western Australia, Australia.

Spigel, R.H.; Imberger, J.; and Rayner, K.N. (1986), "Modeling the diurnal mixed layer," *Limnology and Oceanography,* **31**, 533-56.

Staniforth, A. and Côté, J. (1991). "Semi-Lagrangian integration schemes for atmospheric models – a review," Monthly Weather Review, 119:2206-2223.

Stevens, C. and Imberger, J. (1996). "The initial response of a stratified lake to a surface shear stress," Journal of Fluid Mechanics, 312:39-66.

Ullman, W.J. and R.C. Aller (1982), "Diffusion coefficients in nearshore marine sediments," *Limnol. Oceanogr., 27*, 552-556.

Wanninkhof, R. (1992), "Relationship between wind speed and gas exchange over the ocean," *J. Geophys. Res., 97(C5)*, 7373-7382.

Yeates, Peter (2004). "ELCOM in the Venice Lagoon," from CWR Models: Bytes and Nybbles, Autumn 2004, Issue 10, page 2.

A.3.2 SUPPLEMENTAL REFERENCES

(November 1999), "Course notes, Computational aquatic ecosystem dynamics model, CAEDYM, Special introduction work session," TTF/3/Nov99, Centre for Water Research, University of Western Australia, 51pp.

(January 2000), "Course notes, Estuary & lake computer model, ELCOM, Special introduction training session," TTF/3/JAN2000, Centre for Water Research, University of Western Australia, 21pp+app.

(January 21, 2000) "Instructions for the use of the graphical user interface *modeler* in the configuration & visualization of DYRESM-CAEDYM," Draft version 2, 42pp.

Antenucci, J. and Imberger, J. (1999), "Seasonal development of long internal waves in a strongly stratified lake: Lake Kinneret," *Journal of Geophysical Research* (in preparation).

Antenucci, J. and Imberger, J. (2000), "Observation of high frequency internal waves in a large stratified lake," *5th International Symposium on Stratified Flows, (ISSF5)*, Vancouver, July 2000, **1**, 271-6.

Bailey, M.B. and Hamilton, D.H. (1997), "Wind induced sediment re-suspension: a lake wide model," *Ecological Modeling*, **99**, 217-28.

Burling, M.; Pattiaratchi, C.; and Ivey, G. (1996), "Seasonal dynamics of Shark Bay, Western Australia," *3rd National AMOS Conference*, 5-7 February 1996, University of Tasmania, Hobart, 128.

Chan, C.U.; Hamilton, D.P.; and Robson, B.J. (2001), "Modeling phytoplankton succession and biomass in a seasonal West Australian estuary," *Proceedings, SIL Congress XXVIII* (in press).

Chan, T. and Hamilton, D.P. (2001), "The effect of freshwater flow on the succession and biomass of phytoplankton in a seasonal estuary," *Marine and Freshwater Research* (in press).

De Silva, I.P.D.; Imberger, J.; and Ivey, G.N. (1997), "Localized mixing due to a breaking internal wave ray at a sloping bed," *Journal of Fluid Mechanics,* **350**, 1-27.

Eckert, W.; Imberger, J.; and Saggio, A. (1999), "Biogeochemical evolution in response to physical forcing in the water column of a warm monomictic lake," *Limnology and Oceanography* (submitted).

Gersbach, G.; Pattiaratchi, C.; Pearce, A.; and Ivey, G. (1996), "The summer dynamics of the oceanography of the south-west coast of Australia – The Capes current" *3rd National AMOS Conference*, 5-7 February 1996, University of Tasmania, Hobart, 132.

Hamilton, D.P. (1996), "An ecological model of the Swan River estuary: An integrating tool for diverse ecological and physico-chemical studies," *INTECOL's V International Wetlands Conference 1996 "Wetlands for the Future,"* September 1996, Perth, Australia.

Hamilton, D.P.; Chan, T.; Hodges, B.R.; Robson, B.J.; Bath, A.J.; and Imberger, J. (1999), "Animating the interactions of physical, chemical and biological processes to understand the dynamics of the Swan River Estuary," Combined Australian-New Zealand Limnology Conference, Lake Taupo.

Hamilton, D.P. (2000), "Record summer rainfall induces first recorded major cyanobacterial bloom in the Swan River," *The Environmental Engineer*, **1**(1), 25.

Hamilton, D.; Hodges, B.; Robson, B.; and Kelsey, P. (2000), "Why a freshwater blue-green algal bloom occurred in an estuary: the Microcystis bloom in the Swan River Estuary in 2000," Western Australian Marine Science Conference 2000, Path, Western Australia.

Hamilton, D.P.; Chan, T.; Robb, M.S.; Pattiaratchi, C.B.; Herzfeld, M.; and Hodges, B. (2001), "Physical effects of artificial destratification in the upper Swan River Estuary," *Hydrological Processes*.

Heinz, G.; Imberger, J.; and Schimmele, M. (1990), "Vertical mixing in Überlinger See, western part of Lake Constance," *Aquat. Sci.,* **52**, 256-68.

Herzfeld, M. (1996), "Sea surface temperature and circulation in the Great Australian bight," Ph.D. Thesis, School of Earth Science, Flinders University, South Australia.

Herzfeld, M. and Hamilton, D. (1997), "A computational aquatic ecosystem dynamics model for the Swan River, Western Australia," *MODSIM '97, International Congress on Modeling and Simulation Proceedings*, 8-11 December, 1997, University of Tasmania, Hobart, **2**, 663-8.

Herzfeld, Michael (May 28, 1999), "Computational aquatic ecosystem dynamics model (CAEDYM), An ecological water quality model designed for coupling with hydrodynamic drivers, Programmer's guide," Centre for Water Research, The University of Western Australia, Nedlands, Australia, 133pp.

Hodges, Ben R. (July 1991), "Pressure-driven flow through an orifice for two stratified, immiscible liquids," M.S. thesis, The George Washington University, School of Engineering and Applied Science.

Hodges, Ben R. (March 1997), "Numerical simulation of nonlinear free-surface waves on a turbulent open-channel flow," Ph.D. dissertation, Stanford University, Dept. of Civil Engineering.

Hodges, Ben R. (June 9, 1998), "Heat budget and thermodynamics at a free surface: Some theory and numerical implementation (revision 1.0c)," Working manuscript, Centre for Water Research, The University of Western Australia, 14pp.

Hodges, Ben R. (1999), "Numerical techniques in CWR-ELCOM," Technical report, Centre for Water Research, The University of Western Australia. (in preparation)

Hodges, Ben R. (2000), "Recirculation and equilibrium displacement of the thermocline in a wind-driven stratified lake," *5th International Symposium on Stratified Flows, (ISSF5)*, Vancouver, July 2000, **1**, 327-30.

Hodges, B.R., Herzfeld, M., and Hamilton, D. (1998), "A computational aquatic ecosystem dynamics model for the Swan River," *EOS Trans. AGU*, **79**(1), Ocean Sciences Meet. Suppl. OS11P-02.

Hodges, B.; Herzfeld, M.; Winters, K.; and Hamilton, D. (1998), "Interactions of a surface gravity waves and a sheared turbulent current," *EOS Trans. AGU*, **79**(1), Ocean Sciences Meet. Suppl. OS53.

Hodges, B.R. and Street, R.L. (1999), "On simulation of turbulent nonlinear free-surface flow," *Journal of Computational Physics*, **151**, 425-57.

Hodges, B.R.; Imberger, J.; Laval, B.; and Appt, J. (2000), "Modeling the hydrodynamics of stratified lakes," *Fourth International conference on HydroInformatics*, Iowa Institute of Hydraulic Research, Iowa City, 23-27 July 2000.

Hodges, B.R. and Imberger, J. (2001), "Simple curvilinear method for numerical methods of open channels," *Journal of Hydraulic Engineering*, **127**(11), 949-58.

Hodges, Ben R. and Street, Robert L. (1996), "Three-dimensional, nonlinear, viscous wave interactions in a sloshing tank," *Proceedings of the Fluid Engineering Summer Meeting 1996*, Vol. **3**, FED-Vol. **238**, ASME, 361-7.

Hodges, Ben R. and Street, Robert L. (1998), "Wave-induced enstrophy and dissipation in a sheared turbulent current," *Proceedings of the Thirteenth Australian fluid Mechanics Conference*, M.C. Thompson and K. Hourigan (eds.), Monash University, Melbourne, Australia, 13-18 December 1998, Vol. **2**, 717-20.

Hodges, B.R., Street, R.L., and Zang, Y. (1996), "A method for simulation of viscous, non-linear, free-surface flows," *Twentieth Symposium on Naval Hydrodynamics*, National Academy Press, 791-809.

Hollan, E. (1998), "Large inflow-driven vortices in Lake Constance," in J. Imberger (ed.), *Physical Processes in Lakes and Oceans. Coastal and Estuarine Studies,* **54,** American Geophysical Union, 123-36.

Hollan, E.; Hamblin, P.F.; and Lehn, H. (1990), "Long-term modeling of stratification in Large Lakes: Application to Lake Constance," in: Tilzer, M.M. and C. Serruya (eds.). *Large Lakes, Ecological Structure and Function***,** Berlin: Springer Verlag, 107-24.

Horn, D.A.; Imberger, J.; and Ivey, G.N. (1999), "Internal solitary waves in lakes – a closure problem for hydrostatic models," *Proceedings of 'Aha Halikoa Hawaiian Winter Workshop*, January 19-22, 1999, University of Hawaii, Manoa.

Horn, D.A.; Imberger, J.; and Ivey, G.N. (1999), "The degeneration of large-scale interfacial gravity waves in lakes," under consideration for publication in *Journal of Fluid Mechanics*.

Horn, D.A.; Imberger, J.; Ivey, G.N.; and Redekopp, L.G. (2000), "A weakly nonlinear model of long internal waves in lakes," *5th International Symposium on Stratified Flows, (ISSF5)*, Vancouver, July 2000, **1**, 331-6.

Imberger, J. (1985), "The diurnal mixed layer," *Limnology and Oceanography,* **30**(4), 737-70.

Imberger, J. (1985), "Thermal characteristics of standing waters: an illustration of dynamic processes," *Hydrobiologia,* **125,** 7-29.

Imberger, J. (1994), "Mixing and transport in a stratified lake," Preprints of *Fourth International Stratified on Flows Symposium*, Grenoble, France, June-July 1994, **3** 1-29.

Imberger, J. (1994), "Transport processes in lakes: a review," in R. Margalef (ed.), *Limnology Now: A Paradigm of Planetary Problems,* Elsevier Science, 99-193.

Imberger, J. (1998), "Flux paths in a stratified lake: A review," in J. Imberger (ed.), *Physical Processes in Lakes and Oceans. Coastal and Estuarine Studies,* **54,** American Geophysical Union, 1-18.

Imberger, J. (1998), "How does the estuary work?" WAERF Community Forum, 25 July 1998, The University of Western Australia.

Imberger, J.; Berman, T; Christian, R.R.; Sherr, E.B.; Whitney, D.E.; Pomeroy, L.R.; Wiegert, R.G.; and Wiebe, W.J. (1983), "The influence of water motion on the distribution and transport of materials in a salt marsh estuary," *Limnology and Oceanography*, **28**, 201-14.

Imberger, J. and Hamblin, P.F. (1982), "Dynamics of lakes, reservoirs, and cooling ponds," *Journal of Fluid Mechanics,* **14**, 153-87.

Imberger, J. and Head, R. (1994), "Measurement of turbulent properties in a natural system," reprinted from *Fundamentals and Advancements in Hydraulic Measurements and Experimentation*.

Imberger, J. and Ivey, G.N. (1991), "On the nature of turbulence in a stratified fluid. Part II: Application to lakes," *Journal of Physical Oceanography,* **21**(5), 659-80.

Imberger, J. and Ivey, G.N. (1993), "Boundary mixing in stratified reservoirs," *Journal of Fluid Mechanics,* **248**, 477-91.

Imberger, J. and Patterson, J.C. (1981), "A dynamic reservoir simulation model – DYRESM: 5," In H.B. Fischer (ed.) *Transport Models for Inland and Coastal Waters,* Academic Press, 310-61.

Imberger, J. and Patterson, J.C. (1990), "Physical limnology," In: *Advances in Applied Mechanics,* **27**, 303-475.

Ivey, G.N. and Corcos, G.M. (1982), "Boundary mixing in a stratified fluid," *Journal of Fluid Mechanics,* **121**, 1-26.

Ivey, G.N. and Imberger, J. (1991), "On the nature of turbulence in a stratified fluid. Part I: The energetics of mixing," *Journal of Physical Oceanography,* **21**(5), 650-8.

Ivey, G.N.; Imberger, J.; and Koseff, J.R. (1998), "Buoyancy fluxes in a stratified fluid," in J. Imberger (ed.), *Physical Processes in Lakes and Oceans. Coastal and Estuarine Studies,* **54,** American Geophysical Union, 377-88.

Ivey, G.N.; Taylor, J.R.; and Coates, M.J. (1995), "Convectively driven mixed layer growth in a rotating, stratified fluid," *Deep-Sea Research I.,* **42**(3), 331-49.

Ivey, G.N.; Winters, K.B; and De Silva; I.P.D. (1998), "Turbulent mixing in an internal wave energized benthic boundary layer on a slope," submitted to *Journal of Fluid Mechanics*.

Jandaghi Alaee, M.; Pattiaratchi, C.; and Ivey, G. (1996), "The three-dimensional structure of an island wake," *8th International Biennial Conference. Physics of Estuaries and coastal Seas (PECS)* 9-11 September 1996, the Netherlands, 177-9.

Javam, A; Teoh, S.G.; Imberger, J.; and Ivey, G.N. (1998), "Two intersecting internal wave rays: a comparison between numerical and laboratory results," in J. Imberger (ed.), *Physical Processes in Lakes and Oceans. Coastal and Estuarine Studies***, 54,** American Geophysical Union, 241-50.

Kurup, R.; Hamilton, D.P.; and Patterson, J.C. (1998), "Modeling the effects of seasonal flow variations on the position of a salt wedge in a microtidal estuary," Estuarine Coastal *and Shelf Science*, **47**(2), 191-208.

Kurup, R.G.; Hamilton, D.P.; and Phillips, R.L. (2000), "Comparison of two 2-dimensional, laterally averaged hydrodynamic model applications to the Swan River Estuary," *Mathematics and Computers in Simulation*, **51**(6), 627-39.

Laval, B.; Hodges, B.R.; and Imberger, J. (2000), "Numerical diffusion in stratified lake," *5th International Symposium on Stratified Flows, (ISSF5)*, Vancouver, July 2000, **1**, 343-8.

Lemckert, C. and Imberger, J. (1995), "Turbulent benthic boundary layers in fresh water lakes," Iutam Symposium on Physical Limnology, Broome, Australia, 409-22.

Maiss, M.; Imberger, J.; and Münnich, K.O. (1994), "Vertical mixing in Überlingersee (Lake Constance) traced by SF6 and heat," *Aquat. Sci.,* **56**(4), 329-47.

Michallet, H. and Ivey, G.N. (1999), "Experiments on mixing due to internal solitary waves breaking on uniform slopes," *Journal of Geophysical Research,* **104**, 13467-78.

Nehru, A; Eckert, W.; Ostrovosky, I.; Geifman, J.; Hadas, O.; Malinsky-Rushansky, N.; Erez, J.; and Imberger, J. (1999), "The physical regime and the respective biogeochemical processes in Lake Kinneret lower water mass," *Limnology and Oceanography***,** (in press).

Ogihara, Y.; Zic, K.; Imberger, J.; and Armfield, S. (1996), "A parametric numerical model for lake hydrodynamics," *Ecological Modeling,* **86**, 271-6.

Patterson, J.C; Hamblin, P.F.; and Imberger, J. (1984), "Classification and dynamic simulation of the vertical density structure of lakes," *Limnology and Oceanography,* **29**(4), 845-61.

Pattiaratchi, C.; Backhaus, J.; Abu Shamleh, B.; Jandaghi Alaee, M.; Burling, M.; Gersbach, G.; Pang, D.; and Ranasinghe, R. (1996), "Application of a three-dimensional numerical model for the study of coastal phenomena in south-western Australia," *Proceedings of the Ocean & Atmosphere Pacific International Conference*, Adelaide, October 1995, 282-7.

Riley, G.A., H. Stommel and D.F. Bumpus, "Quantitative ecology of the plankton of the Western North Atlantic," *Bull. Bingham Oceanogr. Coll., 12(3)*, 1-69, 1949.

Robson, B.J.; Hamilton, D.P.; Hodges, B.R.; and Kelsey, P. (2000), "Record summer rainfall induces a freshwater cyanobacterial bloom in the Swan River Estuary," *Australian Limnology Society Annual Congress*, Darwin, 2000.

Saggio, A. and Imberger, J. (1998), "Internal wave weather in a stratified lake," *Limnology and Oceanography,* **43**, 1780-95.

Schladow, S.G. (1993), "Lake destratification by bubble-plume systems: Design methodology," *Journal of Hydraulic Engineering*, **119**(3), 350-69.

Smagorinsky, J. (1963) "General circulation experiments with the primitive equations, ´*Monthly Weather Review, 91*, 99-152.

Spigel, R.H. and Imberger, J. (1980), "The classification of mixed-layer dynamics in lakes of small to medium size," *Journal of Physical Oceanography,* **10**, 1104-21.

Steele, J.H. (1962), "Environmental control of photosynthesis in the sea," *Limnol. Oceanogr., 7*, 137-150.

Taylor, J.R. (1993), "Turbulence and mixing in the boundary layer generated by shoaling internal waves," *Dynamics of Atmospheres and Oceans,* **19**, 233-58.

Thorpe, S.A. (1995), "Some dynamical effects of the sloping sides of lakes," *IUTAM Symposium on Physical Limnology*, Broome, Australia, 215-30.

Thorpe, S.A. (1998), "Some dynamical effects of internal waves and the sloping sides of lakes," in J. Imberger (ed.), *Physical Processes in Lakes and Oceans. Coastal and Estuarine Studies,* **54,** American Geophysical Union, 441-60.

Thorpe, S.A. and Lemmin, U. (1999), "Internal waves and temperature fronts on slops," *Annales Geophysicae,* **17**(9), 1227-34.

Unlauf, L; Wang, Y.; and Hutter, K. (1999), "Comparing two topography-Following primitive equation models for lake circulation," *Journal of Computational Physics*, **153**, 638-59.

Winter, K.B. and Seim, H.E. (1998), "The role of dissipation and mixing in exchange flow through a contracting channel," submitted to *Journal of Fluid Mechanics*.

Winter, K.B.; Seim, H.E.; and Finnigan, T.D. (1998), "Simulation of non-hydrostatic, density-stratified flow in irregular domains," submitted to *International Journal of Numerical Methods in Fluids*.

Zhu, S. and Imberger, J. (1994) "A three-dimensional numerical model of the response of the Australian North West Shelf to tropical cyclones," in: *J. Austral. Math. Soc. Ser.***, B 36,** 64-100.

APPENDIX B

ANIMATIONS

INSTRUCTIONS FOR INSTALLING AND USING FRAMER TO VIEW ANIMATION FILES

Installation of Framer

Copy the files from the CD(s) to a directory on your computer.

Running Framer

1) In the Start Menu, choose "run." In this window, type "framer.exe." This should open a "Framer Open File" window, in which you find the proper directory and choose the file that you wish to view.

2) Commands for running the animation files are in the toolbar in the upper left corner of the framer window.

LIST OF ANIMATIONS

1) SVR_BaseCase_Temperature.rm: Animation of predicted water temperature for the Base Case

2) SVR_BaseCase_DecayingTracer.rm: Animation of predicted decaying tracer concentration for the Base Case

3) SVR_Extended_Drought_DecayingTracer.rm: Animation of predicted decaying tracer concentration for the Extended Drought scenario

4) SVR_Emergency_Drawdown_DecayingTracer.rm: Animation of predicted decaying tracer concentration for the Emergency Drawdown scenario

5) SVR_DesignLocation_BaseCase_DecayingTracer.rm: Animation of predicted decaying tracer concentration using Design Purified Water Inlet Location under the Base Case operating scenario

6) SVR_BaronaArm_BaseCase_DecayingTracer.rm: Animation of predicted decaying tracer concentration using Barona Arm Purified Water Location under the Base Case operating scenario

7) SVR_CurrentAqueduct_BaseCase_DecayingTracer.rm: Animation of predicted decaying tracer concentration using Current Aqueduct Purified Water Inlet Location under the Base Case operating scenario

8) SVR_NewAqueduct_BaseCase_DecayingTracer.rm: Animation of predicted decaying tracer concentration using New Aqueduct Purified Water Inlet Location under the Base Case operating scenario

9) SVR_DesignLocation_ExtendedDrought_DecayingTracer.rm: Animation of predicted decaying tracer concentration using Design Purified Water Inlet Location under the Extended Drought operating scenario

10) SVR_NewAqueduct_ExtendedDrought_DecayingTracer.rm: Animation of predicted decaying tracer concentration using New Aqueduct Purified Water Inlet Location under the Extended Drought operating scenario